CHATTERING SUPPRESSION IN SLIDING MODE

CONTROL SYSTEM

DISSERTATION

Presented in Partial Fulfillment of the Requirements for
the Degree Doctor of Philosophy in
the Graduate School of The Ohio State University

By

Hoon Lee, M.S.

* * * * *

The Ohio State University

2007

Dissertation Committee:

Professor Vadim I. Utkin, Adviser

Professor Chia-Hsiang Menq

Professor Gregory Washington

Professor Andrea Serrani

Approved by

_____

Adviser
Mechanical Engineering
Graduate Program

ABSTRACT

In this dissertation, various known methods to decrease level of chattering caused by unmodeled dynamics are reviewed. And an analysis to understand system behavior in the presence of such unmodeled dynamics and to estimate the amplitude and frequency of chattering using describing function is provided. It is shown that the amplitude is proportional to relay gain of discontinuous control, and the frequency is inversely proportional to the time constant of unmodeled dynamics. Two methods are proposed to change switching magnitude of sliding mode control to reduce chattering. Based on the original idea of Variable Structure System, first method is to use adaptive relay gain which depends on system states. Second method varies switching gain of sliding mode control along the equivalent control. System behaviors with the two controller designs are analyzed, and it is demonstrated by simulations that chattering can be significantly reduced. For systems controlled by on/off switches or fixed switching gain only, chattering also appears if switching frequency is restricted at a finite value. To suppress chattering in such case, a methodology based on the harmonic cancellation is proposed. To fix switching frequency and to obtain desired phase shift between any two consecutive phases, hysteresis loops with adaptive width are implemented in switching elements. The design principle and procedure of the methodology are suggested, and chattering reduction effect of the method is demonstrated by various simulation results. It is also shown that the method using multiple phases may decrease chattering caused by unmodeled dynamics as well with the equivalent width of hysteresis which makes entire phases have the same frequency.

Dedicated to my family

ACKNOWLEDGMENTS

VITA

May, 19, 1970 .... Born - Seoul, Korea, Republic of

1999 .... B.S. Mechanical Engineering,

Hanyang University, Korea, Republic of

2002 .... M.S. Mechanical Engineering,

The Ohio State University, Columbus, Ohio

2002 - 2007 .... Graduate Research and Teaching Associate,

The Ohio State University, Columbus, Ohio

2003 - 2005 .... Graduate Research Fellow,

Research of Control for Electromechanical Systems,

The Ohio State University, Columbus, Ohio

PUBLICATIONS

H. Lee and V.I. Utkin (2006) Chattering Analysis" In: C. Edwards, E. Fossas Colet, Enric, L. Fridman (Eds.) Advances in Variable Structure and Sliding Mode Control, Lecture Notes in Control and Information Sciences, Vol. 334, Springer, Berlin

H. Lee and V.I. Utkin (2007) Chattering Suppression Methods in Sliding Mode Control Systems", Annual Reviews in Control

V.I. Utkin and H. Lee (2006) The Chattering Analysis, Proc. 12th International Power Electronics and Motion Control Conference, EPE-PEMC 2006, Portoroz, Slovenia, pp. 2014-2019

V.I. Utkin and H. Lee (2006) Chattering Problem in Sliding Mode Control Systems, Proc. 9th International Workshop on Variable Structure Systems, VSS 2006, Alghero, Sardinia, Italy, pp. 346-350

J. Lee and H. Lee (2004) Dynamic Simulation of Nonlinear Model-Based Observer for Hydrodynamic Torque Converter System, 2004 SAE World Congress - Transmission & Driveline Symposium, Detroit, Michigan, USA

FIELDS OF STUDY

Major field: Mechanical Engineering

TABLE OF CONTENTS

LIST OF TABLES

LIST OF FIGURES

CHAPTER 1

INTRODUCTION

Since the theory of Variable Structure Systems (VSS) had been orginated in the former Soviet Union, the sliding mode control methodology has become the principal operational mode for the control systems based on VSS [1]. Practically, all design methods for VSS are based on deliberate introduction of sliding modes which have played a remarkable role not only in theoretical developments but also in practical applications [7][8].

The sliding mode control has long been known as a particularly suitable method for handling nonlinear systems with uncertain dynamics and disturbances due to its order reduction property and low sensitivity to disturbances and plant parameter variations, which relaxes the burden of the necessity of exact modeling. Moreover, the sliding mode control may reduce the complexity of feedback control design through decoupling of system into independent subsystems of lower dimension. Because of these properties, diverse applications of the sliding mode control methodology can be found in the areas of electric motors, manipulators, power systems, mobile robots, spacecraft, and automotive control [1]. The most prospective implementation of the discontinuous control has been addressed in [9] by the use of power electronic switching devices.

The main idea of sliding mode control is to enforce the motion of the sliding mode in predefined switching surfaces in the system state space using discontinuous control. The discontinuity surfaces or the switching manifold should be selected such that sliding motion would exhibit desired dynamics of motion in accordance with certain performance criterion. The methods of the conventional control theory, such as eigenvalue placement or Linear-quadratic regulator (LQR) for linear systems, can be applicable to choose proper switching surfaces. Then, the discontinuous control needs to be chosen such that any states outside of the discontinuity surface are enforced to reach the surface in finite time. Accordingly, sliding mode occurs along the surface, and the system follows the desired system dynamics.

Let us consider the following affine system

$$\dot{x} = f(x,t) + B(x,t)u \quad (x, f \in \Re^n, \ B \in \Re^{n \times m}, \ u \in \Re^m). \tag{1.1}$$

Then, the control u is selected as a discontinuous function vector of the state as follows.

$$u_i(x) = \begin{cases} u_i^+(x,t) & if \ \ \sigma_i(x) > 0 \\ u_i^-(x,t) & if \ \ \sigma_i(x) < 0 \end{cases} \tag{1.2}$$

where $i = 1, \ldots, m$, and $u_i^+(x,t)$, $u_i^-(x,t)$, and $\sigma_i(x)$ are continuous state functions. Under a certain condition, sliding mode may be enforced in the intersections of m switching surfaces $\sigma_1(x), \sigma_2(x), \cdots, \sigma_m(x) = 0$, and the condition is equivalent to the stability condition of the motion in subspace $S(x) = [\sigma_1(x), \sigma_2(x), \ldots, \sigma_m(x)]^T$

$$\dot{S}(x) = Gf(x) + GB(x)u \tag{1.3}$$

where $G = (\partial\sigma_i/\partial x_j)$ $(G \in \Re^{m \times n})$. To consider the existence condition of sliding

2

mode, simply let $GB = I$ where I is an $n \times n$ identity matrix. Then, for discontinuous control $u_i = -M sign(\sigma_i)$ with a positive constant M which exceeds the upper estimates of elements in vector Gf, the values $\sigma_i(x)$ and $\dot{\sigma}_i$ have different signs so the sliding mode occurs in each discontinuity surface.

Under assumption that the sliding mode exists at any point of the manifold $S(x) = 0$, the control u may be replaced by u_{eq} which is a solution to the equation $\dot{S}(x) = 0$. For the condition $det(GB) \neq 0$, u_{eq} can be written as

$$u_{eq} = -(GB)^{-1} Gf \tag{1.4}$$

which is well-known as the *equivalent control* [7]. And the sliding mode equation in the manifold $S(x) = 0$ becomes

$$\dot{x} = \{I - B(GB)^{-1}G\}f \tag{1.5}$$

where I is an identity matrix. After sliding mode occurs, motion equation is of reduced order; the order of the motion equation is m less than the order of the original system. Since $S(x) = 0$ in the sliding mode, m components of the state vector x may be found as functions of the rest $(n - m)$, which means the order of the system is reduced from n to $(n - m)$. Thus, enforcing sliding modes enables order reduction, and it leads to decoupling and simplification of design procedure.

As mentioned earlier, the excellent robustness in the presence of parametric uncertainty and disturbance is the most distinguishing feature of the sliding mode. Adding a function $h(x, t)$ to the system (1.1) gives

$$\dot{x} = f(x, t) + B(x, t)u + h(x, t) \quad (h \in \Re^n). \tag{1.6}$$

The vector $h(x, t)$ represents all the factors whose influence on the control process should be eliminated. If the *matching condition* [1]

$$h(x, t) = B(x, t)\lambda(x, t) \tag{1.7}$$

is satisfied for some m-dimensional vector $\lambda(x, t)$, i.e., the disturbances act in control space, then there exists control u_k such that $Bu_k = -h$ and the system is invariant to disturbance h. The physical meaning of (1.7) is that all parametric uncertainties and disturbances should be contained in $span\{B(x, t)\}$, however the control u_k is hard to be implemented since the disturbances may be inaccessible for measurement. As the sliding mode equation in any manifold does not depend on control, it can be shown that the sliding mode does not depend on $h(x, t)$ as well; therefore, the condition (1.7) is the invariance condition for sliding mode control. And only the upper estimate of $h(x, t)$ is needed for designing a sliding mode controller.

In the implementation of sliding mode control theory in real systems, the main obstacle is an undesirable phenomenon of oscillation with finite frequency and amplitude, which is known as 'chattering'. The chattering is harmful because it leads to low control accuracy, high wear of moving mechanical parts, and high heat losses in electrical power circuits. In case that there exist fast dynamics which are neglected in the ideal model, the chattering may appear since an ideal sliding mode may not occur. These 'unmodeled' dynamics are usually from servomechanisms, sensors and data processors with small time constants. The analysis of chattering caused by such unmodeled dynamics and solutions to avoid the chattering are discussed in later chapters of this dissertation. In sliding mode, the control switches between two different values, and the switching frequency should be considerably high enough to make the sliding mode almost ideal. However, in some systems, it may not be

4

possible due to certain limitations in switching device, which also results in chattering like the one caused by unmodeled dynamics. For example, in sliding mode control of power converter systems, a natural way to reduce chattering is increasing switching frequency. However, it is not always possible due to the limitation of switching frequency for losses in power converters. Actually this chattering problem cannot blame sliding mode implementation since it is mainly caused by switching limitations. The challenge in systems such as multi-phase converter lies in reducing chattering to desired level under given switching frequency, and solutions to reduce chattering in this case are also proposed in chapter 4. In digital control system, controllers having finite sampling intervals are used, which causes so called 'discretization chattering'. For this class of systems, the concept 'discrete-time sliding mode control' has been developed [5]. A well-known solution for this case is to use the equivalent control [1], and the methodology is out of scope of this dissertation.

In the literature, various analysis of chattering in the presence of unmodeled dynamics have been studied. The chattering in the sliding mode systems with the fast actuator/sensor dynamics based on singularly perturbed approach has been analyzed in [10]-[14]. In [10], [12], and [13], it is shown that the chattering exponentially tends to zero if the relative degree of the system with actuators or sensors is two. The chattering in the presence of fast actuator dynamics is analyzed via the Poincare maps in [11], [14]. The author provides sufficient conditions for existence and stability of periodic solutions and the correction terms for sliding mode equations. However, the direct use of those maps is not always convenient because there are analytical difficulties for higher order. Therefore, approximation methods are commonly used for chattering analysis. The frequency-domain approach offers a number of advantages compared to state-space methods since the chattering phenomenon having a periodic motion may easily be handled by the frequency-domain methods. One of the first

5

attempts to analyze the phenomenon of oscillation, which later received the name chattering, was in [15]. The describing function method was applied to the analysis of chattering in [16], [17]. Later there were a few attempts to overcome the approximate nature of the describing function method. The Tsypkin's method [18] provides the required functionality and may be conveniently used for this purpose especially when the nonlinearity is a relay. An example of application of this method to analyze the chattering caused by the hysteresis of the relay can be found in [19]. An exact method called the Locus of a Perturbed Relay System (LPRS), which can be used for complex analysis comprising the chattering analysis and analysis of input-output properties of sliding-mode control systems, was proposed in [20]. This method was also extended to the case of non-relay sliding mode control algorithms (relays with state dependent output amplitudes, linear state feedback control with switched gains, etc.) in [21]. This research proposal deals with describing function approach, originating in [15] and applied to variable structure systems with sliding modes [16].

It is known that several solutions have been developed to avoid chattering. One of the solutions is to use a saturation function for the sliding mode controller, which is named 'the boundary layer solution' [22]-[25]. The saturation function approximates the sign function term in a boundary layer of the sliding surface. Since the methodology had been proposed, modifications using various types of saturation function have been suggested in the literature. For example, a state-dependent boundary layer design is proposed in [26]. Many other papers which modify the saturation function approximation using adaptiveness or even fuzzy logic [27][28] can be found in the literature. Basically, the boundary layer approach is to avoid chattering by replacing the discontinuous switching action with a continuous function depending on width of boundary layer. Of course, the width should not be too small so unmodeled dynamics are not excited. From the replacement, the system trajectories

are confined to a small vicinity of the sliding surface, not exactly to $s(t) = 0$ as in ideal sliding mode [1]. This is because real sliding mode does not occur when the switching action is replaced by a continuous approximation. The major problem of the approach is that the system behavior may not be determined within the small vicinity of the boundary layer, and it is not guaranteed that the trajectories in the vicinity converge to zero. Thus, it can be said that the accuracy and robustness of the sliding mode are partially sacrificed by the method.

To suppress chattering preserving the control discontinuities, another solution using asymptotic observers has been proposed, which is called 'observer-based' solution [29][30]. The main idea of using an asymptotic observer to prevent chattering is to generate an ideal sliding mode in the auxiliary loop including the observer. In the observer loop, the sliding mode is generated from the control software; therefore, any unmodeled dynamics which cause chattering can be excluded. As can be seen in Figure (1.1), the controller uses estimated states instead of measured states directly from the plant so the observer is free from any unmodeled dynamics from actuators or sensors and the system behaves as if an equivalent control was applied [6].

Let us consider the following nonlinear system as an example.

$$
\begin{aligned}
\dot{x}_1 &= x_2 \\
\dot{x}_2 &= ax_1 + bx_2 + c\sin x_1 + du
\end{aligned}
\tag{1.8}
$$

And let us assume that there exist certain unmodeled dynamics which cause chattering. For the above system, an asymptotic observer may be designed as follows when only the state x_1 is measurable.

$$
\begin{aligned}
\dot{\hat{x}}_1 &= \hat{x}_2 - L_1(x_1 - \hat{x}_1) \\
\dot{\hat{x}}_2 &= a\hat{x}_1 + b\hat{x}_2 + c\sin \hat{x}_1 + du(t) - L_2(x_1 - \hat{x}_1)
\end{aligned}
\tag{1.9}
$$
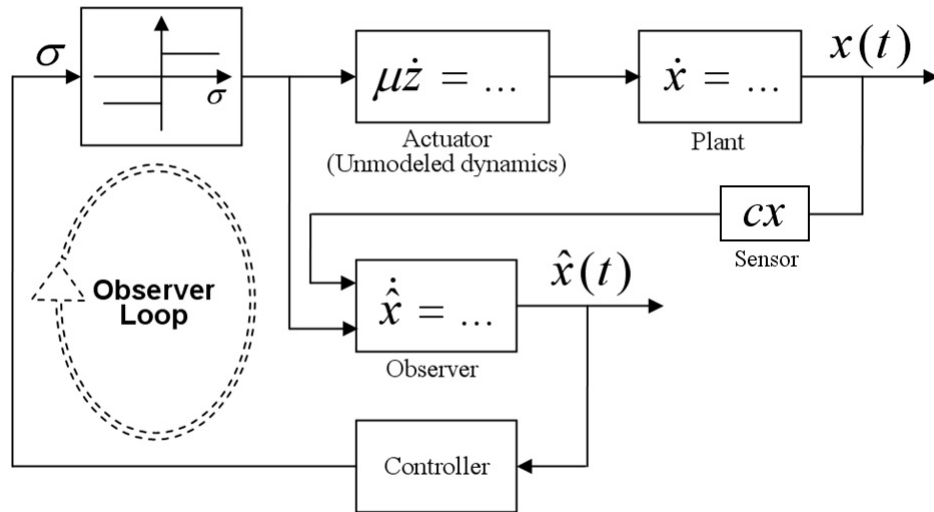
Figure 1.1: Sliding mode control with auxiliary observer loop. The discontinuous control input $u(t)$ does not excite the actuator dynamics, thus, ideal sliding mode occurs in the observer loop.

where L_1 and L_2 are constant values determined such that the error $e = x_1 - \hat{x}_1$ reduces to zero. As can be seen in Figure (1.2), the system is free from chattering by using an observer in auxiliary control loop, as illustrated in Figure (1.1), although $\dot{x}$ becomes continuous, $\dot{\hat{x}}$ in the observer is a discontinuous time function; therefore, a sliding mode may be enforced. The first plot in Figure (1.2) shows the comparison between the system output with and without observer. As can be clearly seen in the second plot which is zoomed in from the first, the system can avoid chattering when an observer is included as if there are no unmodeled dynamics ($\mu = 0$). The third plot is also from the first, and it shows that the system with an observer gives no oscillation even in transient period. However, the observer-based chattering suppression obviously requires additional effort in control design. Moreover, the plant parameters must be known to make a proper observer. But, including an observer in the control system may bring extra benefits such as identification of uncertainties and disturbances, in addition to its value in estimating unavailable states [1].

There are other solutions suggested in the literature. In case that the unmodeled dynamics are not completely unknown, i.e. some parts of information about the dynamics are available, so-called 'regular form solution' may be applicable based on the block control principle [31][32] and the integrator backstepping method [33]. Another method is to obtain an accurate disturbance estimate while avoiding chattering in the main control loop, which can be regarded as a special case of integral sliding mode [7][34]. The main idea is to design a sliding mode controller combining a continuous part and a discontinuous part, and the idea has been employed in the literature [35]. The method using so-called 'higher-order sliding mode (HOSM)' has been known to suppress chattering as well. The methodology generalizes the basic idea of sliding mode acting on the higher-order time derivatives of the system deviation from the constraint ($\sigma = \dot{\sigma} = \ddot{\sigma} = \ldots = \sigma^{(r-1)} = 0$ for so-called r^{th}-*order sliding mode* [38][39]
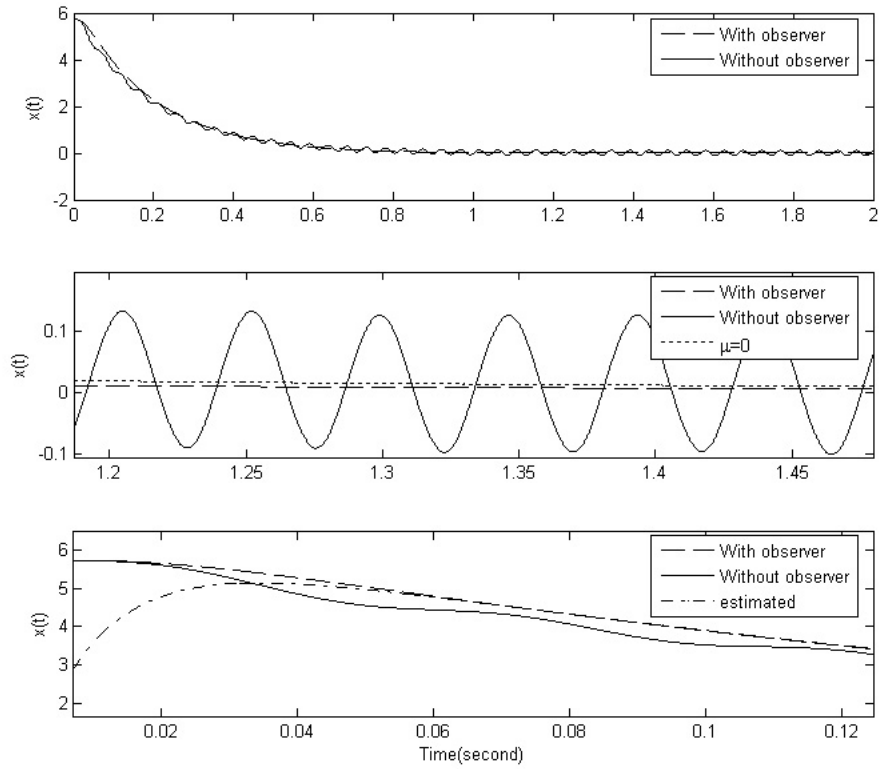
Figure 1.2: With an observer, the system can avoid chattering despite unmodeled dynamics.

where $\sigma = 0$ is a sliding surface) instead of influencing the first deviation derivative $\dot{s}$ like in conventional sliding modes [36][37]. The simulation result provided in [38] shows successful chattering suppression. However, the methodology requires more complicated process to design controller and more computational efforts to calculate control input to the plant than standard sliding mode control.

To modify the original sliding mode control to fit into specific purposes of various systems, there also have been various attempts to combine adaptiveness or other control methods with sliding mode control. To design a sliding mode controller, the bounds of unknown parameter uncertainties and disturbances should be known so that the sliding mode occurs. The adaptive control is introduced into sliding mode control because sometimes such bounds may not be easily found prior to design sliding mode control. Some papers proposed so-called 'adaptive sliding mode control (ASMC)' to estimate the bounds of the uncertainties [40]-[44]. The adaptiveness may possibly estimate the bounds of uncertainties, but is not helpful for chattering reduction. By assuming that the structure of unmodeled dynamics are known, one can possibly identify the parameters of the unmodeled dynamics by using adaptiveness, but the controller may become too complicated.

Researchers also integrated sliding mode control and fuzzy logic control techniques to develop the 'fuzzy-sliding mode control (FSMC)'. Because the fuzzy logic control (FLC) rules are experience oriented and suitable membership function should be selected by the trial and error procedure, the work of the FLC design is time-consuming and the response of the controlled system would be hardly evaluated apriori. So, the main purpose to introduce the sliding mode control to FLC was to overcome such problems, however, it is found that the FSMC can also decrease the chattering due to switching gain change [45]. But the methodology is much complicated than the design of conventional sliding mode controller. The ASMC and

the FSMC (in addition, the adaptive fuzzy sliding mode cotrol [46]) are being implemented for various applications in the literature. There also have been other various attempts to reduce chattering. Some researchers propose various method to improve the 'boundary layer' method, e.g. using time-varying boundary layer thickness [26]. The drawback of varying the boundary layer is that the boundary width becomes too large in some cases [47]. Some papers suggests that the switching gain of sliding mode is designed to be time-varying function [48][49], but not state-dependent as provided in later chapter of this dissertation.

The sliding mode control has been implemented to various power electronic devices, and power converter system is an example of such applications. Traditionally, controls using Pulse Width Modulation(PWM) were common for controlling buck/boost DC-DC converter systems [53], but sliding mode has come to attention as suitable substitute over the PWM strategy because of the benefits in sliding mode control, as mentioned earlier in this chapter, e.g. the ability to achieve desired system responses regardless of a certain level of parameter changes in spite of the fact that the equivalent control of sliding mode is similar to the one obtained from PWM block. In the literature, many papers can be found for related researches [54]-[59]. However, an obstruction of sliding mode implementation in power converters is the fact that the sliding mode yields to variable switching frequencies, which is unacceptable in many applications. The most promising solution to this problem is to adopt a hysteresis loop in switch replacing the signum nonlinearity in standard sliding mode control to fix or further to control switching frequency [60][61], which is mentioned in later chapter.

For applications using on/off switches as only admissible control modes, like general power systems, it is often required to restrict the frequency of switching due to certain reasons such as power losses. Such limitation in switching frequency

leads inevitably to chattering phenomenon or "ripple" in the output. Of course, like any other type of controllers, sliding mode implementation cannot be free from the problem of oscillations which consequently happen in the system output due to the switching restriction. Obviously, neither any well-known chattering suppression methods including the observer based solution and the linear approximation method nor those methodologies based on relay gain adaptation proposed in later chapter of this dissertation are not very helpful to the case since the control input to the system should be either zero or one and can not take any intermediate value.

The attempt to attenuate chattering in such systems may adopt methods of output voltage or current ripple amplitude reduction in power systems that are controlled by on/off switching. Let us consider a multiphase power converter system for example. The system uses on/off switchings in each phase, and the switching frequency is usually restricted at some hundred kHz. The output of the system is generally the sum of currents of all phases or the voltage across the load capacitance and resistance as shown in Figure (1.3). The governing equation for the system can be written as

$$
\begin{aligned}
L\frac{di_1}{dt} + i_1 R_a &= V_s u_1 - V_L \\
L\frac{di_2}{dt} + i_2 R_a &= V_s u_2 - V_L \\
C\frac{dV_L}{dt} + \frac{V_L}{R_L} &= i_1 + i_2
\end{aligned}
\tag{1.10}
$$

where u_1 and u_2 are switching commands for each phase that can be either zero or one (on/off). With parameters $L = 50nH$, $R_a = 0.3m\Omega$, $Vs = 12V$, $R_L = 50m\Omega$, and $C = 600\mu F$, simulation is performed for system (1.11) with PWM controllers with switching frequency of 250kHz. It can be observed in Figure (1.4), the amplitude level of output oscillation $(i_1 + i_2)$ is high when two switching commands, u_1 and u_2 are

13
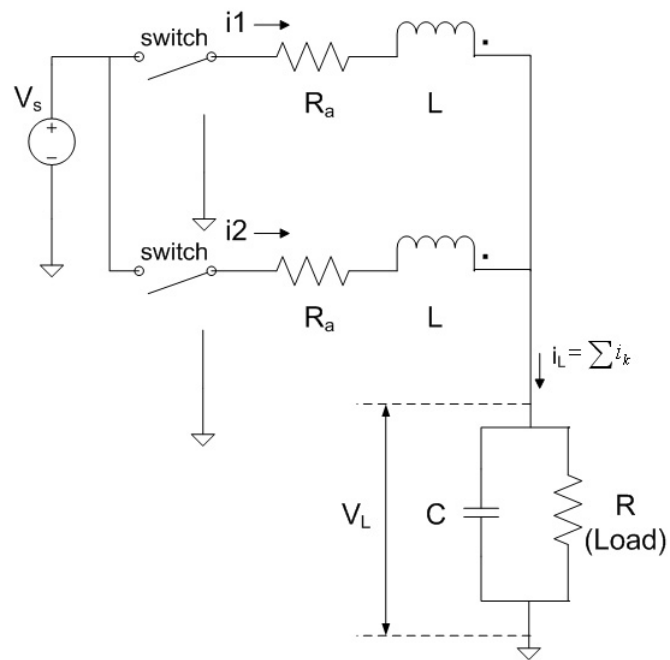
Figure 1.3: A two-phase DC to DC converter.
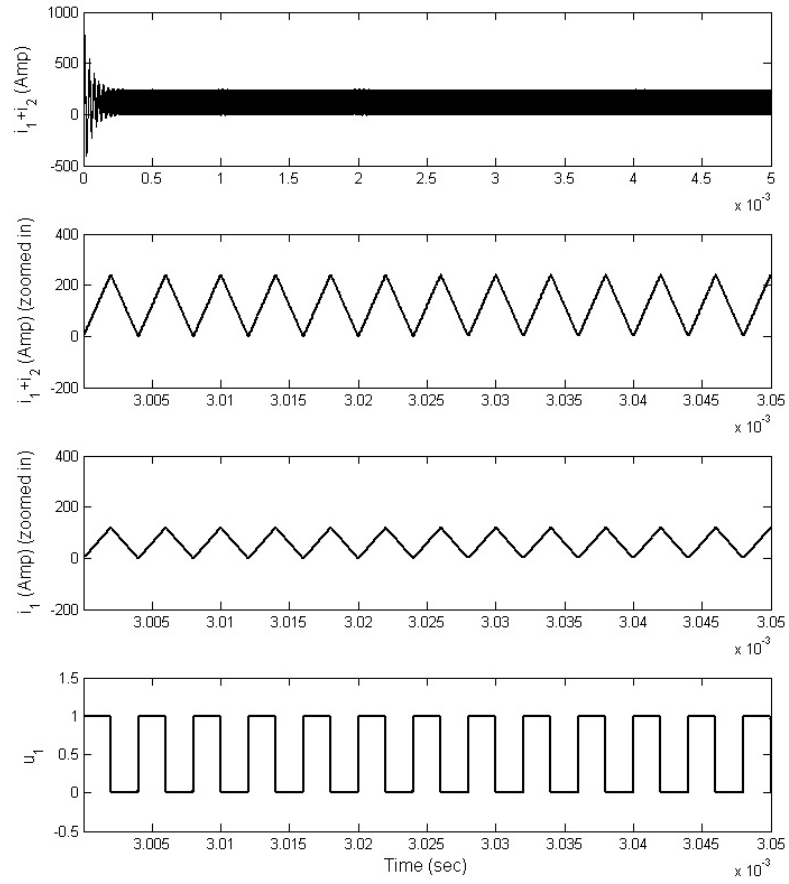
Figure 1.4: Simulated responses from the two-phase DC to DC converter depicted in (1.3) when $u_1 = u_2$.

equal. Then it is obvious that currents in two phases are equal as well ($i_1 = i_2$), and the sum of them will simply be $2i_1$. However, if the second switching u_2 is phase-sifted by half of its period from the first switching u_1, the current i_2 will also be shifted from i_1, which may reduce current ripple in the output. As can be seen in Figure (1.5), the output ripple is totally eliminated by the phase-shift for selected parameters. This methodology to cancel out the ripple in the system output is known as "ripple cancellation" or "harmonic cancellation" method [64]-[66]. For some systems such as voltage regulator module (VRM) to supply power for microprocessors, it may be extremely important to maintain the amplitude of output oscillation at a certain requirement. Of course, the amplitude of the ripple can be reduce if larger inductance L is used. However, using larger inductance may slow down the system response, so it is desired to have small inductance if possible. Thus, the ripple cancellation enables the use of small inductance while it suppresses oscillations in the output current or voltage, which may bring wider range of voltage deviation during the load is varying. One of the attempts to apply this idea have been made such that phases are interconnected so phase shift between phases could be controlled correspondingly, which generally is based on using transformer with primary and secondary coils in different phases. It has used to be related to the converter using PWM control schematic with fixed frequency [67]. The other conventional approaches to suppress ripple in systems with PWM are also based on multiphase channels providing desired phase shifts using delay, filters, set of triangular inputs with selected delays [63]-[65].

For sliding mode implementation, a new methodology to suppress output ripple will be proposed in chapter 4 of this dissertation. The approach stems from the nature of multidimensional sliding mode control with hysteresis loop in switching elements, and it lets the designer have desired phase shift between phases for any frequencies. The method does not need any additional dynamic components such as
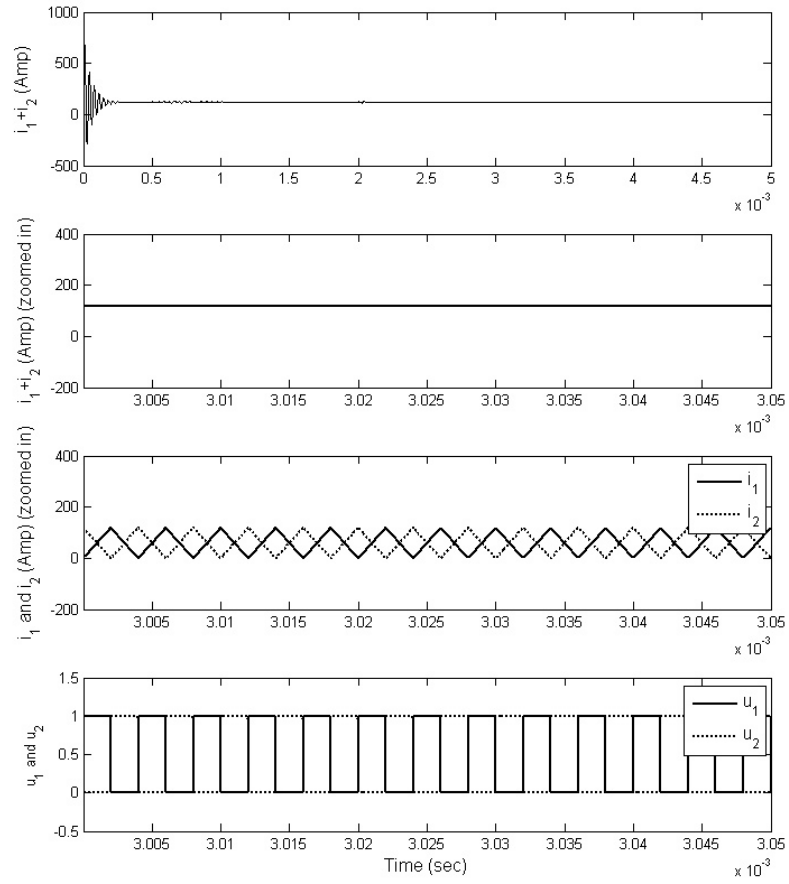
Figure 1.5: Simulated responses from the two-phase DC to DC converter depicted in (1.3) when u_2 is shifted from u_1 by T/2.

transformers, filters, or time delays. A similar research on sliding mode control with ripple cancelation has been done [62]; however, the method in the paper is to use specially designed sliding surfaces, which is different from the method proposed in this dissertation based on adaptive width of hysteresis and multidimensional sliding mode.

This dissertation provides:

- analysis of chattering phenomenon using describing function method to estimate amplitude and frequency of the oscillation in the presence of unmodeled dynamics

- development of a new chattering reduction methodology based on state-dependent switching gain and equivalent-control-dependent gain

- chattering frequency control using hysteresis loop and chattering suppression method using phase shift for sliding mode control in systems under switching frequency limitation.

CHAPTER 2

CHATTERING ANALYSIS

This chapter analyzes the chattering phenomenon analytically using the describing function method. Before the analysis is performed, the system behavior with discontinuous control in the presence of unmodeled dynamics is studied. As mentioned in previous chapter, these unmodeled dynamics are from sensors and/or actuators which have small time constants, and they are often omitted in the principal modeling process since they are significantly faster than the plant dynamics.

2.1   The chattering in the presence of Unmodeled Dynamics

Let us consider the following second-order system as an example.

$$
\begin{aligned}
\dot{x}_1 &= x_2 \\
\dot{x}_2 &= ax_1 + bx_2 + c\sin x_1 + du
\end{aligned}
\tag{2.1}
$$

where a and b are negative constants while c and d have positive constant values. The system is known to be unstable for $c > |a|$. It is assumed that there exist fast dynamics for the actuator, which is stable. They are not taken into account in the

ideal model and governed by the equations

$$
\begin{aligned}
w_1 &= w \\
\dot{w}_1 &= w_2 \\
\dot{w}_2 &= -\frac{1}{\mu^2}w_1 - \frac{2}{\mu}w_2 + \frac{1}{\mu^2}u.
\end{aligned}
\tag{2.2}
$$

The constant μ is regarded as a sufficiently small, positive constant. In the presence of actuator unmodeled dynamics, the actual input to the system is $w(t)$, not $u(t)$ directly from sliding mode controller as can be seen in Figure (2.1). The control input and the sliding surface are chosen as

$$
\begin{aligned}
u &= -Msign(\sigma) \\
\sigma &= \lambda x_1 + x_2
\end{aligned}
\tag{2.3}
$$

where λ and M are positive constants, and M must be sufficiently large to enforce sliding mode in the ideal model ($\dot{\sigma}\sigma < 0$). In real system, the sliding mode cannot be expected to occur since $\dot{x}$ becomes a continuous time function, thus, chattering will be caused. In accordance with the *singular perturbation theory* [50][51], in systems

with continuous control, a fast component of the motion decays rapidly while a slow component depends continuously on the small time constants [52]. In discontinuous control systems the solution depends on the small parameters continuously as well, but, unlike continuous systems, the switching in control excites the unmodeled dynamics, which leads to oscillations in the state at high frequency. Figure (2.2) shows the chattering of the system depicted in Figure (2.1) Because of the second-order actuator dynamics, the actual input $w(t)$ is different from the intended input $u(t)$, thus the output $x(t)$ oscillates with an amplitude of μ-order, and the oscillation occurs in the vicinity of the switching surface. Actually, the system shown in Figure (2.1) is
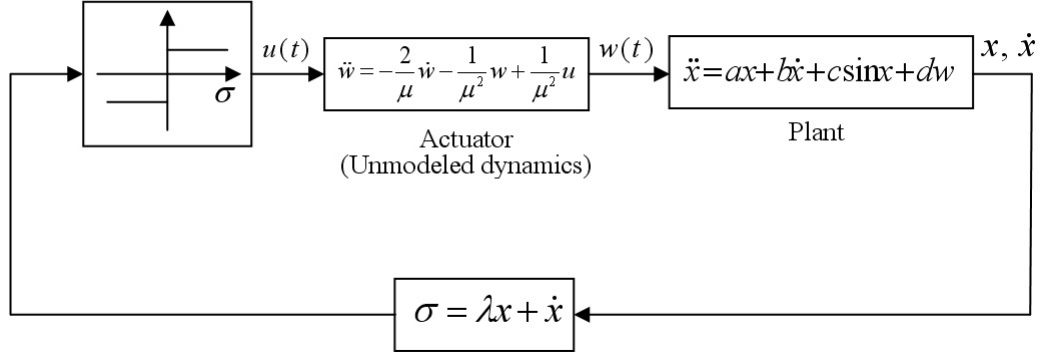
Figure 2.1: An example system: sliding mode control for for system (2.1). There are actuator dynamics which were not included in the ideal system. The high frequency switching action excites these unmodeled dynamics, which causes chattering.

close to a high-gain system with relative degree of 3 since it consists of second-order plant and actuator. Thus, by assuming that $c = 0$ and $d = 1$ for simplification, dynamics of the plant (2.1) and the actuator (2.2) can be combined together to be written as

$$
\begin{aligned}
\ddot{x} &= b\dot{x} + ax + w \\
\ddot{w} &= -\frac{2}{\mu}\dot{w} - \frac{1}{\mu^2}w + \frac{1}{\mu^2}u \\
\sigma &= \lambda x + \dot{x} \\
u &= -M sign(\sigma).
\end{aligned}
\tag{2.4}
$$

It follows from (2.4), the third time derivative of σ may be found in the form

$$
\begin{aligned}
\sigma_1 &= \lambda x + \dot{x} \\
\sigma_2 &= \dot{\sigma}_1 \\
\sigma_3 &= \dot{\sigma}_2 \\
\dot{\sigma}_3 &= F(x, \dot{x}, w, \dot{w}, \mu, \lambda) + \frac{1}{\mu_2}u, \quad F(0,0,0,0,\mu,\lambda) = 0 \\
u &= -M sign(\sigma_1).
\end{aligned}
\tag{2.5}
$$

21
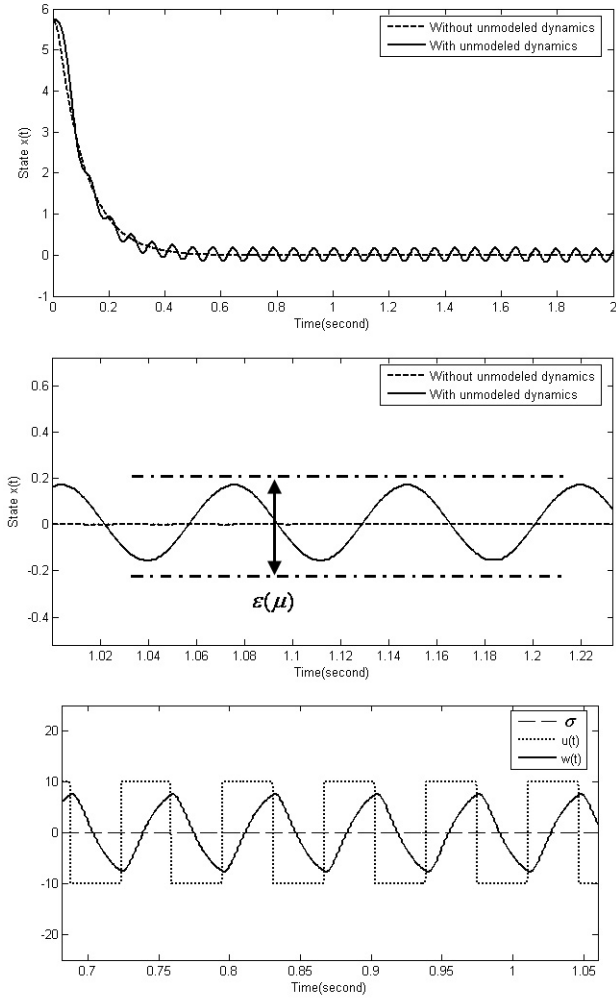
Figure 2.2: Chattering in system (2.1) in the presence of second-order unmodeled dynamics.

22

Since the coordinate transformation from $z = [x, \dot{x}, w, \dot{w}]^T$ to $z^* = [x, \sigma_1, \sigma_2, \sigma_3]^T$ is non-singular, the function $F(x, \dot{x}, w, \dot{w}, \mu, \lambda)$ will be zero also when $x = \sigma_1 = \sigma_2 = \sigma_3 = 0$. From (2.4), the actuator dynamics can be rewritten as

$$
\begin{cases}
w_1 &= w \\
\mu \dot{w}_1 &= w_2 \\
\mu \dot{w}_2 &= -w_1 - 2\mu w_2 + u.
\end{cases}
\tag{2.6}
$$

By considering a Lyapunov function candidate $V = \frac{1}{2}\sigma^2$ for the system (2.5), let us examine convergence of the system trajectory outside a small vicinity ϵ of μ-order around switching surface $\sigma = 0$ where $\epsilon(\mu)$ defines the boundary of chattering. When $\sigma(t)$ is initially outside of ϵ, i.e., $|\sigma(t_0)| > \epsilon$, u is constant for a certain initial time interval $\Delta t = t_1 - t_0$ where t_1 is the time when the first switching happens. Then, since the actuator dynamics are stable with a very small time constant, the output of actuator w in (2.6) converges to its input u within Δt, which makes the time derivative of the Lyapunov function $\dot{V} = \dot{\sigma}\sigma < 0$. It means that the system trajectory converges to ϵ-vicinity. Now, to find the system behavior inside ϵ, the following Lyapunov-like function is selected.

$$
V = \sigma_1 \sigma_3 - \frac{1}{2}\sigma_2^2
\tag{2.7}
$$

Note that the Lyapunov-like function candidate is sign-varying, and the time derivative of the function is

$$
\dot{V} = \sigma_1 F(x, \dot{x}, w, \dot{w}, \mu, \lambda) - \frac{1}{\mu^2}M|\sigma_1|.
\tag{2.8}
$$

The function $\dot{V}$ is negative for the domain $|F| < \frac{1}{\mu^2}M$, which means that the behavior of the system is unstable inside ϵ-vicinity around the sliding surface $\sigma = 0$.

The analysis of system behavior is now extended to a general case. Let us consider the following system as depicted in Figure (2.3) (a)

$$
\begin{aligned}
\dot{x} &= Ax + Bw \quad (x \in \Re^n, w \in \Re^m) \\
u &= -Msign(\sigma), \quad \sigma = Cx \quad (C \in \Re^{m \times n})
\end{aligned}
\tag{2.9}
$$

where w is the output from unmodeled dynamics of actuators as previously. Since the given system is linear, it is possible to represent an equivalent system shown in Figure (2.3) (b) as follows

$$
\begin{aligned}
\dot{x} &= Ax + Bu \quad (u \in \Re^m) \\
u &= -Msign(\sigma^*)
\end{aligned}
\tag{2.10}
$$

and $\sigma = Cx$ is now the input to the unmodeled dynamics block while σ^* is the output from the block. If the gain M is selected properly, then sliding mode occurs in the system without the unmodeled dynamics. Suppose that the unmodeled dynamics in the system may be written as follows

$$
\begin{aligned}
\mu^2 \ddot{z} + \mu D\dot{z} + z = R\sigma \quad (z \in \Re^k, \ R \in \Re^{k \times m} \ D \in \Re^{k \times k}, \ k > m) \\
\sigma^* = Qz, \quad QR = I \quad (Q \in \Re^{m \times k})
\end{aligned}
\tag{2.11}
$$

with $\mu \ll 1$. Then, (2.11) may be also represented in a state-space form

$$
\begin{cases}
z_1 &= z \\
\mu\dot{z}_1 &= z_2 \\
\mu\dot{z}_2 &= -\mu D z_2 - z_1 + R\sigma.
\end{cases}
\tag{2.12}
$$

Since σ is the output of plant dynamics with bounded input, its time derivative $d\sigma/dt = \dot{\sigma}$ is also bounded. Thus, the conventional singular perturbation theory is

24
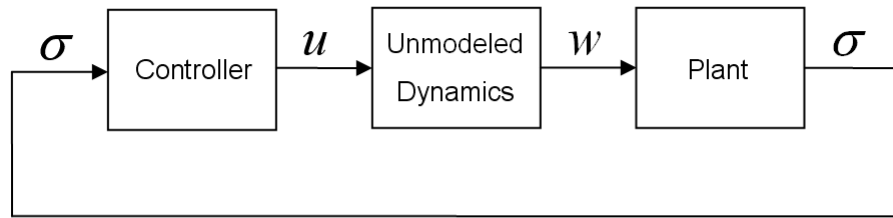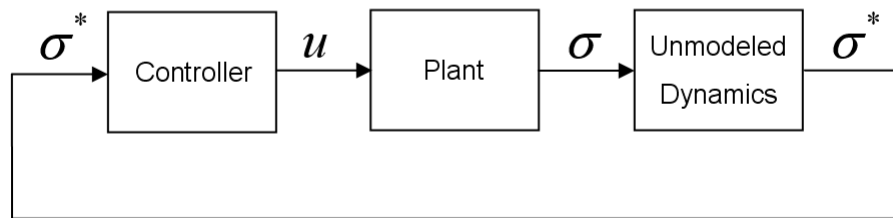
Figure 2.3: Block diagrams of systems with unmodeled dynamics. The two systems (a) and (b) are equivalent when they are linear.

again applicable to (2.12), which implies that after a finite time interval Δt ($\Delta t \to 0$ with $\mu \to 0$), the variable $z = z_1$ converges into a small vicinity of $R\sigma$, i.e.

$$z_1 = R\sigma + \varepsilon_1(\mu, t) \tag{2.13}$$

and

$$\sigma^* = Qz_1 = \sigma + \varepsilon_2(\mu, t) \tag{2.14}$$

where $\varepsilon_1(\mu, t)$ and $\varepsilon_2(\mu, t)$ tend to zero as $\mu \to 0$. It implies that $Msign(\sigma) = Msign(\sigma^*)$ beyond the vicinity $\varepsilon(\mu)$ of $\sigma = 0$, and all the state trajectories are converging into the vicinity.

Now, stability of the system inside the $\varepsilon(\mu)$-vicinity is analyzed. Let us consider the system (2.9) shown in Figure (2.3) (a). Similarly, as assumed in (2.11), the unmodeled dynamics with $\mu \ll 1$ become

$$\mu^2 \ddot{z} + \mu D \dot{z} + z = Ru, \quad w = Qz \quad (u, \, w \in \Re^m) \tag{2.15}$$

where u is the input to the unmodeled dynamics, and w is the input to the plant. It may be rewritten in a state-space form as follows

$$\begin{cases} z_1 & = & z \\ \dot{z}_1 & = & z_2 \\ \dot{z}_2 & = & -\frac{1}{\mu^2} z_1 - \frac{1}{\mu} D z_2 + \frac{1}{\mu^2} Ru. \end{cases} \tag{2.16}$$

The desired eigenvalues of ideal sliding mode can be placed, and $CB = I$ [1]. Then,

26

from (2.16), the third time derivative of $\sigma_1 = \sigma$ may be found as

$$
\begin{aligned}
\dot{\sigma}_1 &= \sigma_2 = CAx + w \\
\dot{\sigma}_2 &= \sigma_3 = CA^2x + CABw + Qz_2 \\
\dot{\sigma}_3 &= CA^3x + CA^2BQz_1 + CABQz_2 + Q\dot{z}_2 \\
&= H(x, z_1, z_2) + \frac{1}{\mu^2}\{-Qz_1 - \mu QDz_2 - Msign(\sigma)\}.
\end{aligned}
\tag{2.17}
$$

To show that the origin in the subspace $(\sigma_1^T, \sigma_2^T, \sigma_3^T)$ is unstable, let us select a sign-varying Lyapunov-like function as follows

$$
V = \sigma_1^T \sigma_3 - \frac{1}{2}\sigma_2^T \sigma_2.
\tag{2.18}
$$

The time derivative of (2.18) can be written as

$$
\begin{aligned}
\dot{V} &= \frac{1}{\mu^2}\sigma_1^T\{\mu^2 H(x, z_1, z_2) - Qz_1 - \mu QDz_2 - Msign(\sigma_1)\} \\
&\leq \frac{1}{\mu^2}|\sigma_1|\{\mu^2|H(x, z_1, z_2)| + |Qz_1| + \mu|QDz_2| - M\}.
\end{aligned}
\tag{2.19}
$$

If it is assumed that sliding mode occurs on $\sigma = 0$, then the control u in (2.16) can be substituted by u_{eq} (solution to $\dot{\sigma} = 0$ with respect to u and $|u_{eq}| < M$ [1]). Therefore, as follows from the singular perturbation theory again, z_1 becomes

$$
z_1 = Ru_{eq} + \varepsilon_3(\mu, t)
\tag{2.20}
$$

and

$$
|Qz_1| = |u_{eq} + \varepsilon_4(\mu, t)| < M.
\tag{2.21}
$$

From (2.19) and (2.21), $\dot{V} < 0$ for small μ while V is sign-varying, which means that the point $(\sigma_1^T, \sigma_2^T, \sigma_3^T) = 0$ in $3m$ dimensional space is unstable. If, at initial time,

$V(0)$ is negative, then this trajectory leaves the small vicinity of μ-order around $\sigma = 0$ since $\dot{V} < 0$. It can be seen from (2.19) that $\dot{V} = 0$ when $\sigma = 0$, but those points are isolated if $(\sigma_1^T, \sigma_2^T, \sigma_3^T) \neq 0$. Thus, the assumption on existence of sliding mode is not correct.

Considering the system behavior inside and outside the $\varepsilon(\mu)$-vicinity, it is concluded that all the state trajectories are converging into the vicinity of sliding manifold $\sigma(t) = 0$, however, the origin of the subspace σ is unstable, and it confirms that the chattering appears in the system with unmodeled dynamics. In the design of the control, it is not possible to consider all the system dynamics including the dynamics of sensors and actuators, i.e. the mathematical models may not perfectly represent the real system usually. Therefore, there always exists the possibility for control engineers to be irritated by the chattering when sliding mode controllers are implemented.

2.2   Describing function method for chattering analysis

For analyzing the influence of mismatches in modeling resulting from neglecting the small time constants of actuators and sensors, the describing function method can be used to estimate the amplitude and frequency of the chattering. Intuitively, the amplitude of the chattering can be related to the value of the constant M somehow where the control input u is either $u^+ = M$ or $u^- = -M$ $(M > 0)$ since larger control action may cause bigger amplitude of chattering.

Let us consider a system with a scalar control

$$
\begin{aligned}
\dot{x} &= f(x) + lu, \quad (x, l \in \Re^n) \\
\sigma &= \sigma(x) \\
u &= -M \operatorname{sign}(\sigma). \quad (M > 0)
\end{aligned}
\tag{2.22}
$$

Then, the time derivative of σ can be written as

$$
\dot{\sigma} = Gf + Glu, \quad G = \left\{ \frac{\partial \sigma}{\partial x} \right\}^T.
\tag{2.23}
$$

When chattering occurs at high frequency, the terms Gf and Gl in (2.23) may be considered to be constant since the system states can be regarded as constant values for a short time interval. Thus, the system in (2.22) becomes

$$
\dot{x} = a + bu \quad (x \in \Re^n)
\tag{2.24}
$$

where the vectors a and b are constant. The system (2.24) is now used to analyze chattering qualitatively. For simplicity, the sliding surface is selected as a linear one

$$
\sigma(x) = cx = 0
\tag{2.25}
$$

where c is a $1 \times n$ row vector with constant elements. Then the control input u becomes $u = -M \operatorname{sign}(cx)$.

Now, let us consider certain sensor dynamics disregarded in ideal model. These unmodeled dynamics are assumed to be linear with small time constant μ, whose state is characterized by an intermediate state vector z $(z \in \Re^m)$ and the state vector x is

regarded as an input to the following subsystem

$$\mu \dot{z} = Az + Bx. \tag{2.26}$$

The time constant μ is a sufficiently small, positive value and A and B are $m \times m$ and $m \times n$ matrices, respectively. The matrix A is assumed to be stable. Instead of the system state vector x, sliding mode controller uses an alternative vector x^* ($x^* \in \Re^n$) which is a linear combination of the elements in the sensor state vector z as follows, and the system configuration is illustrated in Figure (2.4).

$$x^* = Hz \tag{2.27}$$

where H is a constant $n \times m$ matrix which indicates measurement of the sensor. Since the controller is using x^*, not the vector x directly from the plant, the sliding mode surface (2.25) now becomes

$$\sigma^* = cx^* \tag{2.28}$$

with a $1 \times n$ row vector c. With this alternative switching surface, the system (2.24) changes to the following:

$$\dot{x} = a + bu^*, \ u^* = -Msign(\sigma^*). \tag{2.29}$$

 The entire system including sensor dynamics is, again, depicted in Figure (2.4). In static mode, when the left hand side of equation (2.26) is zero, i.e., $\dot{z} = 0$, the vector x^* should follow the state x without any distortion. Therefore, from (2.26) and (2.27),
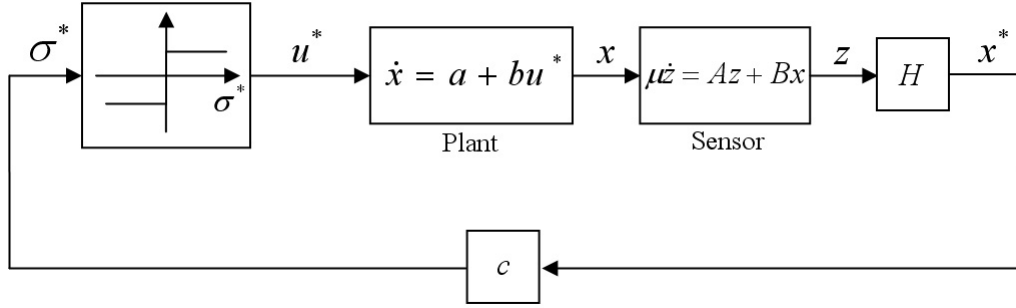
Figure 2.4: The system has fast dynamics (small value of μ) which are not included in the ideal plant model.

relationship between x and x^* becomes

$$x^* = -HA^{-1}Bx \qquad (2.30)$$

and the following equality can be found

$$-HA^{-1}B = I. \qquad (2.31)$$

Note that A^{-1} exists since the unmodeled dynamics are assumed to be stable.

The describing function method is an approximation procedure for analyzing oscillations in nonlinear systems, which may be useful to estimate the magnitude and frequency of chattering. For applying the describing function method, the system (2.26)-(2.29) should be represented in terms of transfer functions due to the nature of the methodology

$$\Sigma^*(s) = cX^*(s) = cHZ(s)$$
$$= cH(\mu sI - A)^{-1}\left\{B\frac{a}{s^2} + B\frac{b}{s}U^*(s) + B\frac{x(0)}{s} + \mu z(0)\right\} \qquad (2.32)$$

where $\Sigma^*(s) = \mathscr{L}\{\sigma^*(t)\}$ and $U^*(s) = \mathscr{L}\{u^*(t)\}$ while $x(0)$ and $z(0)$ are initial conditions. In compliance with the describing function method, the inverse Laplace transformation of (2.32) is assumed to be a harmonic function plus a constant as illustrated in Figure (2.5)

$$\sigma^* = \alpha + \beta \sin \omega t \quad (\alpha < \beta) \tag{2.33}$$

where α, β, and ω are constants. Then, the first two terms of the Fourier expansion of the input function $u^* = -M sign(\sigma)$ can be found as follows

$$
\begin{aligned}
u^* &= u_0^* + u_1^* \sin \omega t \\
u_0^* &= \frac{\omega}{2\pi} \int_0^{2\pi/\omega} u^*(t)dt = -\frac{2}{\pi} M \sin^{-1} \frac{\alpha}{\beta} \\
u_1^* &= \frac{\omega}{\pi} \int_0^{2\pi/\omega} u^*(t) \sin \omega \; t dt = -\frac{4M}{\pi} \cos(\sin^{-1} \frac{\alpha}{\beta}) \\
&= -\frac{4M}{\pi} \sqrt{1 - \left(\frac{\alpha}{\beta}\right)^2}.
\end{aligned}
\tag{2.34}
$$

By substituting $\Sigma^*(s)$ and $U^*(s)$ under assumption of zero time constant μ for simplicity, (2.32) becomes

$$\Sigma^*(s) = \frac{\alpha}{s} + \frac{\beta\omega}{s^2 + \omega^2} = -HA^{-1}B \left\{ \frac{ca}{s^2} + \frac{cb}{s^2} u_0^* + \frac{cb}{s} \left(\frac{\omega u_1^*}{s^2 + \omega^2} \right) + \frac{x(0)}{s} \right\}. \tag{2.35}$$

Note that $-HA^{-1}B$ should be an identity matrix from (2.31). For equality, the term $1/s^2$ in the left hand side of the equation must be eliminated, thus the coefficient of the term should be equal to zero. Therefore, the constant component of the function u^* is determined as

$$u_0^* = -\frac{ca}{cb} \tag{2.36}$$

32
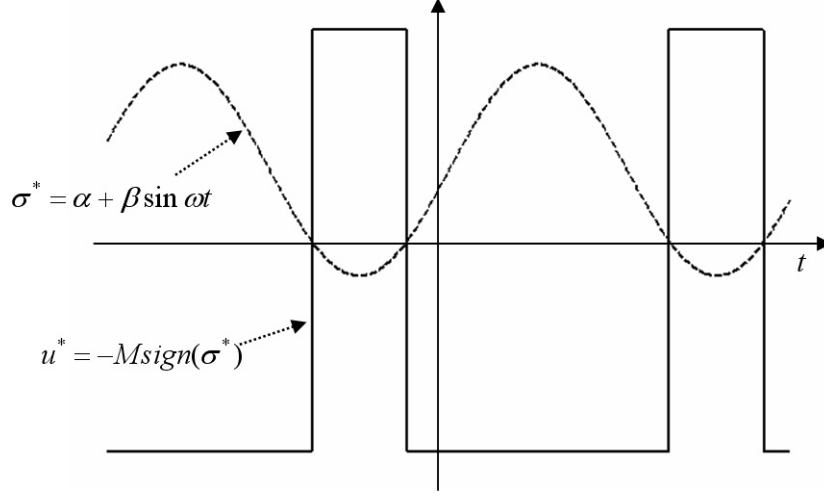
Figure 2.5: The sliding surface σ^* and corresponding control input u^* when σ^* is assumed to be a sinusoidal function in compliance with the procedure of the describing function method.

which is the well-known *equivalent control* [7] because it is nothing but the solution to the following equation from (2.28) and (2.29) with respect to u_{eq} when $x = x^*$

$$\dot{\sigma} = c\dot{x} = ca + cbu_{eq} = 0. \tag{2.37}$$

From (2.34) and (2.36), the coefficient for the first harmonic becomes

$$u_1^* = -\frac{4M}{\pi} \cos\left(\frac{ca}{cb}\frac{\pi}{2M}\right). \tag{2.38}$$

From (2.36) and (2.38), the behavior of the system (2.29) can be written in the form

$$\dot{x} = a + bu^* = a + b(u_0^* + u_1^* \sin \omega t) = a - b\frac{ca}{cb} - b\left\{\frac{4M}{\pi} \cos\left(\frac{ca}{cb}\frac{\pi}{2M}\right)\right\} \sin \omega t. \tag{2.39}$$

33

Therefore, it can be seen from the equation that the amplitude of chattering depends on the value of M; the larger M, the bigger the oscillation amplitude in the chattering, and it confirms the simulation results in Figure (2.6). The methodology is to find the effect of the switching gain M when μ is fixed, so it is assumed that μ is zero in the middle of the process, thus, the result (2.39) does not depend on μ. However, the amplitude must be related to the change of μ as well because it is intuitively expected that larger time constant in unmodeled dynamics would lead to bigger amplitude of oscillations with discontinuous control.

By neglecting $1/s^2$ term and initial conditions in (2.32), the phase of the first harmonic in the input and the output can be found as follows

$$\arg\left\{cH(\mu j\omega I - A)^{-1}B\frac{b}{s}\right\} = \arg\left\{\frac{\Sigma^*(j\omega)}{U^*(j\omega)}\right\} = \pm k\pi \quad (k = 1, 3, 5, \ldots) \qquad (2.40)$$

since $\sigma(t)$ and $u(t)$ always have different signs. The equation (2.40) gives

$$-\frac{\pi}{2} + \arg\left\{cH(j\omega^* I - A)^{-1}Bb\right\} = \pm k\pi \quad (k = 1, 3, 5, \ldots) \qquad (2.41)$$

where $\omega^* = \mu\omega$. If it is assumed that the equation (2.41) always has a solution for ω^*, the solution $\tilde{\omega}$ can be written as

$$\omega = \frac{\tilde{\omega}}{\mu} \qquad (2.42)$$

which makes (2.39)

$$\dot{x} = a - b\frac{ca}{cb} - b\left\{\frac{4M}{\pi}\cos\left(\frac{ca}{cb}\frac{\pi}{2M}\right)\right\}\sin\frac{\tilde{\omega}}{\mu}t \qquad (2.43)$$

and it can be said that the frequency of chattering increases as the time constant

μ decreases, and it has nothing to do with the switching gain M. It can be seen in Figure (2.6), the frequency of chattering does not change as the gain M changes. And the simulated result in Figure (2.7) verifies that the chattering frequency is inversely proportional to μ as it shows that the frequency is doubled as μ is reduced to half.

In this chapter, using describing function method it is shown that the magnitude and the frequency of chattering depend on the switching gain of sliding mode control and the time constant of unmodeled dynamics. Since higher amplitude of the chattering is caused by larger magnitude of discontinuous control, a way of chatter reduction is by reducing the magnitude but such that a sliding mode still exists. Based on this idea, methodologies to reduce chattering using time-varying switching gain are proposed in the following chapter.
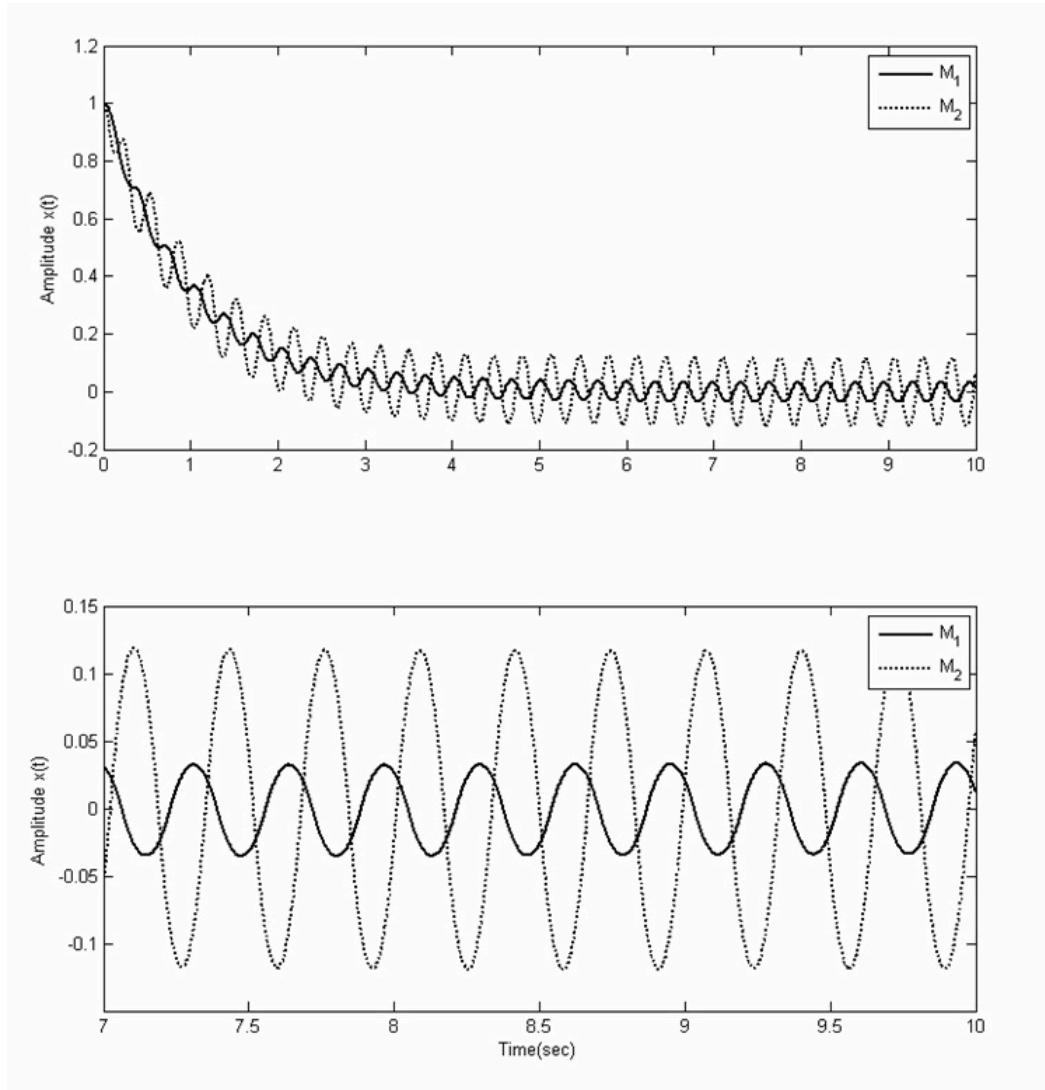
Figure 2.6: Simulation results for the system in Figure (2.4). The plots are the state x_1 versus time. With a fixed μ, it can be seen that the amplitude of chattering depends on the value M ($M_1 < M_2$).
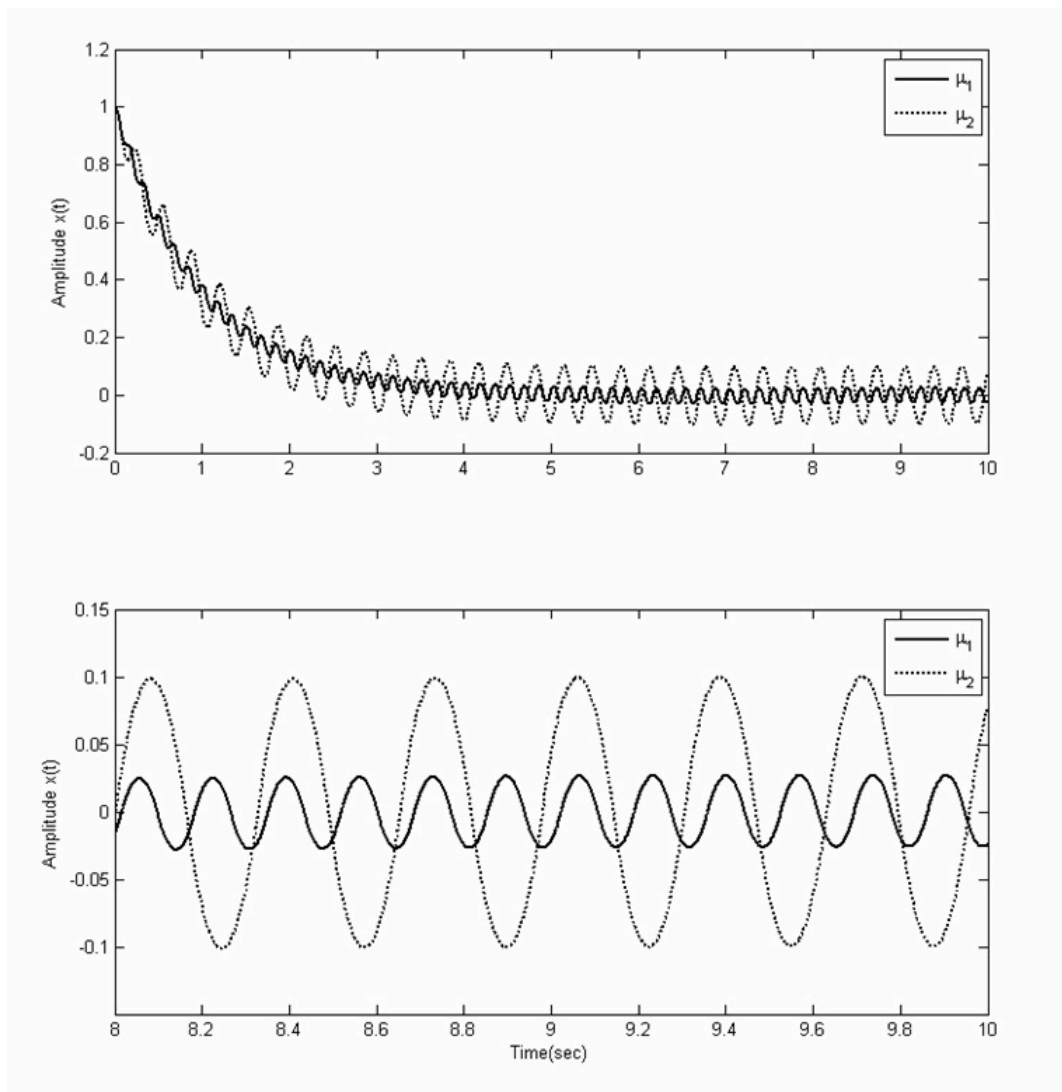
Figure 2.7: Simulation results for the system in Figure (2.4). The switching gain M is fixed and $\mu_1 = \mu_2/2$ The chattering in x_1 with μ_2 shows about twice higher frequency than the one with μ_1.

CHAPTER 3

CHATTERING REDUCTION BASED ON TIME-VARYING SWITCHING GAIN

3.1 State-dependent gain method

This chapter provides methodology to suppress chattering without designing an additional dynamic system such as asymptotic observers. In the previous chapter, it was analytically studied that the magnitude of chattering is proportional to the switching gain of sliding mode control. Thus the methodology for decreasing chattering issued by unmodeled dynamics is to reduce the magnitude of the switching gain while the existence of sliding mode is preserved. The idea which uses time-varying switching gain was actually originated from the principle design idea in variable structure systems [7].

Let us consider stabilization for the following second-order system as an example

$$
\begin{aligned}
\dot{x}_1 &= x_2 \\
\dot{x}_2 &= a_1 x_1 + a_2 x_2 + u.
\end{aligned}
\tag{3.1}
$$

To stabilize the system a standard sliding mode controller may be designed as follows

$$\sigma = cx_1 + x_2$$

$$u_1 = -M_0 sign(\sigma) \tag{3.2}$$

where c is a positive constant. It is obvious that a constant gain M_0 should be selected such that sliding mode exists. The time derivative of the sliding variable σ is found as

$$\dot{\sigma} = c\dot{x}_1 + \dot{x}_2 = (a_1 - ca_2 - c^2)x_1 - M_0 sign(\sigma) \tag{3.3}$$

with $x_2 = cx_1$ when $\sigma = 0$, and the domain of sliding becomes

$$|x_1| < \frac{M_0}{|a_1 - ca_2 - c^2|}. \tag{3.4}$$

It can be seen that σ and $d\sigma/dt$ have different signs for the domain (3.4).

In order to decrease chattering, the switching gain M_0 is modified as follows. For system stabilization, as the state x_1 approaches to steady-state, the system does not need much control action; therefore, the relay gain may be reduced as x_1 tends to zero, which can lead to lower level of chattering. A modified control is proposed as

$$u_2 = -M_0^*(|x_1| + \delta)sign(\sigma). \tag{3.5}$$

where c and M_0^* are positive constant values and δ is a sufficiently small, positive constant. Note that the gain M is not fixed value but proportional to the state x_1. Again, the constant gain M_0 should be selected to enforce sliding mode to occur along

the switching surface. It may be found analytically from (3.1) and (3.5) that

$$\dot{\sigma} = (a_1 - a_2 c - c^2)x_1 - M_0(|x_1| + \delta)sign(\sigma). \tag{3.6}$$

Thus a sliding mode exists if the following condition holds

$$M_0 \geq |a_1 - a_2 c - c^2|. \tag{3.7}$$

Now the following second-order actuator dynamics are introduced to the system (3.1)

$$
\begin{aligned}
w_1 &= w \\
\dot{w}_1 &= w_2 \\
\dot{w}_2 &= -\frac{1}{\mu^2}w_1 - \frac{2}{\mu}w_2 + \frac{1}{\mu^2}u
\end{aligned}
\tag{3.8}
$$

then, the control input u to the system (3.1) is substituted with w, the output from the actuator. Now it can be said that the system schematic is not different from the one depicted in Figure (2.3)(a). Both controls u_1 and u_2 may stabilize the given system, but the difference is that u_1 uses a fixed switching gain as a standard sliding mode control while u_2 has time-varying one. The term δ is a small constant added to deal with disturbances and uncertainties; $M_0\delta$ must be large enough to overcome them. To handle disturbances, a modified method that eliminates the need of δ will be discussed in later part of this section. Figure (3.1) provides simulation results of the system (3.1) under unmodeled dynamics (3.8). It can be seen that the amplitude of the discontinuous control input is significantly reduced by using the proposed control u_2 comparing to the conventional sliding mode control u_1. It is obvious that the switching gain decreases while x is decreasing, which leads to lower level of chattering.
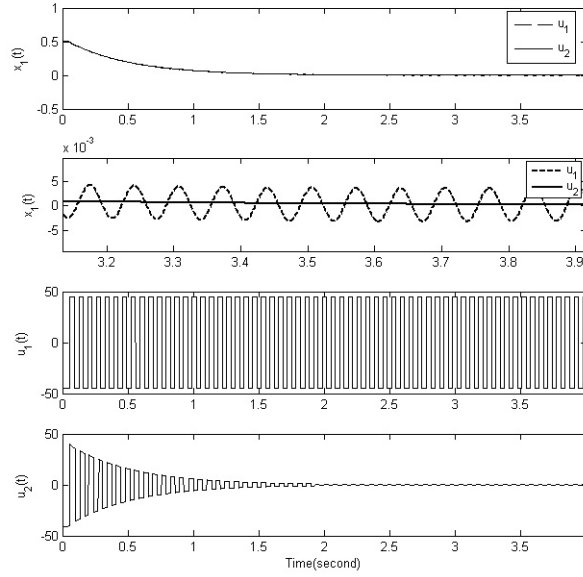
Figure 3.1: Chattering is reduced by using the control input $u_2(t)$ in (3.5).

Thus, in the presence of unmodeled dynamics, chattering arises, but the magnitude of chattering is reduced by using the state-dependent gain $M(x,t)$ as expected.

The proposed controller is tested for a time-varying system which is governed by a nonlinear differential equation

$$\ddot{x} - 10x\dot{x} - 10x\cos x = u. \tag{3.9}$$

In this case, unmodeled dynamics are from sensors, not actuators like in the previous example, and each of the two sensors to read x and $\dot{x}$ have the same structures as given in (3.8) with the time constant $\mu = 0.02$. Two controllers are designed for comparison, which are $u_1 = -5sign(\sigma)$ and $u_2 = -40|x|sign(\sigma)$ where $\sigma = x + \dot{x}$. Simulation results from the system is shown in Figure (3.2). As can be seen, chattering is nearly eliminated by using control u_2. Next, the proposed controller is evaluated
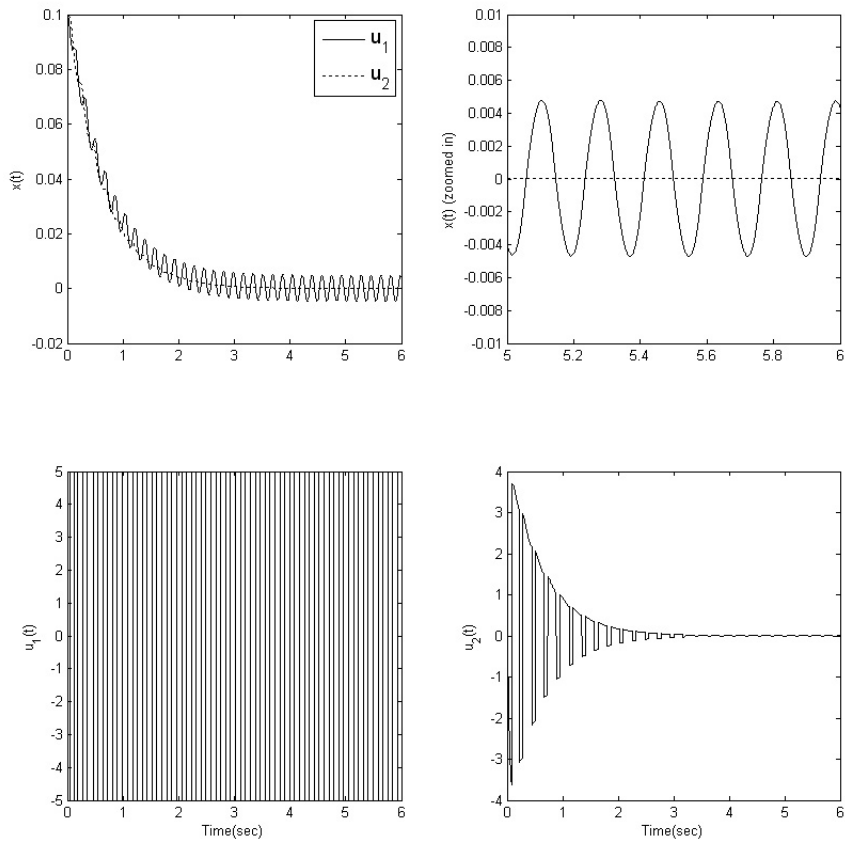
41

Figure 3.2: Chattering is reduced by the proposed control $u_2(t)$ for the system in the presence of two unmodeled sensors.

for a second-order system with two-dimensional vector control:

$$\begin{pmatrix} \dot{x}_1 \\ \dot{x}_2 \end{pmatrix} = \begin{pmatrix} -3 & -1 \\ -5 & 5 \end{pmatrix} \begin{pmatrix} x_1 \\ x_2 \end{pmatrix} + \begin{pmatrix} u_1 \\ u_2 \end{pmatrix} \tag{3.10}$$

and it is assumed that there exist unmodeled dynamics for two actuators associated with control $u = [u_1 \ u_2]^T$ having the same structure as given in (3.8) ($\mu = 0.03$). Two controllers are suggested to stabilize the system

$$
\begin{aligned}
\sigma &= [\sigma_1 \ \sigma_2]^T = [x_1 \ x_2]^T \\
u^1 &= [u_1^1 \ u_2^1]^T = [-M_1 sign(\sigma_1) \quad - M_1 sign(\sigma_2)]^T \\
u^2 &= [u_1^2 \ u_2^2]^T = [-M_2|x_1|sign(\sigma_1) \quad - M_2|x_2|sign(\sigma_2)]^T
\end{aligned}
\tag{3.11}
$$

and it can be seen that u^1 is designed as a standard sliding mode control whereas u^2 adopts a state-dependent gain. It is obvious that $\sigma_i \dot{\sigma}_i < 0$ ($i = 1, 2$) for $M_1 \geq \sup\{|-3x_1 - x_2|, |-5x_1 + 5x_2|\}$ and $M_2 \geq \sup\{|-3x_1 - x_2|/|x_1|, |-5x_1 + 5x_2|/|x_1|\}$, which implies both x_1 and x_2 converges to zero in finite time interval if above inequalities hold. Simulation result is depicted in Figure (3.3), and again, chattering is nearly eliminated by the control u^2. The proposed methodology is applicable to another system written as

$$
\begin{aligned}
\dot{x}_1 &= x_2 \\
\dot{x}_2 &= \sin(x_1) + x_2 + x_3 + u_1 \\
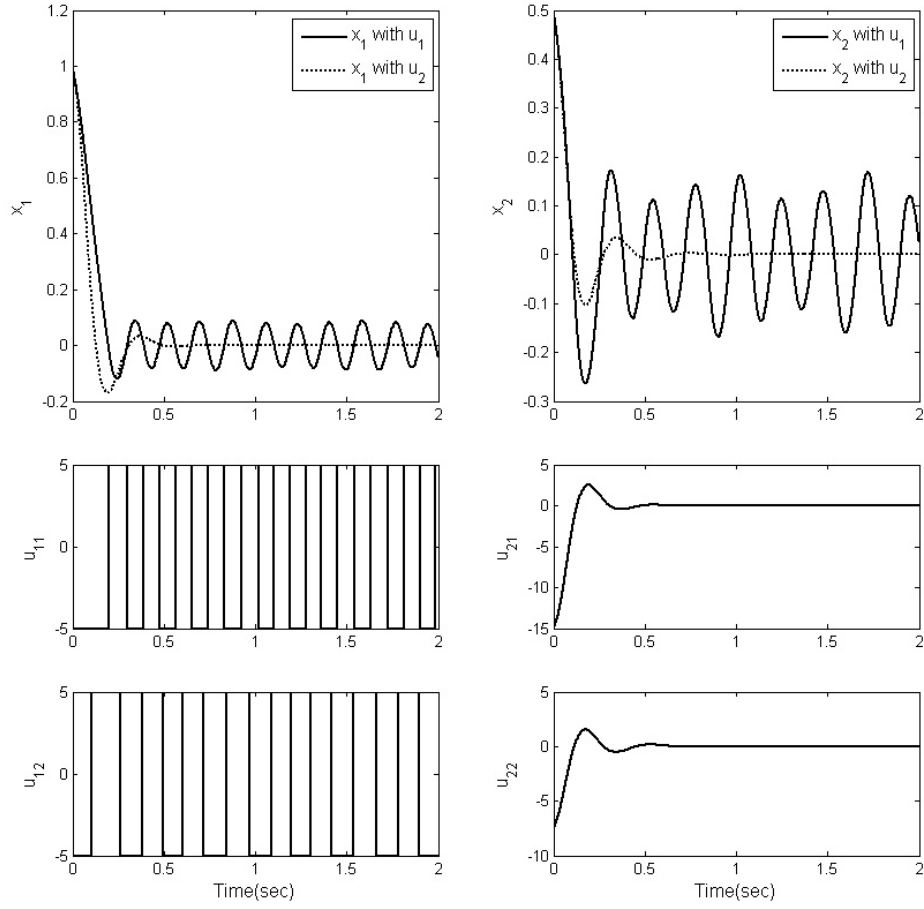\dot{x}_3 &= 2\sin(x_2) + u_2
\end{aligned}
\tag{3.12}
$$

Figure 3.3: The amplitude of chattering is significantly decreased by the control $u^2 = [-15|x_1|sign(x_1) \quad -15|x_2|sign(x_2)]^T$ compared with a standard sliding mode control $u^1 = [-5sign(x_1) \quad -5sign(x_2)]^T$.

and the control $u = [u_1 \ u_2]^T$ is chosen as follows

$$
\begin{aligned}
\sigma_1 &= x_1 + x_2 \\
\sigma_2 &= x_1 + x_2 + x_3 \\
u^1 &= [u_1^1 \ u_2^1]^T = [-M_{11}sign(\sigma_1) \ -M_{12}sign(\sigma_2)]^T \\
u^2 &= [u_1^2 \ u_2^2]^T = [-M_{21}|x_1 + x_2|sign(\sigma_1) \ -M_{22}|x_3|sign(\sigma_2)]^T
\end{aligned}
\tag{3.13}
$$

where M_{ij} $(i, j = 1, 2)$ are positive constant, and u^1 is a standard sliding mode control while u^2 utilizes switching gain adaptation. For control u^1, σ_2 and $\dot{\sigma}_2$ have different signs if $M_{12} > |2x_2 + x_3 + \sin(x_1) + 2\sin(x_2)| + M_{11}$. Then the surface $\sigma_2 = 0$ is reached after a finite time interval which induces the state trajectories to follow the motion $x_3 = -x_1 - x_2$. Thus the second equation in (3.12) becomes $\dot{x}_2 = -x_1 + \sin(x_1) + u_1$, and $\sigma_1\dot{\sigma}_1 < 0$ for $M_{11} > |-x_1 + \sin(x_1)|$, which implies that the system trajectories get to the intersection of two surfaces $\sigma_1 = 0$ and $\sigma_2 = 0$ after a finite time interval. Finally, the system is stabilized since the first equation in (3.12) becomes $\dot{x}_1 = -x_1$. It is obvious that the system behavior with control u^2 may simply be analyzed in a similar manner. Figure (3.4) provides simulation results for the system (3.12) with the proposed controls, and it can be observed that chattering is considerably reduced by using sliding mode control u^2 with gain adaptation.

The chattering problem becomes more serious for the system under disturbances. Let us consider the following systems under a disturbance for an example

$$
\begin{aligned}
\dot{x}_1 &= x_2 \\
\dot{x}_2 &= f(x_1, x_2) + u(t) + h(t)
\end{aligned}
\tag{3.14}
$$

where the function $h(t)$ represents a disturbance which is assumed to be bounded,
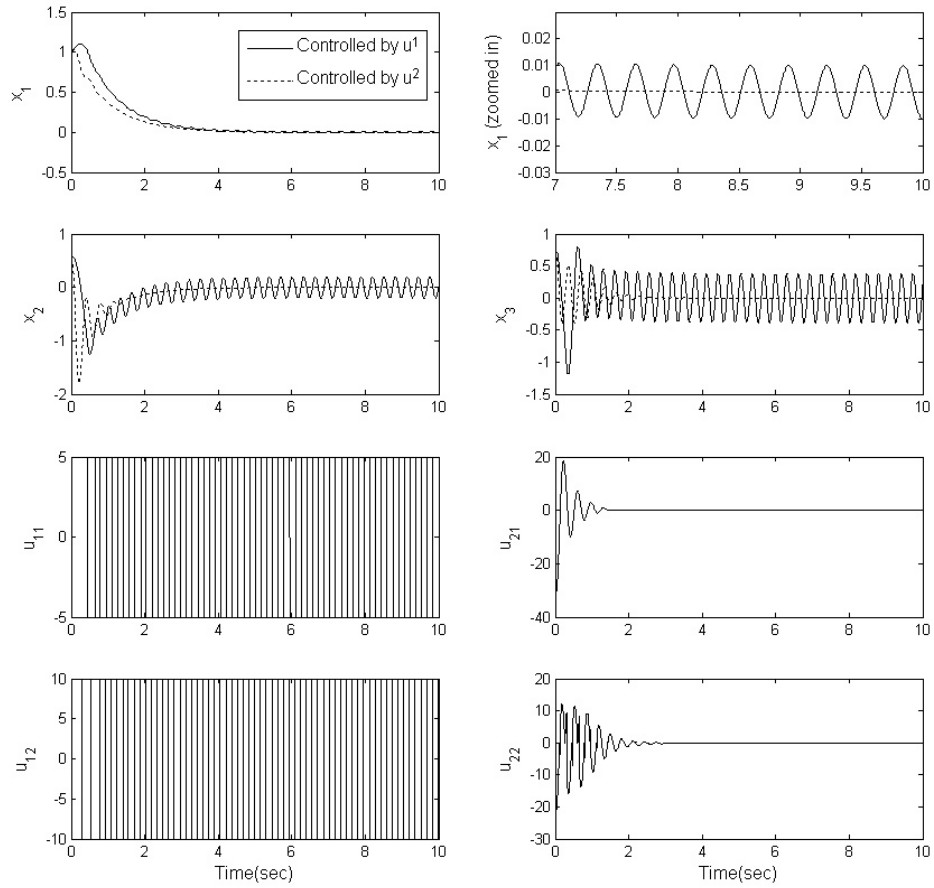
Figure 3.4: The level of chattering is significantly decreased by the control u^2 ($M_{21} = 20, \ M_{22} = 30$) compared with a standard sliding mode control u^1 ($M_{11} = 5, \ M_{12} = 10$) in (3.13).

and $f(x_1, x_2) = 0$ for $x_1 = x_2 = 0$. If there is no unmodeled dynamics, the control

$$u(t) = -Msign(\sigma)$$
$$\sigma = cx_1 + x_2 \ (c > 0)$$

(3.15)

stabilizes the system when the constant gain satisfies the condition $M > |-c^2x_1 + f(x_1, x_2) + h(t)|$ for an ideal sliding mode occurs, which make the state trajectory to move along the surface $\dot{x}_1 = -cx_1$ in a finite time interval. It is noticed that the gain M have larger value than the one under no disturbance since M must suppress the additional term $h(t) \neq 0$, and it apparently causes higher level of chattering in the presence of unmodeled dynamics as analyzed in previous chapter. Moreover, if there exists unmodeled dynamics of actuators, the switching gain should be selected even larger because the actual magnitude of control input to the plant can be smaller than originally designed value as can be seen in Figure (3.5), and it consequently leads to even bigger amplitude of chattering. As proposed earlier in this section, control $u(t)$ may be modified using time-varying relay gain for chattering reduction:

$$u(t) = -M(|x_1| + \delta)sign(\sigma)$$

(3.16)

where δ has a positive constant value. However, with the control (3.16), chattering may not be diminished down to satisfactory level since the term $M\delta$ always needs to be larger than the upper bound of $|h(t)|$, and it still remains after x_1 converges to zero. From (3.15), the time derivative of σ becomes

$$\dot{\sigma} = -c^2x_1 + f(x_1, x_2) + h(t) + u(t).$$

(3.17)

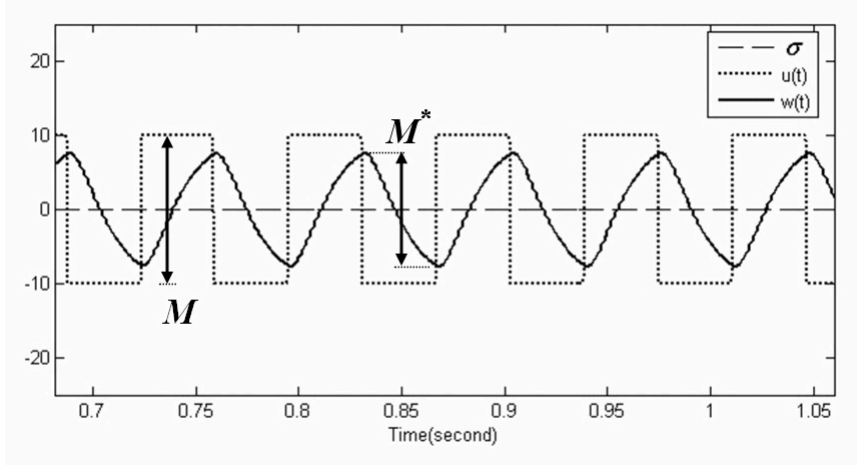If $\delta = 0$, it is found from (3.17) that σ and $\dot{\sigma}$ have different signs if $M > M_{min}$ when

Figure 3.5: The magnitude M^* of the actual input $w(t)$ to the plant is less than M of control $u(t) = -Msign(\sigma)$ because consecutive switching in the input to actuator unmodeled dynamics may occur before the output of the actuator $w(t)$ reaches steady-state. See Figure (2.1) for the system block diagram.

$M_{min} = |-c^2x_1 + f + h|/|x_1|$. It means that $M_{min} \to \infty$ as $|x_1| \to 0$ for $h \neq 0$; In order to enforce sliding mode, M should be infinity, which may not be possible.

Therefore, it is suggested that the control (3.16) is remedied based on disturbance cancelation as follows

$$u(t) = -M|x_1|sign(\sigma) - \tilde{h}(t) \tag{3.18}$$

where $\tilde{h}(t)$ is an estimation of the disturbance function $h(t)$. By assuming that $\tilde{h}(t) \approx h(t)$, $\sigma\dot{\sigma} < 0$ for $M > |-c^2x_1 + f|/|x_1|$ from (3.17), and M is a finite value $(f \to 0$ as $x_1, x_2 \to 0)$. As a solution to the equation $\dot{\sigma} = 0$ the equivalent control of $u(t)$ is written as
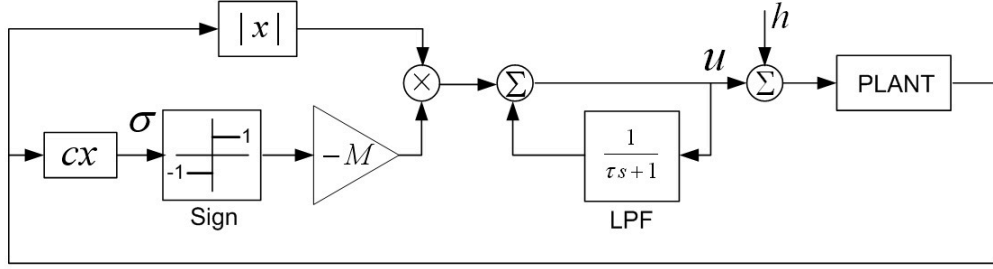
$$u_{eq} = c^2x_1 - f(x_1, x_2) - h(t) \tag{3.19}$$

48

Figure 3.6: The system block diagram with a modified version of state-dependent gain method as suggested in (3.20).

and it can be seen that $u_{eq} \to -h(t)$ as x_1 converges to zero. So, the control $u(t)$ in (3.19) may become

$$u(t) = -M|x_1|sign(\sigma) + u_{eq} \qquad (3.20)$$

and u_{eq} is the average value of discontinuous control $u(t)$ that can be obtained by using a first-order low-pass filter $\tau\dot{\eta} + \eta = u(t)$. The system schematic with control (3.20) is illustrated in Figure (3.6). Figure (3.7) shows simulation results for the following second-order nonlinear system under disturbance

$$\ddot{x} + 20\dot{x}^2 \sin(2x) - 25\dot{x}\sin(3x) = u + h \qquad (3.21)$$

with unmodeled actuator dynamics given in (3.8), and the control laws for the system are

$$
\begin{aligned}
\sigma &= cx + \dot{x} \\
u_1 &= -M_1 sign(\sigma) \qquad\qquad (3.22)\\
u_2 &= -M_2|x|sign(\sigma) + u_{eq}.
\end{aligned}
$$

The control u_1 is a standard sliding mode control while u_2 is designed by suggested methodology of disturbance cancelation. For simulation, parameters are selected as
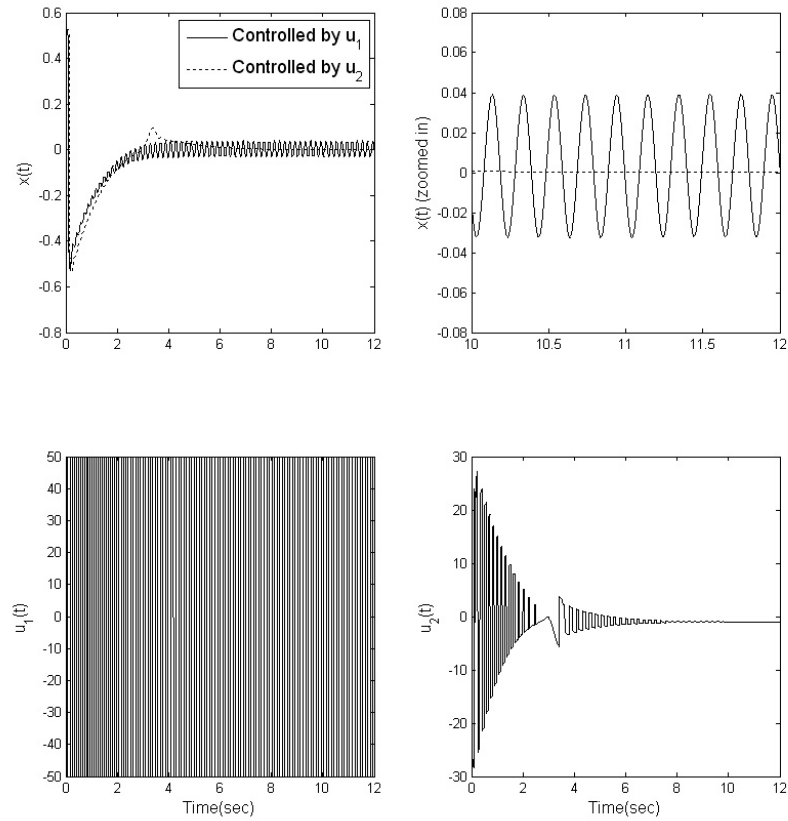
49

Figure 3.7: Simulation results for the system (3.21) with control (3.22).

follows: $M_1 = 50$, $M_2 = 50$, $\mu = 0.03$, $c = 1$, and $h = 1$. The equivalent control u_{eq} is acquired from a first-order low-pass filter having a time constant $\tau = 1.4$. It is observed that u_2 based on disturbance cancelation enables nearly chattering-free system.

The state-dependent gain method may be implemented for the other control tasks. For tracking control of the system (3.1), the following controller may be offered using the state-dependent gain method to substitute a conventional sliding mode

controller

$$e = x_1 - x_d$$

$$\sigma = \lambda e + \dot{e}, \quad (\lambda > 0)$$

$$u = -\{M_0(|e| + \delta) + |a_1 x_d|\} \, sign(\sigma) \qquad (3.23)$$

where the constant x_d is the desired value of x, and δ is sufficiently small, positive constant. M_0 is a constant, which should be large enough to force a sliding mode ($M_0 \geq |a_1 - a_2\lambda - \lambda^2|$). In this case, the gain M depends on the error e. When the control input is bounded as $|u| \leq u_{max}$, we may attach a limiter to modify the control law as follows

$$u^* = \begin{cases} u_{max} & \text{if} \quad u \geq u_{max} \\ -\{M_0(|e| + \delta) + |a_1 x_d|\} \, sign(\sigma) & \text{if} \quad -u_{max} < u < u_{max} \\ -u_{max} & \text{if} \quad -u < -u_{max} \, . \end{cases} \qquad (3.24)$$

Figure (3.8) shows the system behavior using the control law (3.23)-(3.24) ($u_1 = u^*$ and $u_2 = -u_{max} sign(\sigma)$ with the same sliding mode surface σ in (3.23)). Again, the controller proposed in (3.23)-(3.24) engenders smaller magnitude of chattering than standard sliding mode controllers. The methodology proposed in this section can significantly reduce chattering with a simple modification to the conventional design of sliding mode control.

Although the system was confined to examples of low orders, the analysis and design methodology is applicable directly for arbitrary systems. The amplitude and frequency of oscillations can be estimated by the describing function method in chapter 2 which may be applied to a system of an arbitrary order.
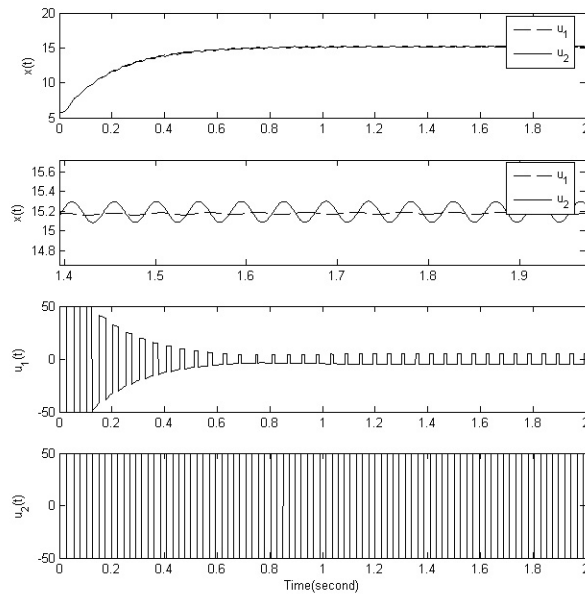
Figure 3.8: Control input $u_1(t)$ with variable gain generates less chattering compared to $u_2(t)$ designed conventionally.

3.2   Equivalent-control-dependent gain method

Actually, any method would be helpful for lessening of chattering if it can cut down the switching gain M effectively. In the previous section, reducing the relay gain M along the system states is suggested. In fact, the gain can be adjusted in other ways, e.g., M may be a function of the equivalent control u_{eq}. In other words, u_{eq} which can be found by using a low pass filter confines the magnitude of discontinuous control. This methodology also looks promising since u_{eq} decreases as sliding mode occurs along the discontinuity surface $\sigma = 0$, in addition, u_{eq} enables to evaluate and cancel disturbances which may exist in the system.

For the simplest first order, arbitrary affine system with scalar control

$$\dot{x} = f(x,t) + bu \quad (x, f, b \in \Re^n) \tag{3.25}$$

a control law is of form

$$\begin{aligned} \sigma &= \sigma(x) \\ u &= -(M_0|\eta| + \delta)sign(\sigma) \end{aligned} \tag{3.26}$$

where M_0 and δ are positive constants, and η is the average value of $sign(\sigma)$ ($\eta = \{sign(\sigma)\}_{eq}$). The system schematic with the proposed controller is illustrated in Figure(3.9). By using a low-pass filter $\tau\dot{\eta} + \eta = sign(\sigma)$ ($\tau =$const.), the average of the discontinuous function $sign(\sigma)$ can be found. Then the time derivative of σ yields

$$\dot{\sigma} = Gf + Gbu = 0. \tag{3.27}$$

where $G = [\partial\sigma/\partial x_1 \ldots \partial\sigma/\partial x_n]$, and it is assumed that $Gb > 0$.
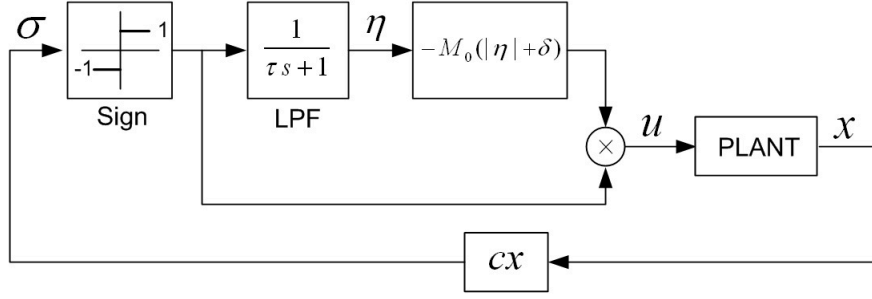
Figure 3.9: A Block diagram for the system with the equivalent-control-dependent gain method.

Theorem. *For the system $\dot{x} = f(x) + bu$ where $u = -(M_0|\eta| + \delta)sign(\sigma)$, sliding mode exists for $M_0 \geq |Gf(x)|/Gb$.*

Proof. From (3.27),

$$\frac{Gf}{Gb(M_0|\eta| + \delta)} = \{sign(\sigma)\}_{eq} = \eta \qquad (3.28)$$

or

$$M_0|\eta|\eta + \delta\eta - g = 0 \quad (g = \frac{Gf}{Gb}) \qquad (3.29)$$

where $\{sign(\sigma)\}_{eq} = u_{eq}/(-M_0|\eta| - \delta)$, and u_{eq} is a solution to $\dot{\sigma} = 0$. If $|\eta| < 1$, sliding mode exists.

(i) If $Gf > 0$ ($\eta > 0$), then (3.29) becomes $M_0\eta^2 + \delta\eta - g = 0$, and $\eta = \frac{-\delta+\sqrt{\delta^2+4M_0g}}{2M_0}$. Since $M_0 \geq g$, $0 < \eta < 1$.

(ii) Similarly, if $Gf < 0$ ($\eta < 0$), then $\eta = \frac{\delta-\sqrt{\delta^2-4M_0g}}{2M_0}$. Since $M_0 \geq -g$, $-1 < \eta < 0$. $\qquad \square$

It means that $|\eta| = |\{sign(\sigma)\}_{eq}| < 1$. Then, (3.27) can be written as

$$
\begin{aligned}
\dot{\sigma} &= Gf - Gb(M_0|\eta| + \delta)sign(\sigma) \\
&= Gb(M_0|\eta| + \delta)[\{sign(\sigma)\}_{eq} - sign(\sigma)].
\end{aligned} \tag{3.30}
$$

Since $|\{sign(\sigma)\}_{eq}| < |sign(\sigma)|$, it is evident that the condition $\dot{\sigma}\sigma < 0$ holds, and sliding mode exists. As the average of $sign(\sigma)$ decreases, the switching gain $M(\eta) = M_0|\eta| + \delta$ lowers.

The simulation results in Figure (3.10) show that the chattering may be successfully decreased by using the suggested method of adjusting the gain M. The simulation is performed for a system $\dot{x}_1 = x_2$, $\dot{x}_2 = 5x_1 + 3x_2 + u$, and a switching variable is selected as $\sigma = 3x_1 + x_2$. Unmodeled dynamics having the structure in (3.8) exist in the simulated system ($\mu = 0.003$). The control $u_1 = -10sign(\sigma)$ has a fixed switching gain, and $u_2 = -30|\eta|sign(\sigma)$ is as proposed in (3.26) where η is obtained using a low-pass filter ($\tau = 1.2$). The result with control u_2 shows almost zero chattering amplitude. Another set of simulation results to compare the proposed controllers is shown in Figure (3.11). The plant dynamics are given as $\ddot{x} + 20\dot{x}^2\cos(2x) - 25\dot{x}\sin(x) = u$, and unmodeled actuator dynamics are the same as (3.8) with $\mu = 0.01$. The sliding variable is chosen as $\sigma = \dot{x} + 2x$. The first and the second control are the same as $u_1 = u_2 = -50sign(\sigma)$, but the second system has an auxiliary observer loop while the first one does not. The third control is $u_3 = -80|e|sign(\sigma)$ when the error $e = x - x_d$ when x_d is desired output. The fourth control is $u_4 = -300|\eta|sign(\sigma)$, and $\eta = \{sign(\sigma)\}_{eq}$ is acquired by a first-order filter. It can be observed in the simulation that the control u_3 and u_4 give similar levels of lowered chattering as the one from the system with an asymptotic observer.
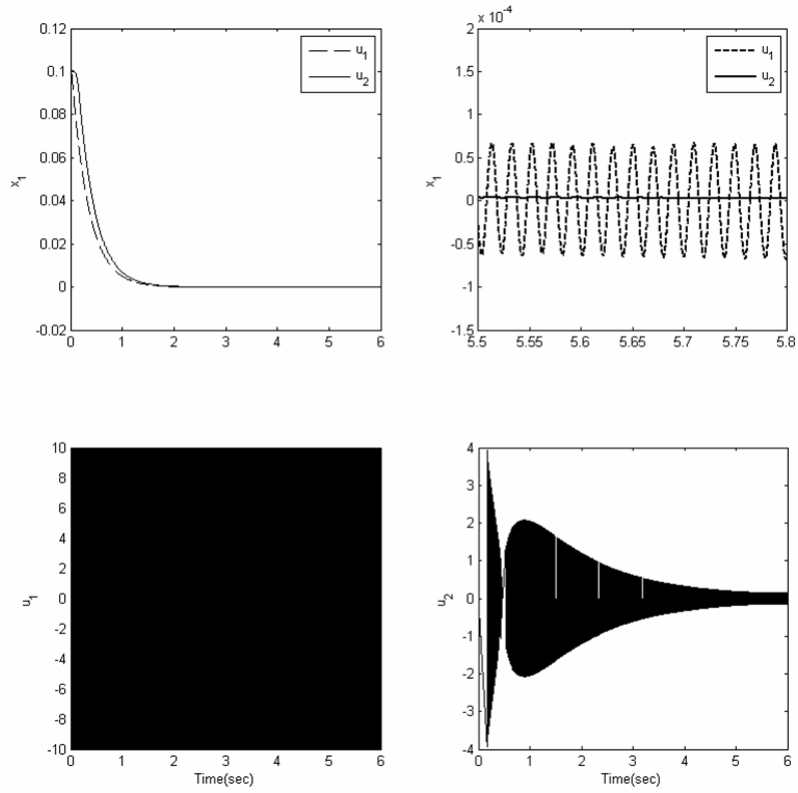
Figure 3.10: Simulation results with the controller proposed in (3.26). The control u_1 is a standard sliding mode control ($u_1 = -10sign(\sigma)$), and u_2 is designed by the proposed methodology using the equivalent control ($u_2 = -30|\eta|sign(\sigma)$). The chattering is significantly reduced with u_2.
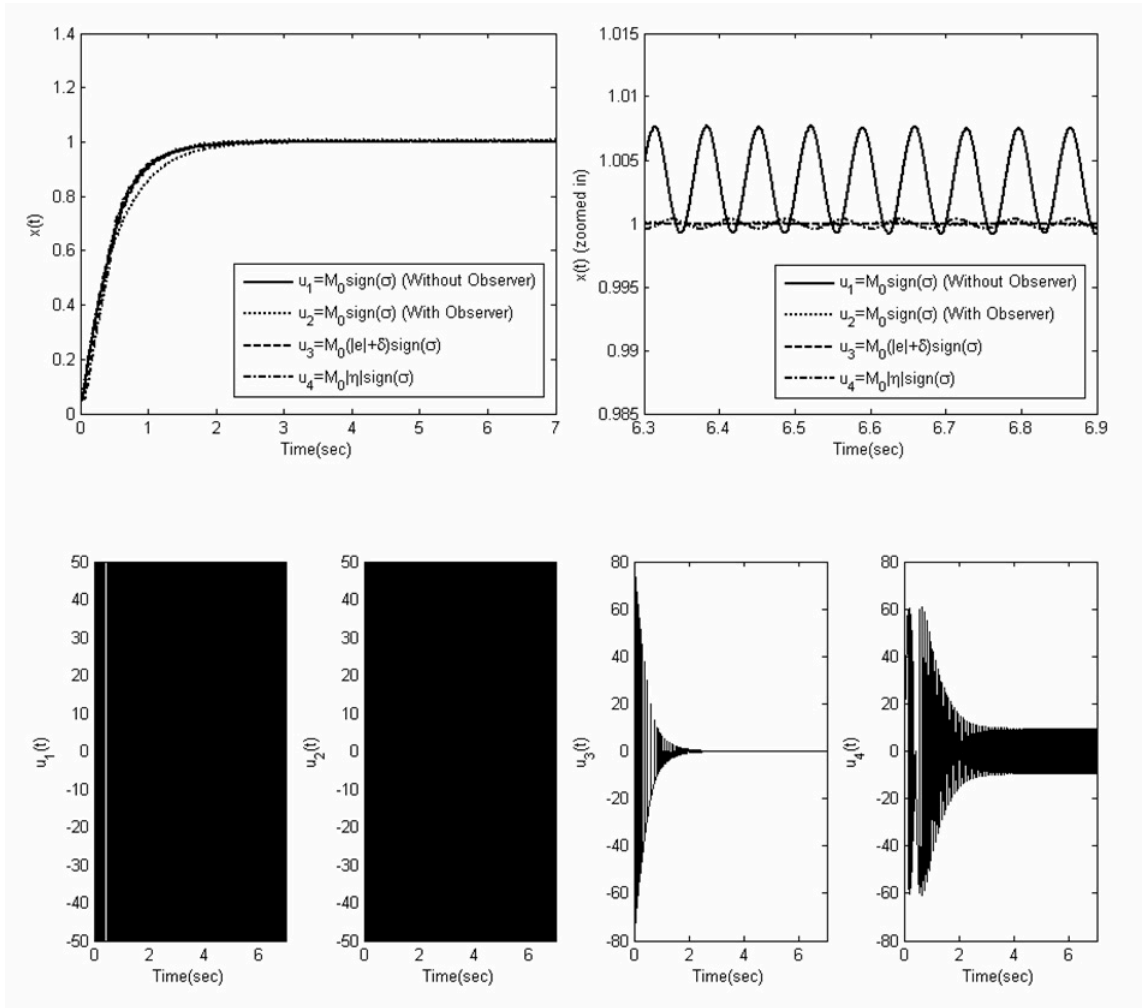
Figure 3.11: Simulation results from four different sliding mode controllers. Three types of controllers, u_2, u_3, and u_4 show similar levels of chattering.

57

The proposed controller is now applied to two-dimensional vector control case as given in (3.12). The control $u = [u^1 \; u^2]^T$ is designed as follows

$$
\begin{aligned}
\sigma_1 &= x_1 + x_2 \\
\sigma_2 &= x_1 + x_2 + x_3 \\
u^1 &= [u_{11} \; u_{12}]^T = [-5sign(\sigma_1) \; -10sign(\sigma_2)]^T \\
u^2 &= [u_{21} \; u_{22}]^T = [-5|\eta_1|sign(\sigma_1) \; -10|\eta_2|sign(\sigma_2)]^T
\end{aligned}
\tag{3.31}
$$

where $\eta_1 = \{sign(\sigma_1)\}_{eq}$, and $\eta_2 = \{sign(\sigma_2)\}_{eq}$. Again, there are two actuator dynamics ignored in the system model, and each of them has the structure given in (3.8) ($\mu = 0.04$). The control u^1 is a standard sliding mode control whereas u^2 utilizes equivalent-control-dependent gain. Simulation is performed for the system and the results can be found in Figure (3.12). As can be noticed, nearly chattering-free system is achieved by using u^2.

Not like the state-dependent gain method in previous section, δ does not need to deal with disturbances. Let us consider the following system

$$
\dot{x} = f(x,t) + u(t) + h(t)
\tag{3.32}
$$

where $h(t)$ represents the disturbance. Then, with control (3.26) ($\sigma = x$), the time derivative of sliding variable can be rewritten as

$$
\dot{\sigma} = f(x,t) + h(t) - M_0|\eta|sign(\sigma) = f^*(x,t) - M_0|\eta|sign(\sigma)
\tag{3.33}
$$

with $\delta = 0$, and $f^* = f + h$. Note that η is now $\eta = \{sign(\sigma)\}_{eq} = f^*/(M_0|\eta|)$ ($f^* \leq M_0$), and it can be found that η evaluates f^* which includes disturbance h. From the same manner provided in the proof for the theorem above, $|\eta| < 1$ again, which
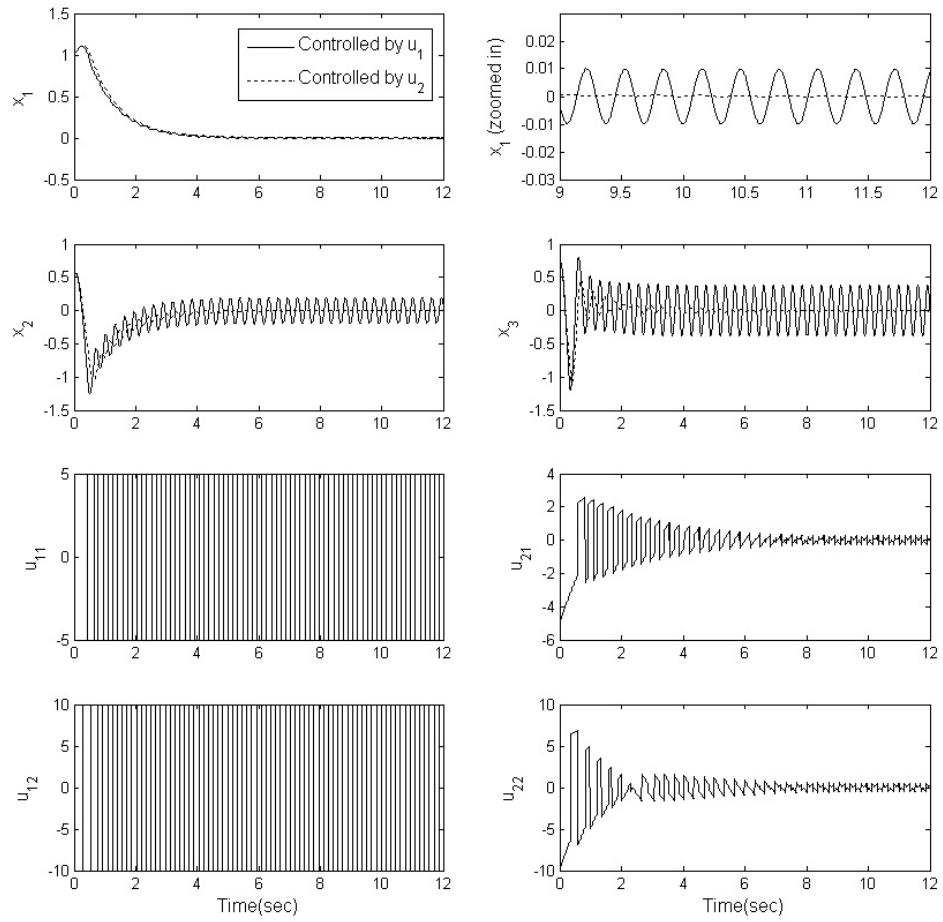
Figure 3.12: Simulation results for vector valued control case with equivalent-control-dependent gain method.

implies that sliding mode still exists even if $\delta = 0$ with any disturbances. However, the problem here is that $|\eta|$ may not be decreased desirably as system states are stabilized since f^* does not converge to zero when $h \neq 0$, and it may result in a certain level of chattering. Therefore a similar modification as suggested in (3.22) may be applied again. The sliding mode control for the system (3.32) with equivalent-control-dependent gain in (3.26) is revised as

$$u(t) = -M_0|\eta|sign(\sigma) + u_{eq} \tag{3.34}$$

where u_{eq} is the average value of control input $u(t)$ acquired by using a low-pass filter. As discussed in previous section, u_{eq} tends to $-h(t)$ as $x \to 0$; $\dot{\sigma}$ in (3.33) becomes

$$\dot{\sigma} = f(x,t) + h(t) - M_0|\eta|sign(\sigma) + u_{eq} = f(x,t) - M_0|\eta|sign(\sigma) \tag{3.35}$$

and sliding mode is enforced along the switching surface $\sigma = 0$ for $M_0 > |f/\eta|$. Then, it is noted that the term $\eta = \{sign(\sigma)\}_{eq}$ does not evaluate the disturbance anymore. It implies that $|\eta|$ decreases as desired, thus the amplitude of discontinuous control will be lessened accordingly, which leads to reduced chattering. A block diagram of the system schematic for the equivalent-control-dependent switching gain with disturbance cancelation is illustrated in Figure (3.13). Simulation is performed for the system (3.21) with unmodeled actuator dynamics given in (3.8). The control laws are constructed as

$$\begin{aligned} \sigma &= cx + \dot{x} \\ u_1 &= -M_1 sign(\sigma) \\ u_2 &= -M_2|\eta|sign(\sigma) + u_{eq} \end{aligned} \tag{3.36}$$

and u_1 is a conventional sliding mode control while u_2 is from the suggested method-
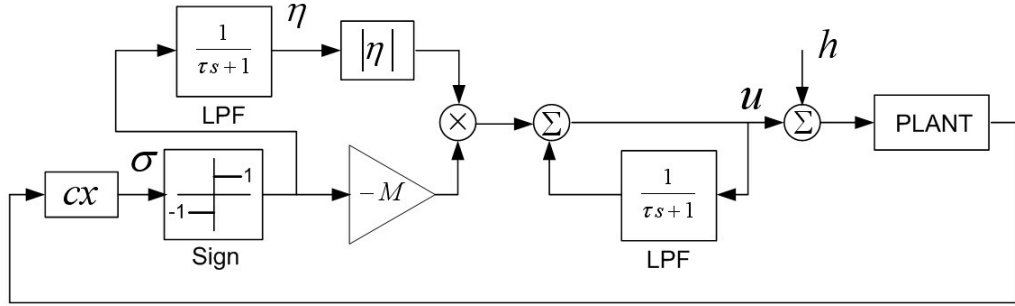
Figure 3.13: The system block diagram with a modified version of equivalent-control-dependent gain method as suggested in (3.34).

ology ($M_1 = 50$, $M_2 = 30$, $\mu = 0.03$, $c = 1$, and $h = 1$). Again, u_{eq} is obtained by a first-order low=pass filter ($\tau = 1.4$). It can be seen in Figure (3.14) that proposed control u_2 based on disturbance cancelation creates almost zero amplitude of chattering for the system.

In this chapter, two sliding mode control strategies using state-dependent and equivalent-control-dependent relay gains are provided. It is advantageous that those two methods with switching gain adaptation result in significantly lowered chattering while they require much less complicated design process than adding an observer or other chattering suppression methods. However, it is not possible to apply the methodology to systems which should be controlled by fixed switching gains or have only "on/off" switching modes. For such systems, a chattering reduction method based on phase shift will be discussed in later chapter of this dissertation.
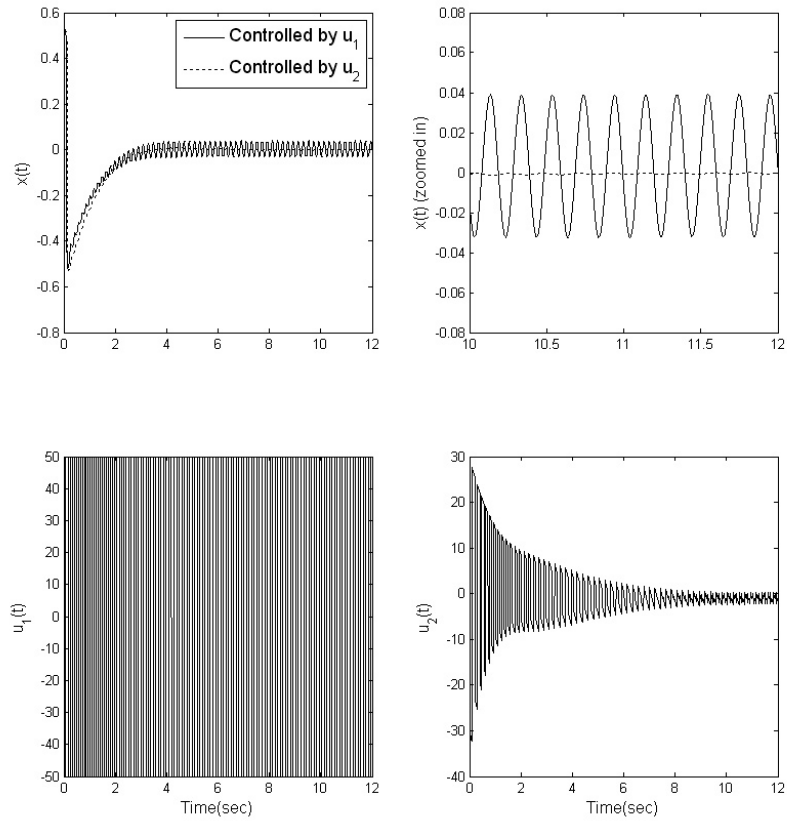
Figure 3.14: Simulation results for the system (3.21) with control (3.36).

CHAPTER 4

MULTIPHASE SLIDING MODE CONTROL
FOR CHATTERING SUPPRESSION

As mentioned in the introduction chapter, chattering may appear in systems controlled by on/off switching under a limitation of switching frequency, and power converter is one of such systems. In order to achieve better accuracy, the switching frequency needs to be increased; however, it may lead to higher power loss. Thus, to restrict the frequency, hysteresis loop is introduced in switching element, which causes chattering or ripple in current due to the lowered frequency. To minimize such chattering, multiple number of phases have been commonly used with harmonic cancellation methods.

In this chapter, analysis of the system with hysteresis in switching device is performed. Then, chattering suppression method based on multidimensional sliding mode with hysteresis loop will be considered.

4.1 Chattering frequency control using hysteresis loop

In systems controlled by on/off switchings, invariable switching frequency is often required. For sliding mode implementation, a hysteresis loop is introduced in switching device to keep the frequency at a desired level.

Let us consider the system

$$\dot{x} = f(x) + b(x)u \quad (x \in \Re^n) \tag{4.1}$$

with a scalar control

$$u = -Msign(\sigma), \; \sigma = cx \tag{4.2}$$

where M is positive constant and assumed to be large enough to enforce sliding mode along the surface $\sigma = 0$. Then the time derivative of sliding variable σ gives

$$\dot{\sigma} = F(x) + d(x)u \tag{4.3}$$

where

$$
\begin{aligned}
F(x) &= \{grad(\sigma)\}^T f(x) \\
d(x) &= \{grad(\sigma)\}^T b(x)
\end{aligned}
\tag{4.4}
$$

with $grad(\sigma) = [\partial\sigma/\partial x_1 \; \ldots \; \partial\sigma/\partial x_n]^T$. It is found that σ and $\dot{\sigma}$ have different signs if $d(x)M > |F(x)| \; (d(x) > 0)$. A hysteresis loop with a width of Δ in switching element can be implemented as depicted in Figure (4.1) with hysteresis loop gain $K = \Delta/M$. The oscillation in the vicinity of sliding surface can be illustrated as in Figure (4.2). It is assumed that Δ is small, and within two consecutive switchings x can be considered as constant. For the segment of trajectory during the time period δt_1, the slope of the line is defined as $d\sigma/dt = \Delta/\delta t_1$; therefore, the period of oscillation is

$$T = \delta t_1 + \delta t_2 = \frac{\Delta}{|\dot{\sigma}^+|} + \frac{\Delta}{|\dot{\sigma}^-|} \tag{4.5}$$
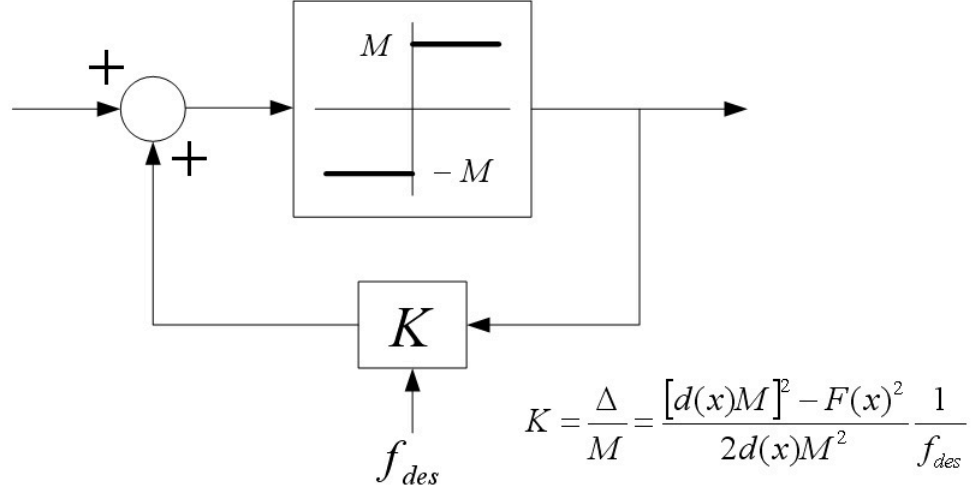
Figure 4.1: Implementation of the switching element with hysteresis loop. The width of hysteresis $\Delta = KM$.

where $\dot{\sigma}^+$ is $\dot{\sigma}$ when $\sigma > 0$, and $\dot{\sigma}^-$ is otherwise. Then, from (4.3), it is found that $|\dot{\sigma}^+| = |F(x) - d(x)M| = d(x)M - F(x)$, and $|\dot{\sigma}^-| = F(x) + d(x)M$. Thus, the period T can be rewritten as

$$T = \frac{\Delta}{d(x)M - F(x)} + \frac{\Delta}{d(x)M + F(x)} = \frac{2d(x)M\Delta}{\{d(x)M\}^2 - F(x)^2}. \tag{4.6}$$

For the desired value of frequency $f_{des} = 1/T_{des}$ where T_{des} is desired period of oscillation, the width of the hysteresis loop can be found as

$$\Delta = \frac{\{d(x)M\}^2 - F(x)^2}{2d(x)M} T_{des} = d(x)\frac{M^2 - \left\{\frac{F(x)}{d(x)}\right\}^2}{2M}\frac{1}{f_{des}}. \tag{4.7}$$
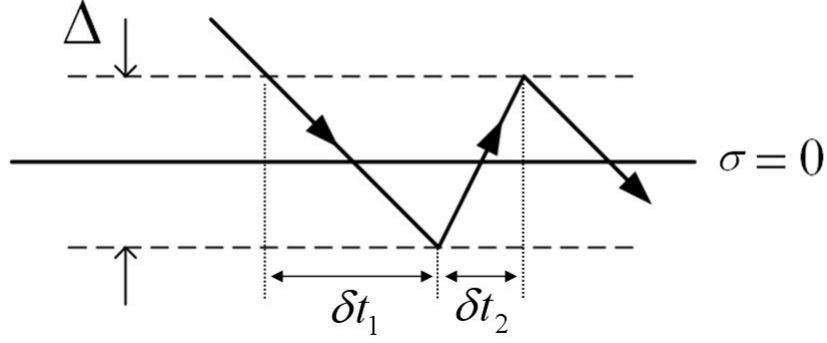
65

Figure 4.2: Oscillation in the vicinity of sliding surface.

Hence the gain K in the hysteresis loop shown in Figure (4.1) becomes

$$K = \frac{\Delta}{M} = \frac{\{d(x)M\}^2 - F(x)^2}{2d(x)M^2}\frac{1}{f_{des}} = d(x)\frac{M^2 - \left\{\frac{F(x)}{d(x)}\right\}^2}{2M^2}\frac{1}{f_{des}} \qquad (4.8)$$

and by using the adaptive gain $K = K(x)$ switching frequency will be fixed at the desired value. For hysteresis loop adaptation, the width of hysteresis Δ should be calculated in order to maintain switching frequency at a desired level, which requires the availability of the term $\frac{F(x)}{d(x)}$. In case that the function $b(x)$ is known, but $f(x)$ is unknown in the system equation (4.1), the term may be obtained by using a low-pass filter because it is indeed equal to the equivalent control u_{eq}. From (4.3), it is seen that the solution to the equation $\dot{\sigma} = 0$ with respect to u is nothing but $u_{eq} = F(x)/d(x)$, and it can be acquired by filtering out high frequency components from a discontinuous control as mentioned in previous chapter [1]. Figure (4.3) illustrates simulation results for a second-order system $\ddot{x} + \dot{x} + x = u$ ($u = -M sign(\dot{e} + e)$, $e = x - x_{ref}$, $F(x) = -x$ and $d(x) = 1$) with a hysteresis loop. It can be seen that an adaptive gain $K(x)$ for the hysteresis loop as in (4.8) results in fixed switching frequency at a desired level even when reference input changes.
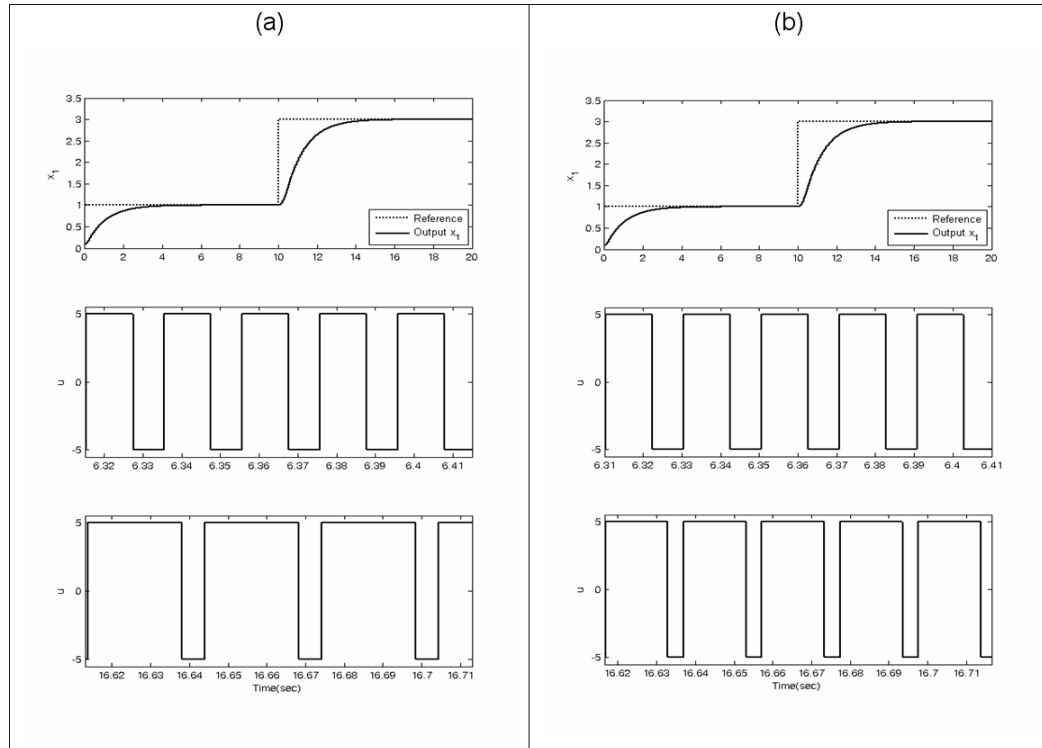
Figure 4.3: The switching gain $M = 10$ and the desired frequency $f_{des} = 50$Hz. (a) The hysteresis loop has a fixed gain K ($K = 0.0048$). The switching frequency varies as reference input changes. (b) The gain K depends on system states ($K = K(x)$) as depicted in Figure (4.1). The switching frequency maintains at the desired level.

4.2 Multidimensional sliding mode

Let us consider the following system that is similar to the one in the introduction chapter.

$$\dot{x} = f(x,t) + B(x,t)u + h(x,t) \quad (x, f, h \in \Re^n, \ B \in \Re^{n \times m}, \ u \in \Re^m) \tag{4.9}$$

The control u is vector-valued, and the components of u undergo discontinuities in m switching surfaces $s_1(x) = 0, \ s_2(x) = 0, \cdots, \ s_m(x) = 0$. The disturbance function $h(x,t)$ satisfies matching condition [1]: there exists a matrix Λ such that $h = B\Lambda$. Under a certain condition, sliding mode may be enforced in manifold $s(x) = [s_1(x) \ s_2(x) \cdots s_m(x)]^T = 0$, and the condition is equivalent to the stability condition of the motion in subspace $s(x)$

$$\dot{s}(x) = Gf(x) + GB(x)u \tag{4.10}$$

where $G = (\partial s_i / \partial x_j) \ (G \in \Re^{m \times n})$. After sliding mode occurs, motion equation is of reduced order, and it does not depend on the disturbance vector $h(x,t)$ which satisfies the matching condition [1]. Due to these two properties: order reduction and low sensitivity to variation of plant dynamics, sliding mode control is an efficient tool to control high order, nonlinear dynamic plants operating under uncertainty conditions.

As mentioned, to enforce sliding mode, stability in subspace $s(x)$ should be provided. The common approach to solve this problem implies proper selection of the vector $s(x)$ such that the matrix $GB(x)$ in (4.10) is diagonal. Then, the problem is reduced to the set of scalar ones: for each component of vector $s(x)$, the condition $s_i \dot{s}_i < 0 \ (i = 1, \cdots, m)$ should hold [1]. If there exist unmodeled dynamics, chattering
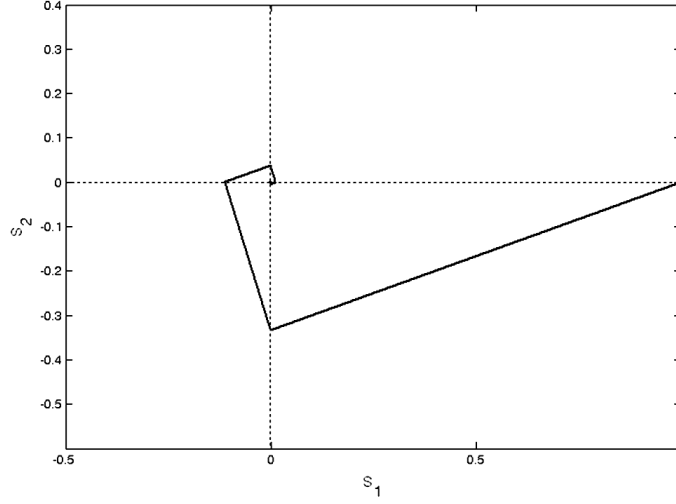
68

Figure 4.4: Sliding mode with two-dimensional control (initial conditions $s_1(0) = 1$, $s_2(0) = 0$).

may appear in each control channel, and oscillations of the chattering in each channel are independent; however, if all of them are interconnected (the interconnection depends on the matrix GB), the phases of oscillations are correlated as well. A simple example for two-dimensional sliding surface is shown in (4.11) and Figure (4.4).

$$\dot{s}_1 = -sign(s_1) + 2sign(s_2)$$
$$\dot{s}_2 = -2sign(s_1) - sign(s_2)$$
(4.11)

As can be seen in Figure (4.4), switching in one control channel depends on the previous switching instant of the other control channel. In the example, the trajectory is converging to the origin $s(x) = 0$, which is the goal of control, while the switching frequency increases. Note that sliding mode does not exist at each switching surface taken separately. However, in real system, chattering may appear due to various imperfections including unmodeled dynamics. The desire to have better accuracy of

69

the system by increasing switching frequency leads to higher frequency of oscillation, which can come into conflict with admissible level of losses in some systems such as power converters.

In following sections, a design methodology to reduce chattering or ripple in output of a system to the desired level under given switching frequency will be developed. The method is based on the opportunity to control phase-shifts in different control channels.

4.3 Design principle

In this section, a procedure for designing sliding mode controller to achieve desired phase-shift between multiple phases of power converter system is discussed.

For system (4.9) with $h(x) = 0$, it is assumed that control should be designed as a continuous function of state variables $u_0(x)$. This situation is common for so-called "Cascade Control" used for electric motors with current as a control input. To implement the desired control, power converter (PC) often utilizes PWM as a principle operation mode. Sliding mode is one of the tools to implement this mode as a substitute for PWM based on the feedback approach as shown in Figure (4.5), which illustrates that the output u tracks the reference input $u_0(x)$ in sliding mode. With a positive constant M, sliding mode variable s is written as

$$s = u_0(x) - u, \quad \dot{u} = v = Msign(s)$$
$$\dot{s} = g(x) - Msign(s), \quad g(x) = [grad(u_0)]^T(f + bu) \tag{4.12}$$

and it is evident that sliding mode with $u \equiv u_0(x)$ exists if $M > |g(x)|$. If the control is implemented with a hysteresis loop, chattering with oscillation amplitude $A = \frac{\Delta}{2}$ in sliding variable s is illustrated in Figure (4.6). Under the assumption that the
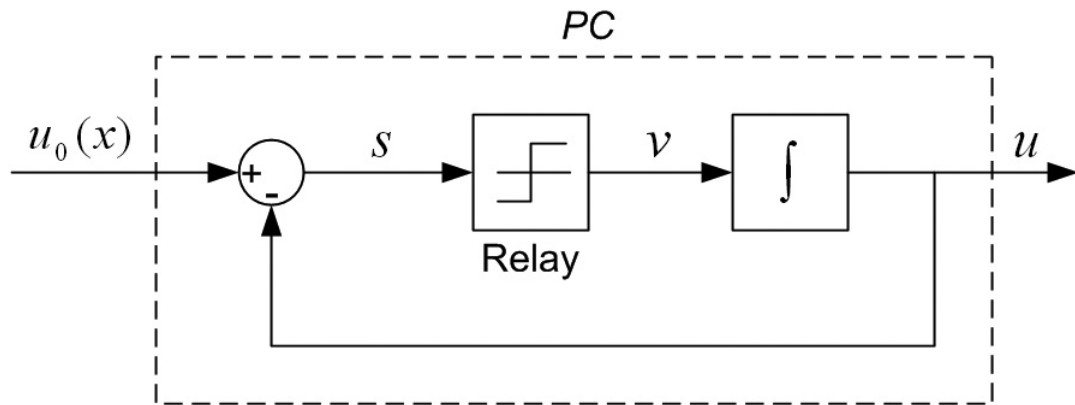
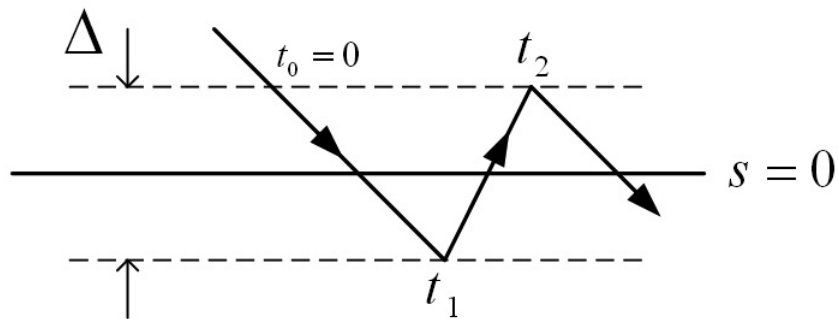Figure 4.5: Sliding mode control for a simple power converter model.

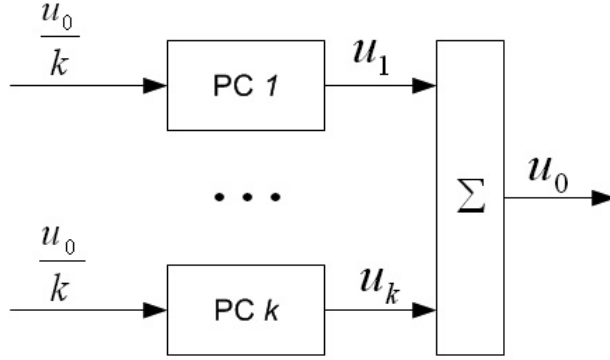Figure 4.6: The oscillation in the vicinity of sliding surface.

Figure 4.7: A k-phase converter with evenly distributed reference input.

switching frequency is high enough, the state x can be considered as constant within the time interval $[t_0, t_2]$ in macroscopic perspective, and the switching frequency is found as $f = \frac{1}{t_1 + t_2}$ where $t_1 = \frac{\Delta}{M - g(x)}$, $t_2 = \frac{\Delta}{M + g(x)}$ since slope of the trajectory line is $ds/dt = \dot{s}$. So, Δ can be selected to maintain the switching frequency at desired level; however, the magnitude of oscillation may be unacceptable.

Let us assume now that the desired control is implemented by k power converters with $s_i = \frac{u_0}{k} - u_i$, $(i = 1, 2, \cdots k)$ and $\frac{u_0}{k}$ as reference inputs as shown in Figure (4.7). If each power converter operates properly, the output is equal to the desired control $u_0(x)$. Amplitude and frequency in each converter can be found as follows:

$$ A = \frac{\Delta}{2}, \quad f = \frac{M^2 - \{\frac{g(x)}{k}\}^2}{2M\Delta}. \tag{4.13} $$

The amplitude of chattering in u_0 depends on the oscillation in each converter phase, and in the worst case, it can be k times higher than that of each converter. For the system in Figure (4.7), phases depend on initial conditions and cannot be controlled. This manner of implementation will be further referred to multiphase power converter or converter with k phases.
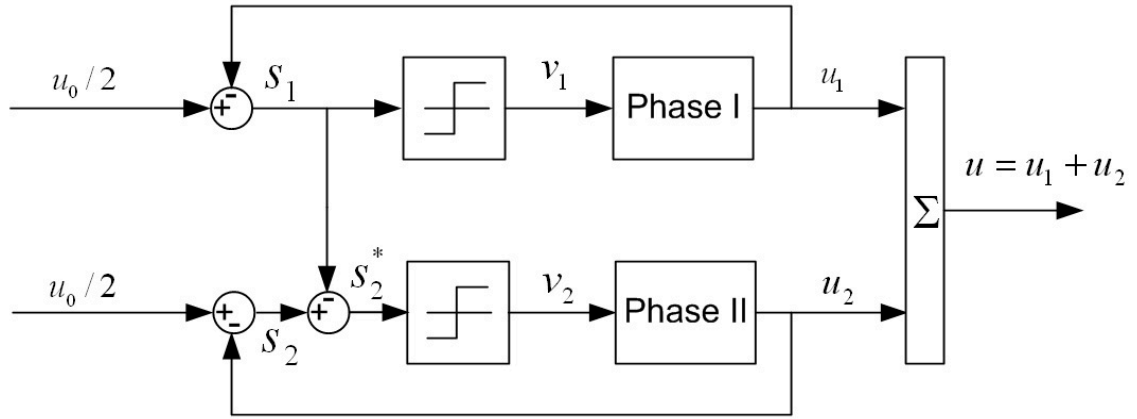
72

Figure 4.8: A power converter model with two interconnected phases.

As demonstrated in the example of multidimensional sliding mode (4.11), switching instants or phase shift between oscillations in different control channels are not independent in case the channels are interconnected. Now it is shown that the phase shift between oscillations in two different phases can be controlled by sliding mode with hysteresis.

Let two power converters be implemented as shown in Figure (4.8), and the switching function for the second converter is proposed as $s_2^* = s_2 - s_1$ where $s_1 = u_0/2 - u_1$, $s_2 = u_0/2 - u_2$, $v_1 = Msign(s_1)$, and $v_2 = Msign(s_2^*)$. Then, time derivatives of s_1 and s_2^* become

$$
\begin{aligned}
\dot{s}_1 &= a - Msign(s_1) \quad (a = \tfrac{g(x)}{k}) \\
\dot{s}_2^* &= Msign(s_1) - Msign(s_2^*).
\end{aligned}
\tag{4.14}
$$

After sliding mode occurs along the manifold of two surfaces $s_1 = 0$ and $s_2^* = 0$, each of u_1 and u_2 equals to $u_0/2$; therefore, the sum of u_1 and u_2, becomes u_0, the desired control. Now the system behavior on the plane s_1 versus s_2^* is analyzed where widths

73

of hysteresis loops for the two sliding surfaces are Δ and $\alpha\Delta$ respectively. First, the case $a = 0$ and $\alpha = 1$ is considered. As can be seen from Figure (4.9), phase shift between v_1 and v_2 turns out to be equal to quarter of the period of oscillation T because the time taken for the trajectory in Figure (4.9) (a) to travel between any two consecutive points is $T/4$. From the fact that $|\dot{s}_1| = M$ for $a = 0$, the period is found to be $T = \frac{2\Delta}{M}$. It is evident that for any initial conditions different from point 0 (for instance 0'), the motion represented in Figure (4.9) will appear in time less than $\frac{T}{2}$. A similar analysis may be performed for the case $a \neq 0$ (of course $M > |a|$) and $\alpha \neq 1$. In Figure (4.10), s-plane is demonstrated for $a > 0$ and $\alpha > 1$. Also, the period of oscillations T can be easily found from the equation with respect to s_1 as follows:

$$T = \frac{\Delta}{M - a} + \frac{\Delta}{M + a} = \frac{2M\Delta}{M^2 - a^2}. \qquad (4.15)$$

The time interval t_a in Figure (4.10) (c) can be calculated from the slope of line segment of s_2^* during that time. From equations (4.14), it can be written as

$$\frac{ds_2^*}{dt} = 2M = \frac{\alpha\Delta}{t_a}. \qquad (4.16)$$

Therefore, the phase shift becomes

$$\phi = \frac{\alpha\Delta}{2M} \qquad (4.17)$$

which is equal to the time interval t_a for changing s_2^* from $\frac{\alpha\Delta}{2}$ to $-\frac{\alpha\Delta}{2}$ or vice versa. From (4.15) and Figure (4.10), it can be seen that the period of oscillation in s_2^* is equal to the period T in s_1.
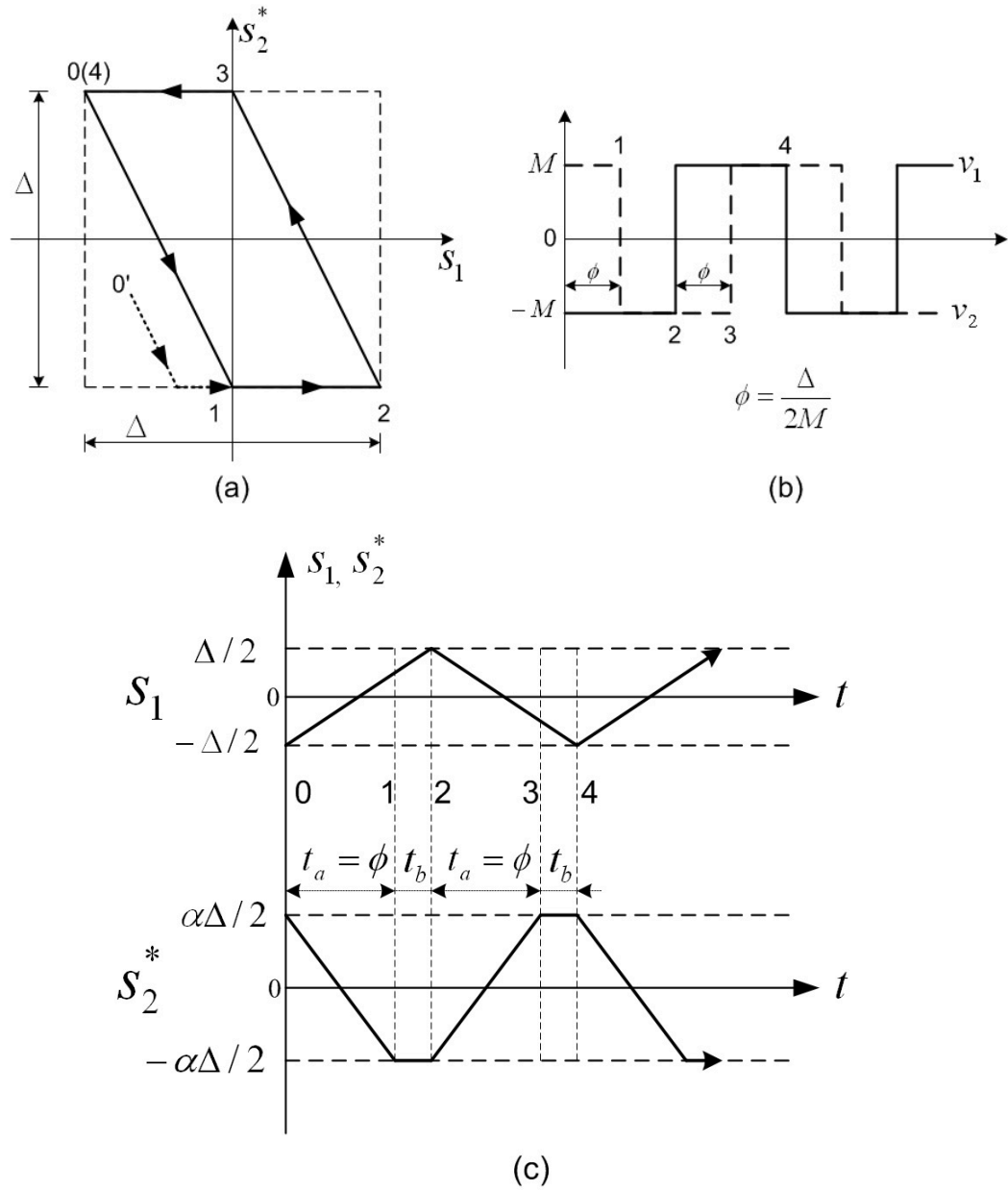
Figure 4.9: (a) The system behavior in s-plane where $\alpha = 1$. (b) The phase controls v_1 and v_2. (c) s_1 and s_2^* in time domain.
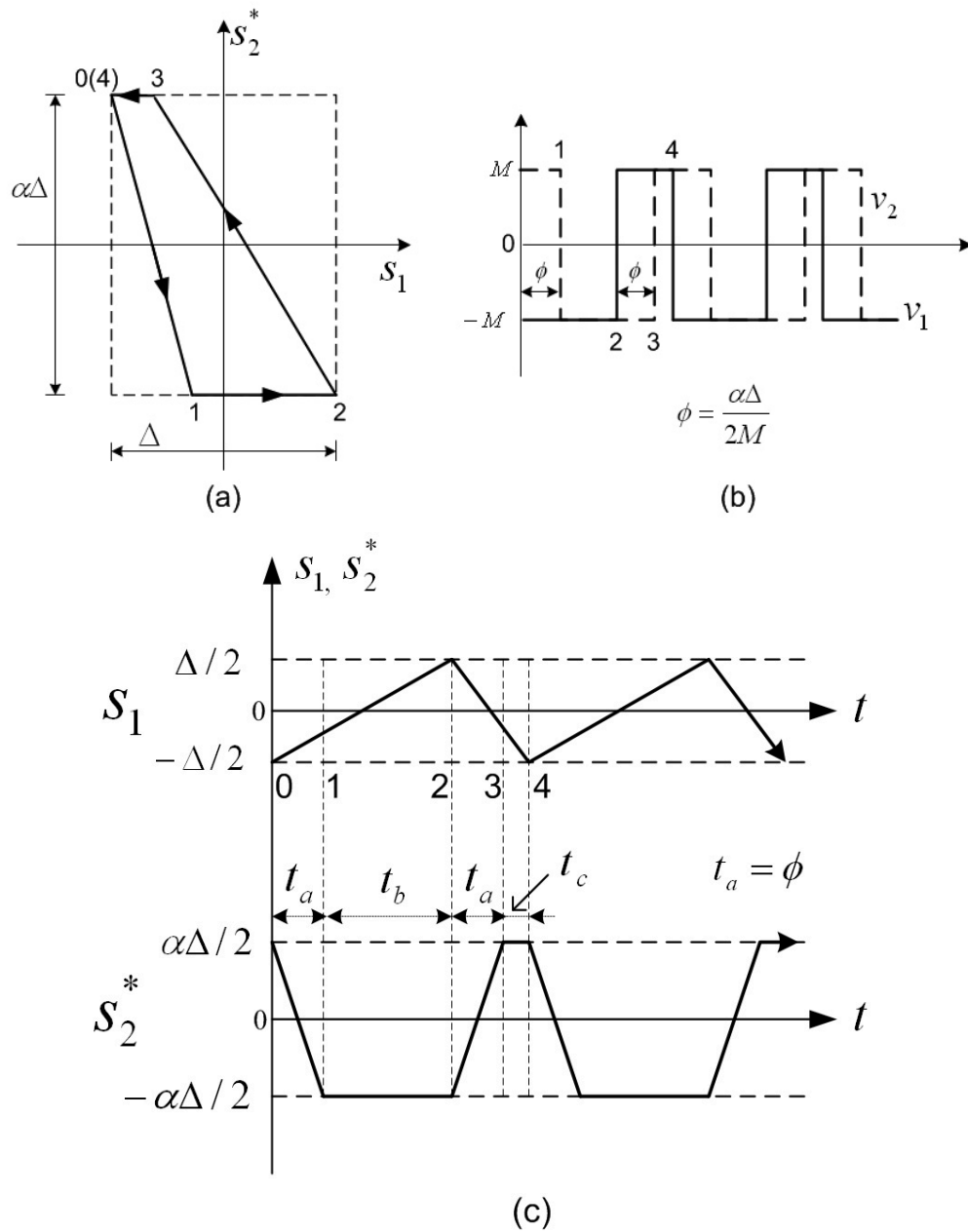
Figure 4.10: (a) The system behavior in s-plane where $\alpha \neq 1$. (b) The phase controls v_1 and v_2. (c) s_1 and s_2^* in time domain.

76

The switching illustrated in Figure (4.10) takes place if

$$\frac{\alpha\Delta}{2M} < \frac{\Delta}{M + |a|} \tag{4.18}$$

otherwise, for the trajectory starting from point 2 in Figure (4.10), v_1 will switch from M to $-M$ before v_2 switches from $-M$ to M at point 3. Thus, to obtain desired phase shift ϕ, the condition (4.18) should hold.

As follows from this example, a phase shift between oscillations of two phases can be selected by proper choice of α for any switching frequency without using dynamic elements, e.g., transformers and filters. The chattering exists in any phase with the same frequency and amplitude. The oscillation amplitude in the output is equal to the sum of outputs from individual phase channels and depends on the phase shifts between phases. They can be controlled, and further the phases will be selected such that the amplitude of chattering is minimized.

4.4   Selection of phase number

Suppose that a multiphase converter with m phases is to be designed such that the period of chattering T is the same in each phase, and two subsequent phases have phase shift $\frac{T}{m}$. Since chattering is a periodic time function, it can be represented by Fourier series with frequencies

$$\omega_k = \omega \cdot k, \ \omega = \frac{2\pi}{T} \ (k = 1, 2, \cdots, \infty). \tag{4.19}$$

Since the phase difference between the first phase and i-th phase can be written as $\phi_i = \frac{2\pi}{\omega m}(i - 1)$, the effect of k-th harmonic in the output signal, which is sum of

individual outputs from all of phases, can be calculated as follows

$$\sum_{i=0}^{m-1} sin\left[\omega_k(t - \frac{2\pi}{\omega m}i)\right] = \sum_{i=0}^{m-1} Im\left[e^{j(\omega_k t - \frac{2\pi k}{m}i)}\right]$$

$$= Im(e^{j\omega_k t}Z), \quad Z = \sum_{i=0}^{m-1} e^{-j\frac{2\pi k}{m}i}.$$

(4.20)

To find Z, let us multiply it by $e^{-j\frac{2\pi k}{m}}$ to have

$$
\begin{aligned}
Ze^{-j\frac{2\pi k}{m}} &= \sum_{i=0}^{m-1} e^{-j\frac{2\pi k}{m}(i+1)} \\
&= \sum_{i'=1}^{m} e^{-j\frac{2\pi k}{m}i'}.
\end{aligned}
$$

(4.21)

Thus, from (4.21), it can be written that

$$Ze^{-j\frac{2\pi k}{m}} = Z$$

(4.22)

since the term for $i' = m$ is equal to that for $i' = 0$. The function $e^{-j\frac{2\pi k}{m}}$ is equal to 1 only if $\frac{k}{m}$ is integer or $k = m, 2m, \cdots$, which means that Z must be zero for all other cases. This analysis shows that all harmonics except for lm $(l = 1, 2, \cdots)$ are suppressed in the output signal. As a result, the amplitude of chattering can be reduced to the desired level by increasing number of phases providing desired phase shift between two subsequent phases from the methodology proposed in the previous section.

Now it is shown that the selection of phase number depends on the range of the function a. First, the value α, which is related to width of hysteresis, is calculated to provide the desired phase shift. Since ϕm must be equal to period T, α can be

found from (4.15) and (4.17) as

$$\alpha = \frac{4M^2}{m(M^2 - a^2)} \tag{4.23}$$

where the function a is assumed to be bounded as $|a| < a_{max} < M$. According to (4.18) and (4.23) for a positive a, the following condition should hold to have proper phase shifts.

$$\frac{4M^2}{m(M^2 - a^2)}\frac{\Delta}{2M} < \frac{\Delta}{M + a}$$

or

$$m > \frac{2M}{M - a_{max}}. \tag{4.24}$$

Similarly, it also can be shown that the same condition should hold for a negative a.

The above results may be summarized as the design procedure for the multi-phase converter:

- Select the width of hysteresis loop as a state function such that the switching frequency in the first phase is maintained at desired level.

- Determine number of phases for given range of function $a(x)$ variation.

- Find the parameter α as a function of $a(x)$ such that the phase shift between two subsequent phases is equal to $\frac{1}{m}$ of the oscillation period of the first phase.

Remark 1. *As follows from (4.18) and (4.23), the condition for a should hold:*

$$|a| < M\left(1 - \frac{2}{m}\right) \quad (m \geq 2). \tag{4.25}$$

If not, it can lead to the collapse of switching sequence, and also frequency of the second phase may be changed. To preserve the switching sequence and frequency even

in case $|a| > a_{max}$ ($a_{max} = M\left(1 - \frac{2}{m}\right)$), the condition (4.18) must be always fulfilled. Therefore, the function α should be selected as in (4.23) for (4.25) and in compliance with (4.18) otherwise, i.e.,

$$
\alpha = \begin{cases}
\dfrac{4M^2}{m(M^2 - a^2)} & if \ |a| < M\left(1 - \dfrac{2}{m}\right) \\[4mm]
\dfrac{2M}{M + |a|} & if \ a_{max} < |a| < M.
\end{cases}
\tag{4.26}
$$

4.5   Master-slave mode

In this section, another version of multiphase converter is proposed based on phase shift control with sliding mode. As illustrated in Figure (4.11), the second phase is under open-loop control which inherits switching command from the first phase and provides necessary phase shift. The first phase (master) is connected to the next phase (slave) through an additional first-order system as a shifter such that the discontinuous input v_2 to the slave has desired phase shift from v_1 without changing switching frequency.

To demonstrate the design idea, a two-phase converter system which is similar to the one in previous section is considered. The equation of the first phase

$$
\dot{s}_1 = a - v_1, \quad v_1 = Msign(s_1)
\tag{4.27}
$$

is complemented by the following equation of an additional first-order dynamic system

$$
\dot{s}_2^* = K(v_1 - v_2), \quad v_2 = Msign(s_2^*).
\tag{4.28}
$$

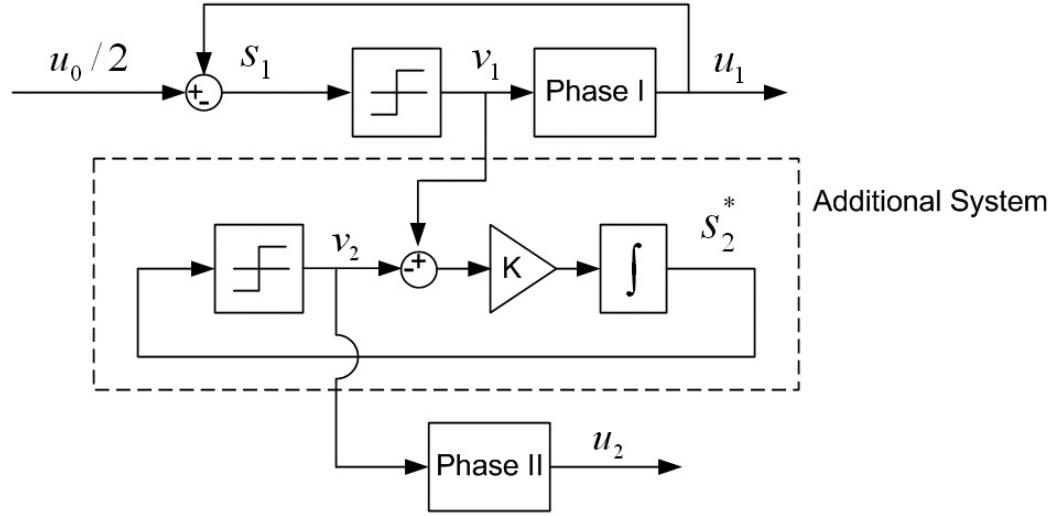The above equation is similar to (4.14), but s_2^* is acquired by integration of $\dot{s}_2^*$ in this

Figure 4.11: Two-phase power converter model in the master-slave mode with an additional first-order system for s_2^*.

case since sliding variable for the second phase s_2 is undefined. The analysis of the system behavior can be performed in the same manner as in previous sections. As depicted in Figure (4.12), the two phases have the same width of hysteresis loop Δ. Then, the slope of the line of s_2^* between switching instant 2 and 3 is found as

$$\dot{s}_2^* = 2KM = \frac{\Delta}{t_a} \tag{4.29}$$

and the time interval t_a is phase shift between v_1 and v_2, which can be written as

$$\phi = t_a = \frac{\Delta}{2KM} \tag{4.30}$$

while the phase shift from the earlier design principle can be found in (4.17). In master-slave mode, a desired phase shift can be achieved by selecting proper value of K. If the desired value of phase shift is T/m for m-phase converter where T is period
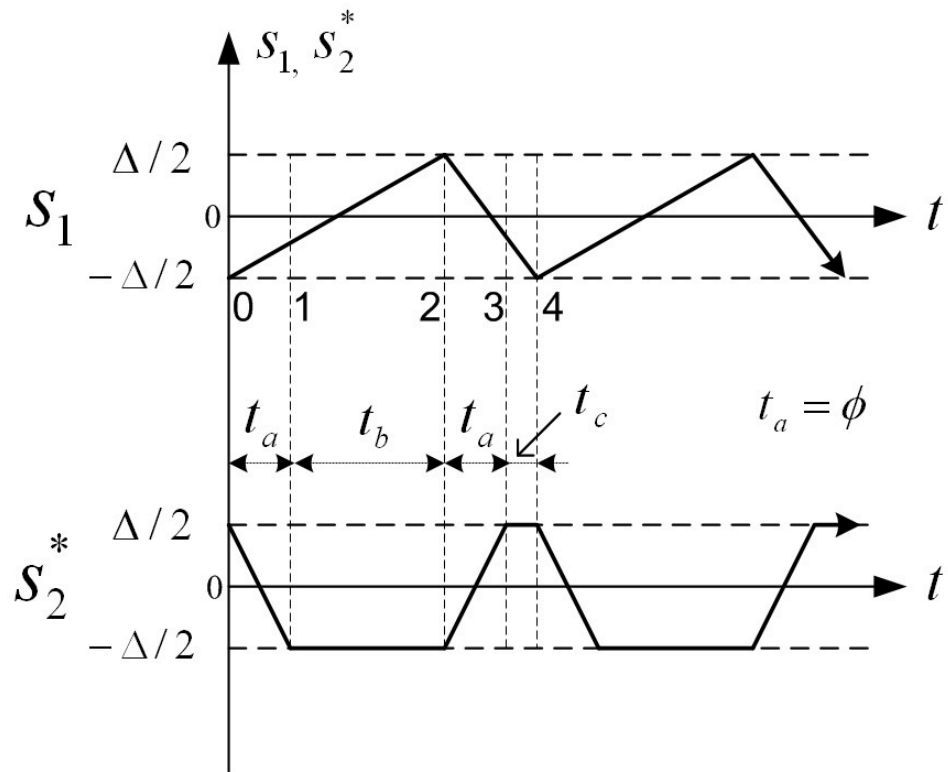
Figure 4.12: The switching variables s_1 and s_2^* in master-slave mode.

of oscillation in each phase, from (4.15) and (4.30), the value of K becomes

$$K = \frac{m(M^2 - a^2)}{4M^2}. \tag{4.31}$$

Note that $K = 1/\alpha$ from (4.23).

For multiphase converter, the desired control of each phase can be obtained similarly from the control of the previous phase; the input to k-th phase, v_k, is a phase-shifted signal from the input to the previous phase v_{k-1}.

Remark 2. *In the additional dynamic system (4.28), the width of hysteresis loop $\tilde{\Delta}$ ($\tilde{\Delta} = \alpha\Delta$) and the amplitude of both discontinuous functions $\tilde{M}$ ($\tilde{M} = \beta M$) may be chosen arbitrarily ($\alpha,\ \beta = const.$). Then, the phase shift becomes*

$$\tilde{\phi} = \frac{\alpha\Delta}{2K\beta M} = \frac{\Delta}{2\tilde{K}M}, \quad (\tilde{K} = \frac{K\beta}{\alpha}) \tag{4.32}$$

*and $\tilde{K}$ should be selected properly from (4.31).*

4.6 Simulation results for multiphase power converter model

The objective of simulation is to demonstrate to what extent chattering can be suppressed in multiphase power converter with proposed phase shift control methodology and to check the range of the function a for which the chattering suppression takes place. In simulation, the "master-slave method" is accepted. The gain K is selected as in (4.26) ($K = 1/\alpha$) to maintain switching frequency at the desired level in all phases even if a is beyond the admissible domain (4.25).

First, the basic simulation block Figure (4.13a) providing the desired phase shift is demonstrated. As can be seen in Figure (4.13b), the phase shift is equal to $1/4$ of the period.
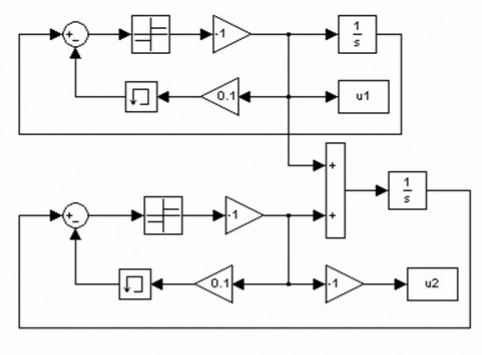
(a)
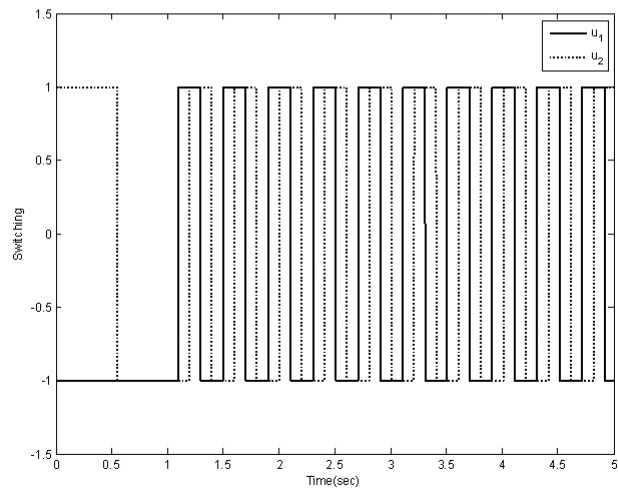
(b)

Figure 4.13: (a) Simulink block diagram for (4.14) with $a = 0$ (b) u_2 is shifted from u_1 by $T/4$.

For further simulation, the governing equations of multiphase power converter are given as follows

$$\dot{I}_k = \frac{1}{L}\left(-I_k R_a + u_k - V_L\right) \quad (k = 1, 2, \cdots, m)$$
$$\dot{V}_L = \frac{1}{C}\left(\sum_{k=1}^{m} I_k - \frac{V_L}{R_L}\right) \tag{4.33}$$

with m phases, and the system schematic is illustrated in Figure (1.3). The following control law is used for a two-phase power converter $(m = 2)$ represented in (4.33):

$$s_1 = I_1 - \frac{I_{ref}}{m}, \quad I_{ref} = \frac{V_{ref}}{R_L}$$
$$u_1 = V_s \frac{1 - sign(s_1)}{2}, \quad u_2 = V_s \frac{1 - sign(s_2^*)}{2} \tag{4.34}$$

where V_{ref} and I_{ref} are reference voltage input and corresponding load current respectively. The desired phase shift $T/2$ is obtained using two additional blocks providing phase shift $T/4$ each of them.

$$
\begin{aligned}
\dot{s}_1 &= \frac{1}{L}\left[-R_a s_1 - \frac{V_s}{2}sign(s_1) + \left(\frac{V_s}{2} - \frac{I_{ref}R_a}{m} - V_L\right)\right] \\
&= -b_1 sign(s_1) - b_2 s_1 + a^* \\
\dot{s}_2^* &= b_1\left[sign(s_1) - sign(s_2^*)\right] \\
\dot{s}_3^* &= b_1\left[sign(s_2^*) - sign(s_3^*)\right]
\end{aligned} \tag{4.35}
$$

where $a^* = \frac{V_s}{2L} - \frac{I_{ref}R_a}{mL} - \frac{V_L}{L}$, $b_1 = \frac{V_s}{2L}$, $b_2 = \frac{R_a}{L}$, and $a = a^*/b_1$. As it follows from (4.25), the only admissible value of a is equal to zero for $m = 2$. As it is shown in Figure (4.14), chattering is suppressed in the output current. Now, four-phase converter $(m = 4)$ is simulated with switching frequency control of the first phase by appropriate choice of hysteresis width or hysteresis loop gain K_h as shown in Figure (4.15). Simulation in Figure (4.16)-(4.18) is performed for several values of a

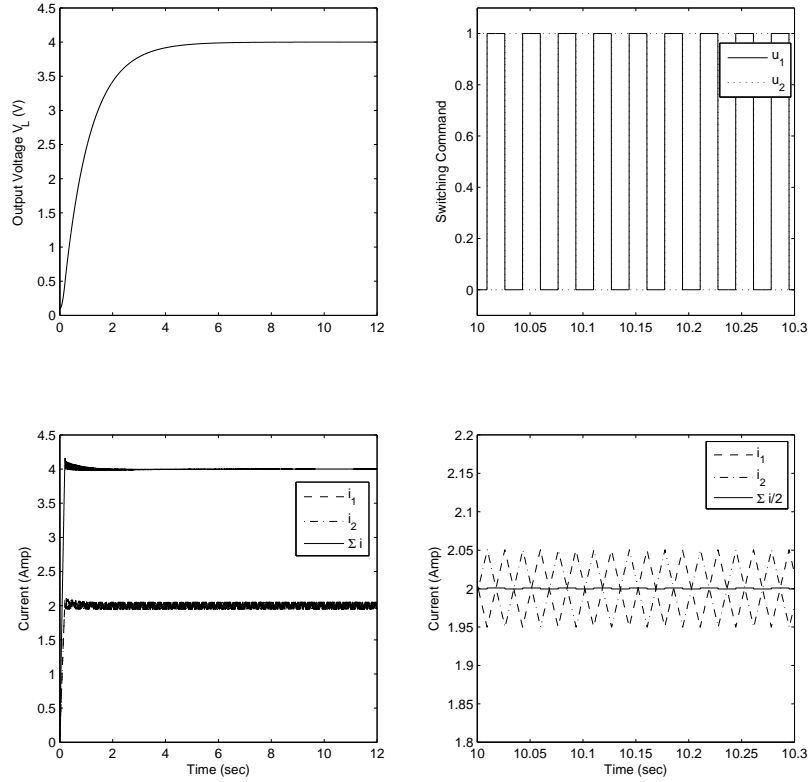| Parameter	Set I	Set II
L (H)	1	5×10^{-8}
C (F)	1	1×10^{-3}
R_a (Ω)	1	3×10^{-4}
R_L (Ω)	1	1×10^{-2}
V_s (V)	12	12

Table 4.1: Parameter values for simulation.

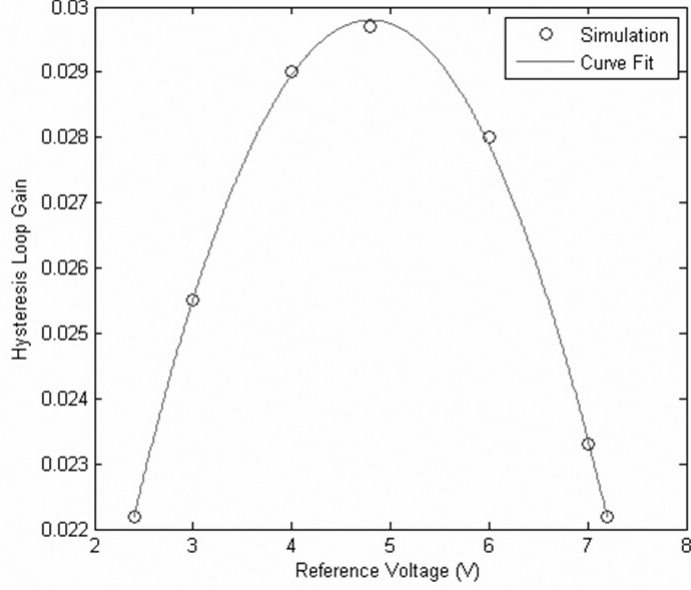Figure 4.14: Simulation result for two phases (4.33)-(4.35) ($a = 0$) with parameter Set I in Table (4.1).

Figure 4.15: Hysteresis loop gain K_h to maintain switching frequency at 50Hz $(K_h(V_{ref}) = -0.0013V_{ref}^2 + 0.0127V_{ref} - 0.0007)$.

in admissible domain with the following control law:

$$
\begin{aligned}
u_1 &= V_s\tfrac{1-sign(s_1)}{2}, \quad u_k = V_s\tfrac{1-sign(s_k^*)}{2}, \quad (k = 1, \cdots, m) \\
\dot{s}_1 &= -b_1 sign(s_1) - b_2 s_1 + a^* \\
\dot{s}_2^* &= Kb_1[sign(s_1) - sign(s_2^*)] \\
\dot{s}_k^* &= Kb_1[sign(s_{k-1}^*) - sign(s_k^*)]
\end{aligned}
\tag{4.36}
$$

and K is chosen from (4.31) with $a = a^*/b_1$. Since a can be out of admissible range in transient period, chattering appears at the beginning of the process. Note that in the simulation, control (4.36) is used without the modified one (4.26). Again, chattering suppression is observed, and the switching frequency is maintained at the same level.

Figure (4.19) shows simulation results from the control (4.36) with modification of K. Since the system is in master-slave mode, K, instead of α, should be adjusted
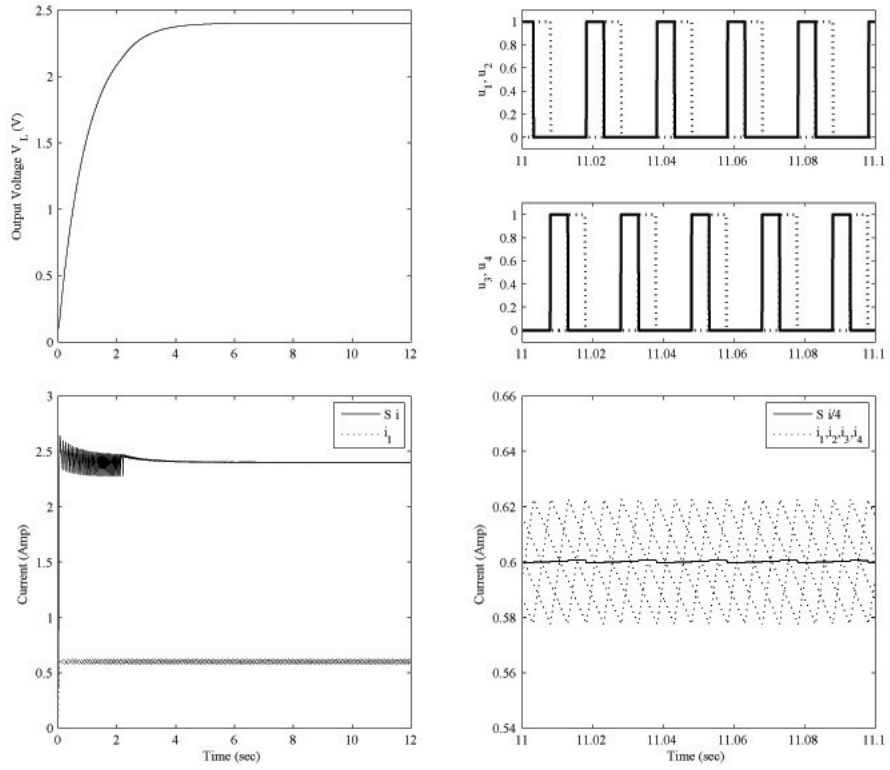
87

Figure 4.16: Simulation result for 4 phases with control (4.36) when $V_{ref} = 2.4V$ (parameter Set I in Table (4.1), $K_h = K_h(V_{ref})$, $a = 0.5$, and $S\ i = \sum_{k=1}^{4} i_k$).
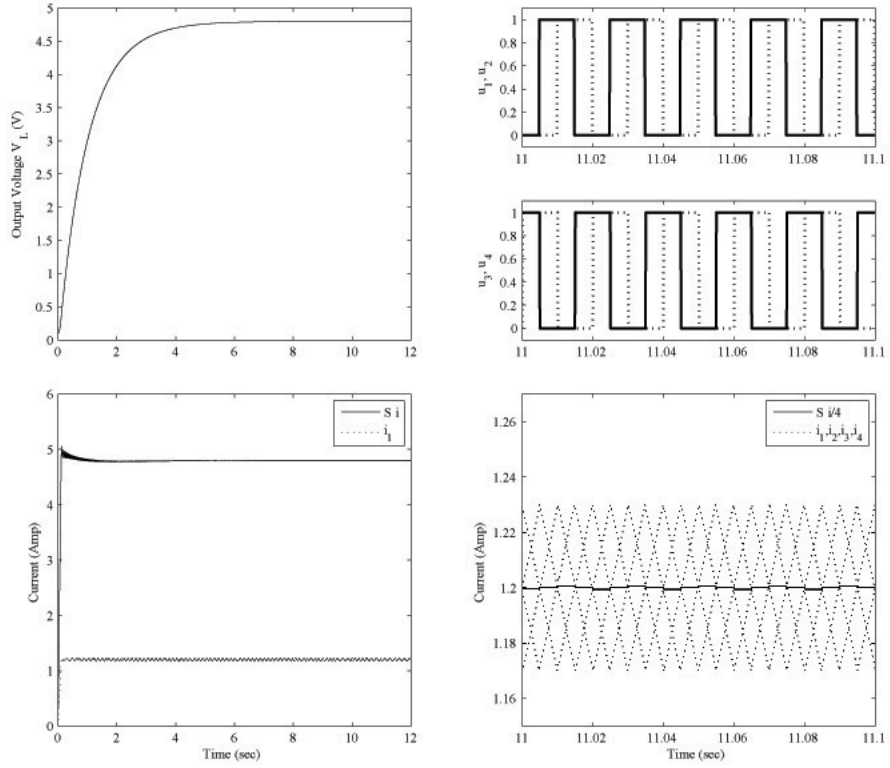
Figure 4.17: Simulation result for 4 phases with control (4.36) when $V_{ref} = 4.8V$ (parameter Set I in Table (4.1), $K_h = K_h(V_{ref})$, $a = 0$, and $S\ i = \sum_{k=1}^{4} i_k$).
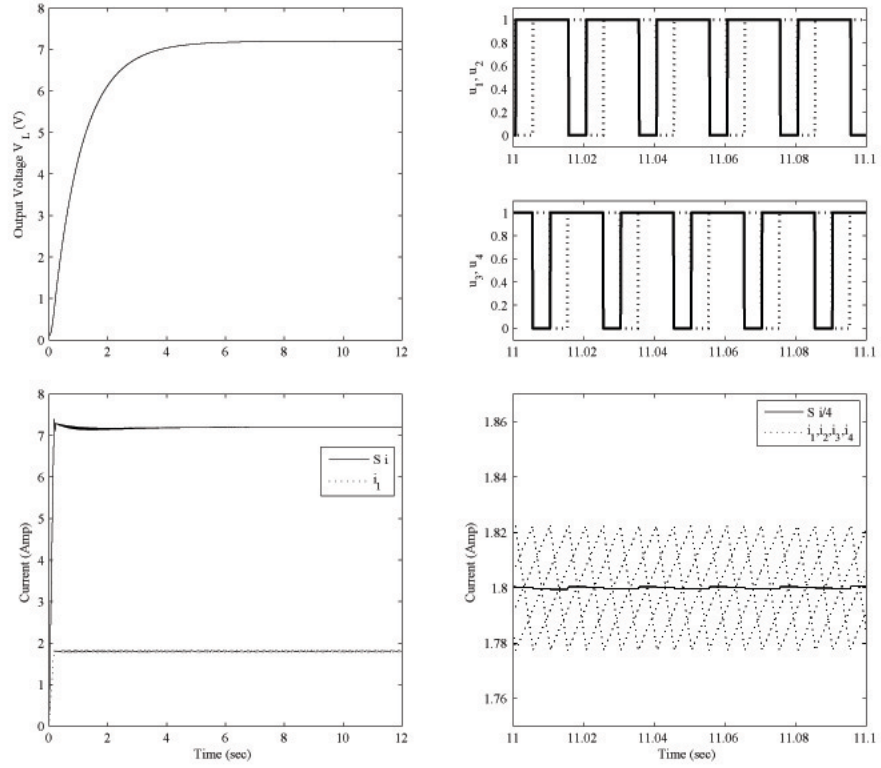
Figure 4.18: Simulation result for 4 phases with control (4.36) when $V_{ref} = 7.2V$ (parameter Set I in Table (4.1)), $K_h = K_h(V_{ref})$, $a = -0.5$, and $S\ i = \sum_{k=1}^{4} i_k$).

as proposed in (4.26); therefore, the value K in (4.36) may be selected as follows $(K = 1/\alpha)$.

$$
K = \begin{cases} \dfrac{m(M^2 - a^2)}{4M^2} & if \ |a| < M\left(1 - \dfrac{2}{m}\right) \\[4mm] \dfrac{M + |a|}{2M} & if \ a_{max} < |a| < M. \end{cases}
\tag{4.37}
$$

Comparing with the results in Figure (4.16), transient response is improved.

The design methodology is developed under the assumption that state variables are constant within one period of oscillation. Further simulation is performed for time-varying reference input with control (4.26) and (4.36). Simulation result in Figure (4.20) demonstrates that efficient chattering suppression for both transient time interval and steady-state modes.

Next set of simulation result is related to 6-phase converter with control law (4.36) ($m = 6$). In Figure (4.21)-(4.28), it can be seen that the admissible range of reference input is wider for 6-phase converter comparing with that of 4-phase ($V_{ref,min}$ is equal to 1.714V and 2.4V respectively). The chattering suppression effect demonstrated for 4-phase converter with time-varying V_{ref} can be observed for 6-phase converter as well in Figure (4.24). For both cases, the modified control (4.26) instead of (4.23) or (4.31) decreases chattering considerably in transient intervals.

For the real-life 4-phase DC to DC power converter with parameters from Set II in Table, simulation is performed for different reference inputs. The power converter is a voltage regulator for certain type of microprocessors, and it has very small inductance value for rapid response, which makes the chattering issue more significant. The effect of chattering suppression for reference inputs 3, 6, and 8V is demonstrated in Figure (4.25)-(4.27), and it can be observed that the proposed methodology successfully reduces output current ripple.
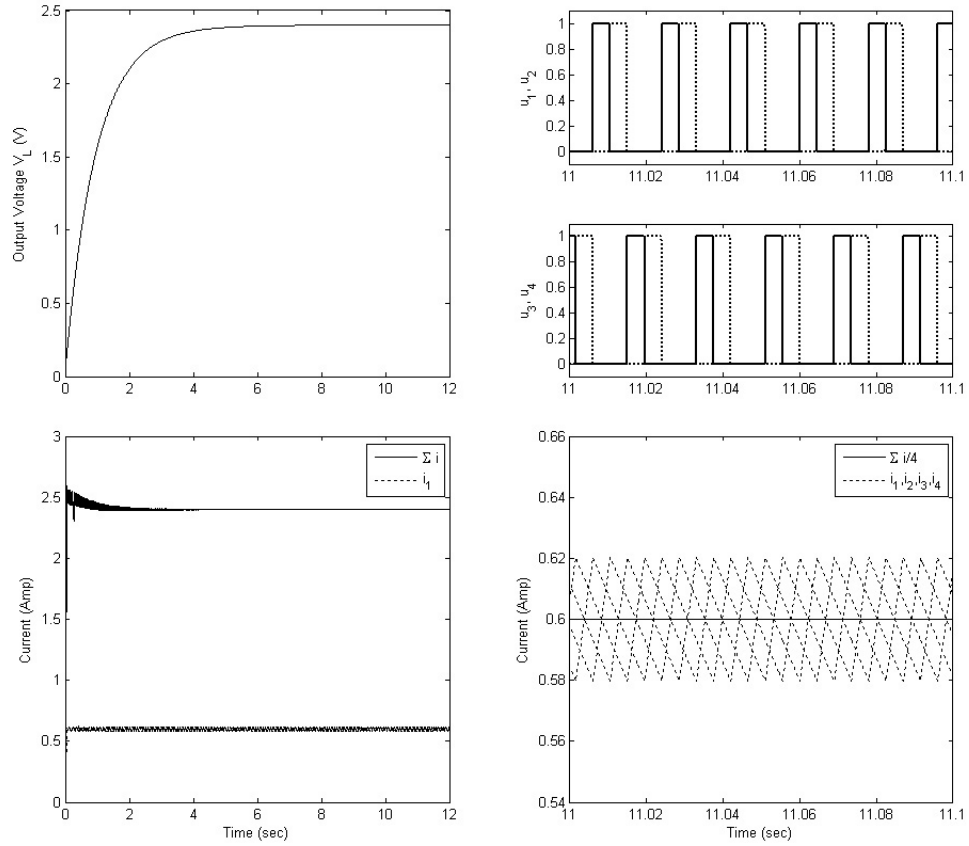
Figure 4.19: Simulation result for 4 phases with control (4.36) with modification (4.37) when $V_{ref} = 2.4V$ (parameter Set I in Table (4.1), $K_h = K_h(V_{ref})$, and $a = 0.5$).
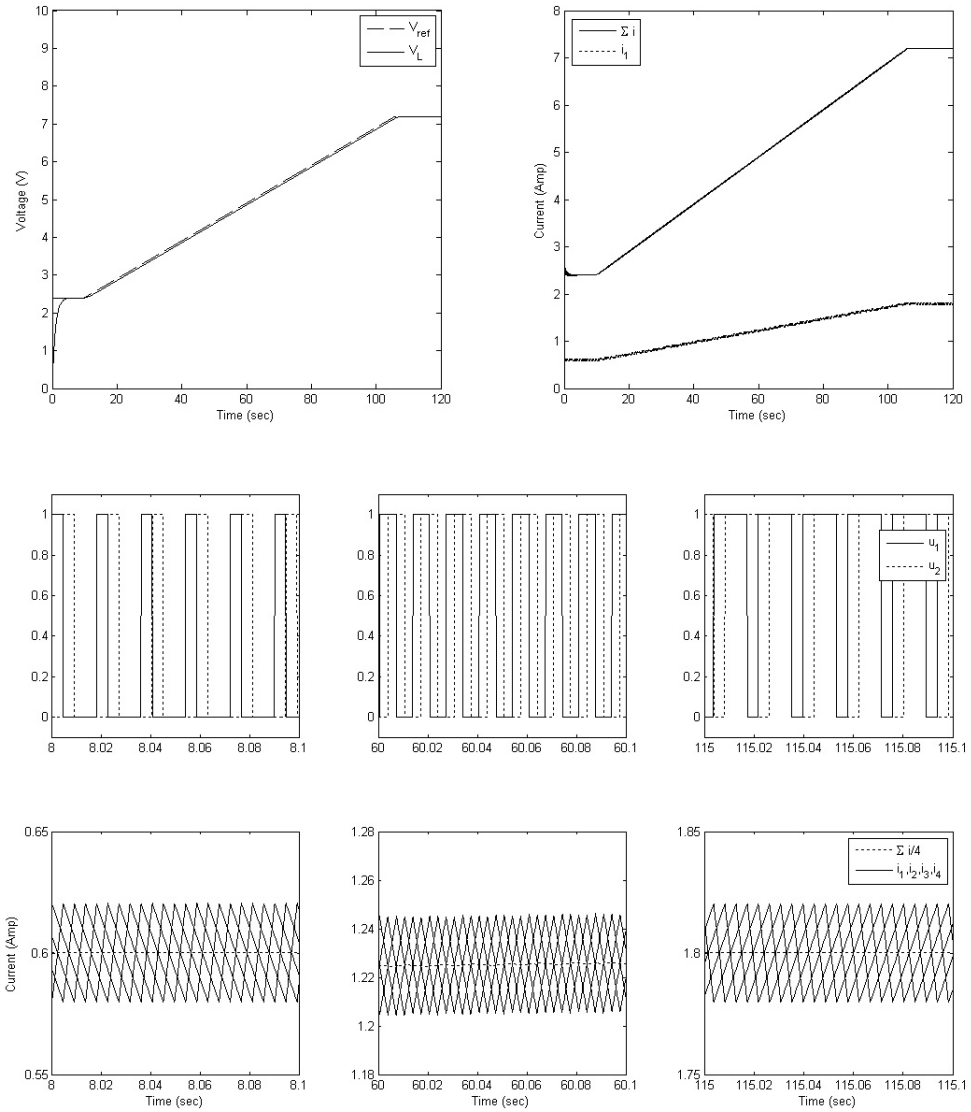
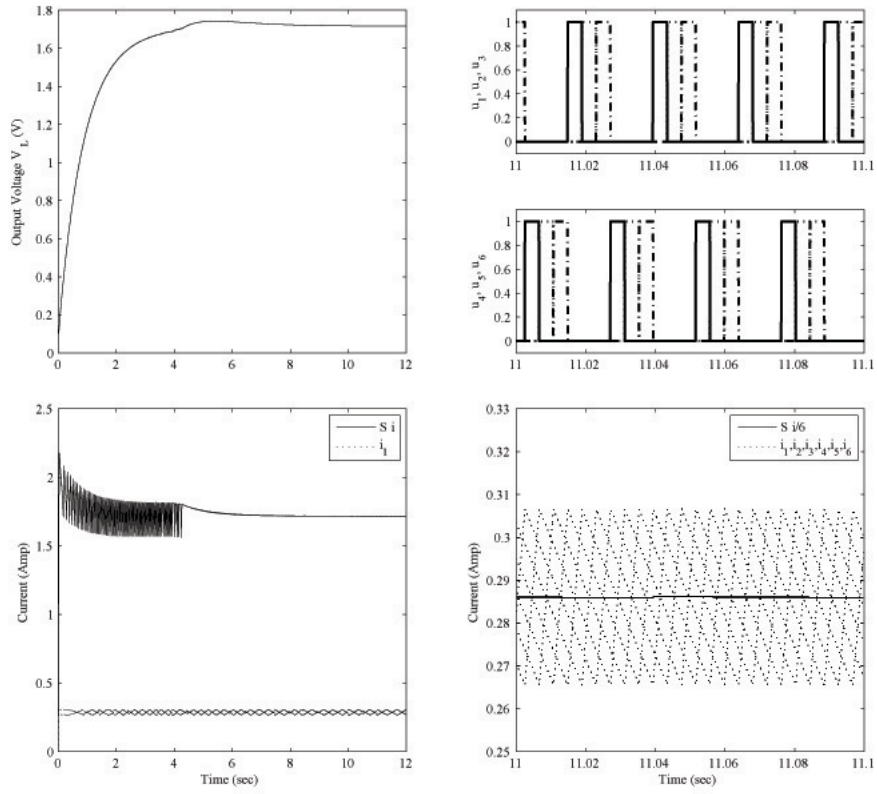Figure 4.20: Simulation result for 4 phases with time-varying $V_{ref}(t)$.

Figure 4.21: Simulation result for 6 phases with control (4.36) when $V_{ref} = 1.714V$ (parameter Set I in Table (4.1), $a = 2/3$, and $S\ i = \sum_{k=1}^{6} i_k$). K is fixed as in (4.31).
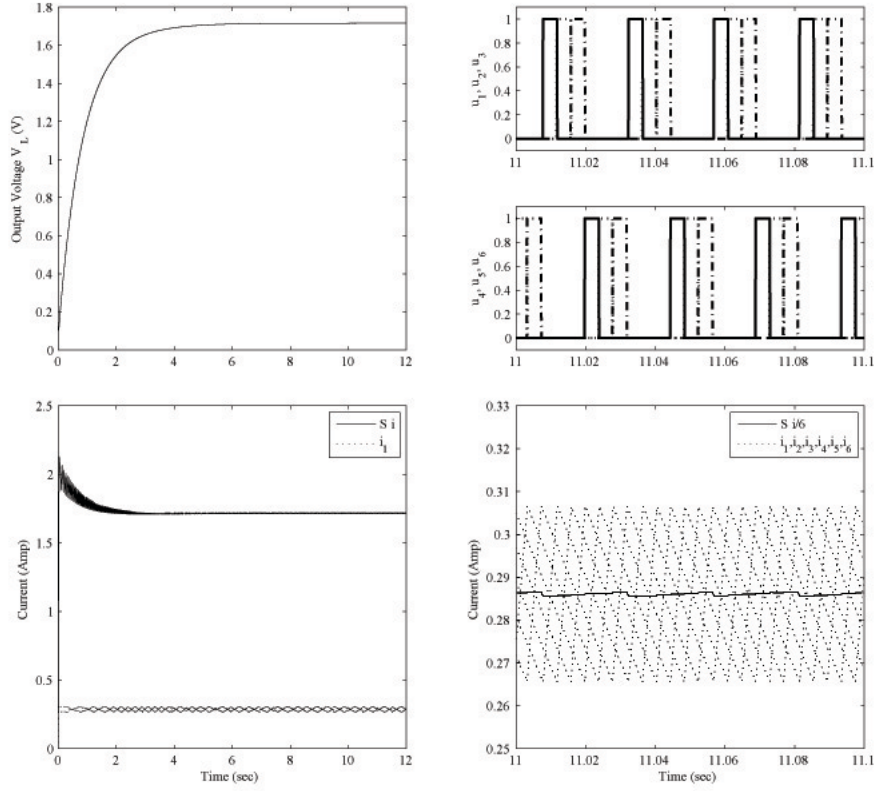
Figure 4.22: Simulation result for 6 phases with control (4.36) when $V_{ref} = 1.714V$ (parameter Set I in Table (4.1), $a = 2/3$, and $S\ i = \sum_{k=1}^{6} i_k$). Chattering level in transient interval is reduced comparing with Fig. (4.21) since K is chosen from (4.26).
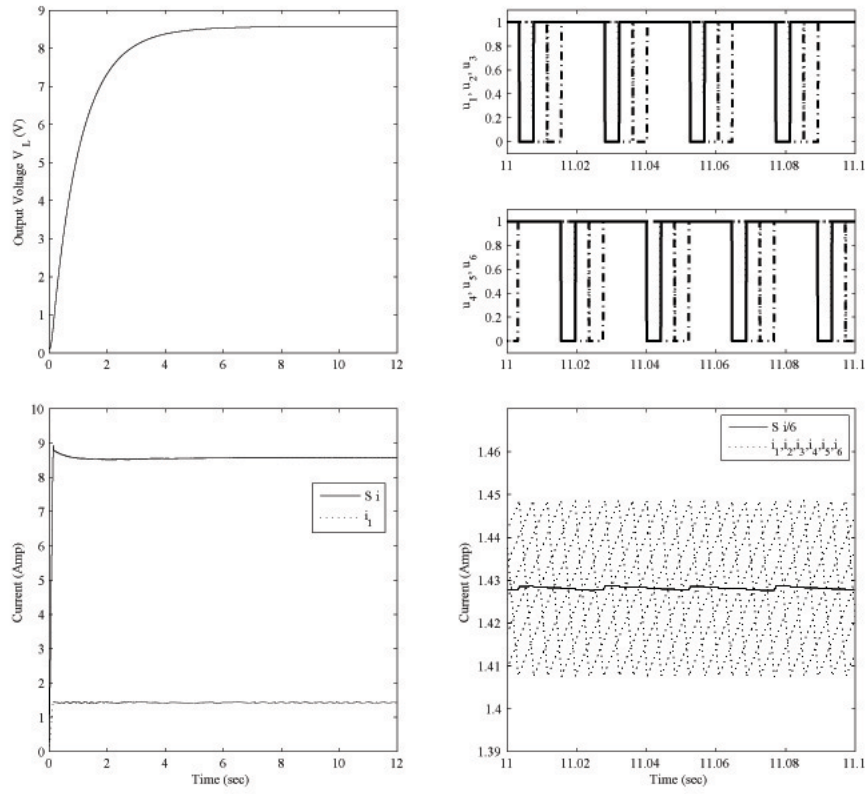
Figure 4.23: Simulation result for 6 phases with control (4.36) when $V_{ref} = 8.571V$ (parameter Set I in Table (4.1), $a = -2/3$, and $S\ i = \sum_{k=1}^{6} i_k$).
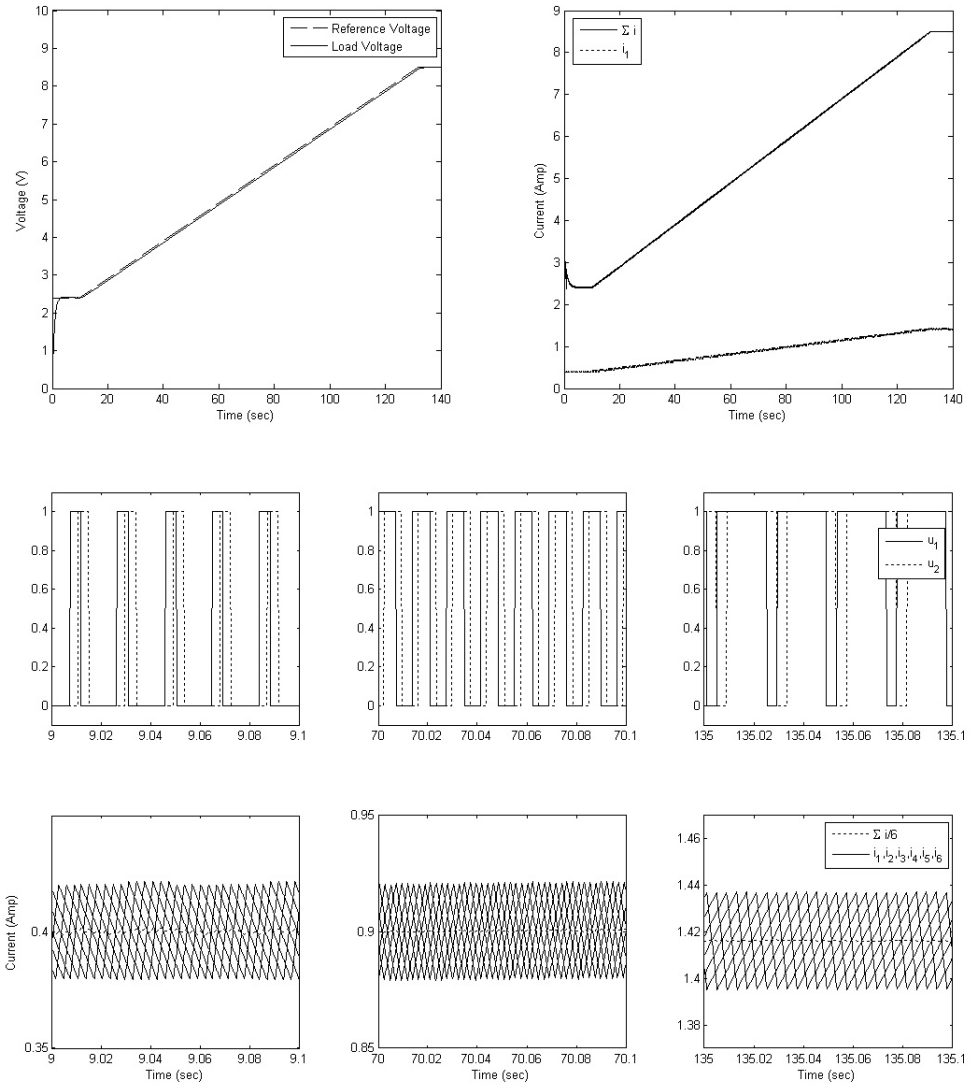
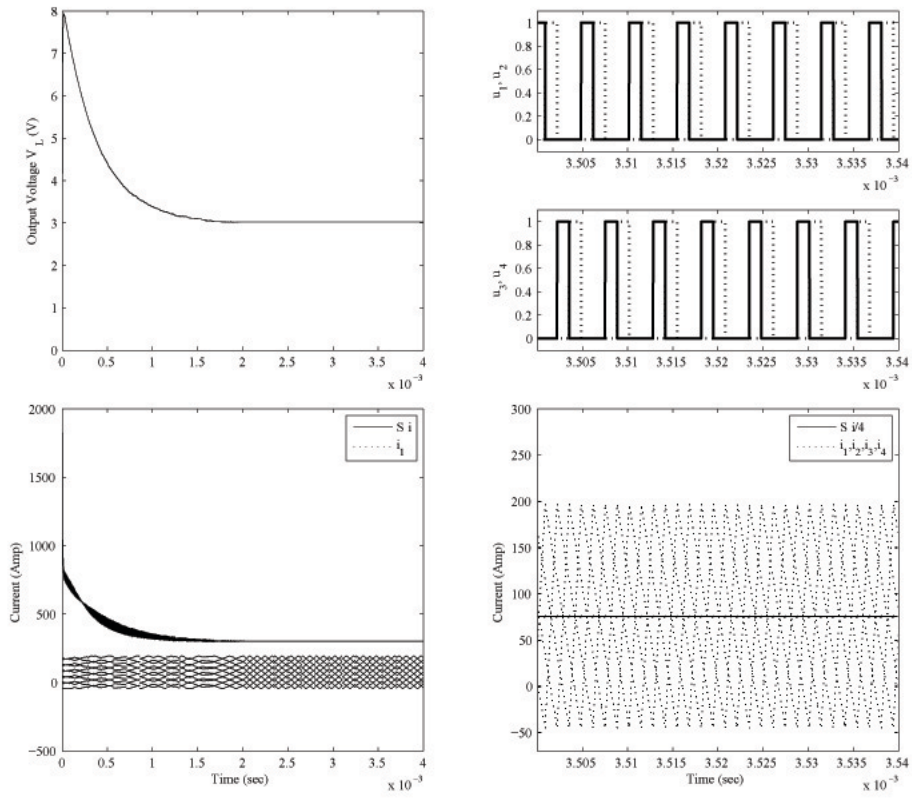Figure 4.24: Simulation result for 6 phases with time-varying $V_{ref}(t)$.

Figure 4.25: Simulation result for 4 phases with control (4.36) when $V_{ref} = 3V$ (parameter Set II in Table (4.1), $S\ i = \sum_{k=1}^{4} i_k$).

Figure 4.26: Simulation result for 4 phases with control (4.36) when $V_{ref} = 6V$ (parameter Set II in Table (4.1), $S\ i = \displaystyle\sum_{k=1}^{4} i_k$).

Figure 4.27: Simulation result for 4 phases with control (4.36) when $V_{ref} = 8V$ (parameter Set II in Table (4.1), $S\ i = \sum_{k=1}^{4} i_k$).
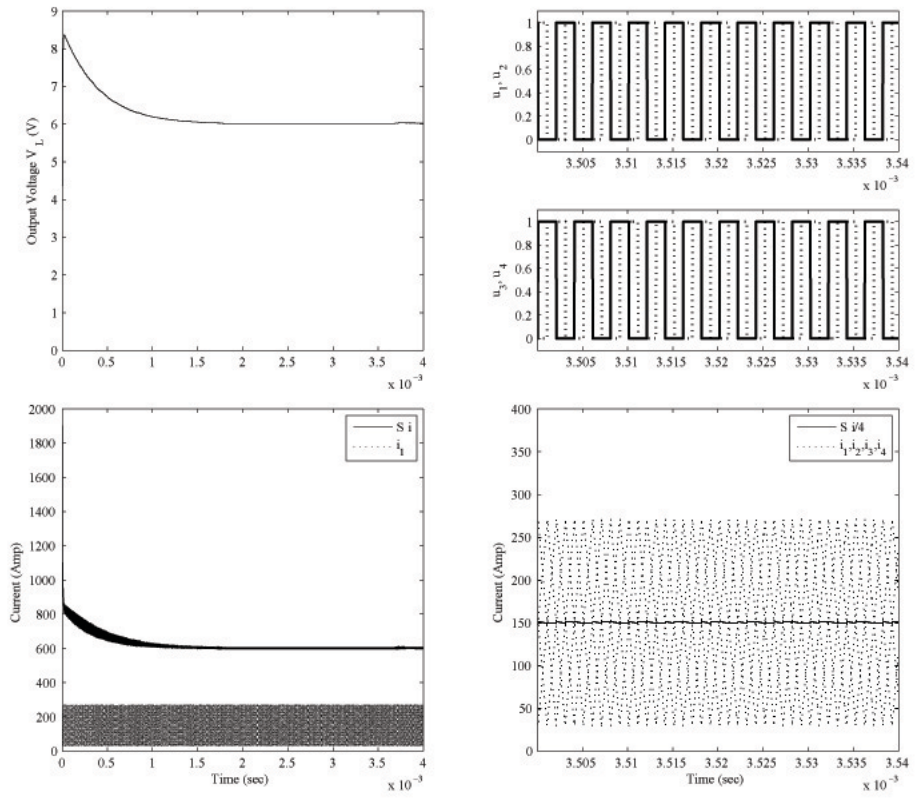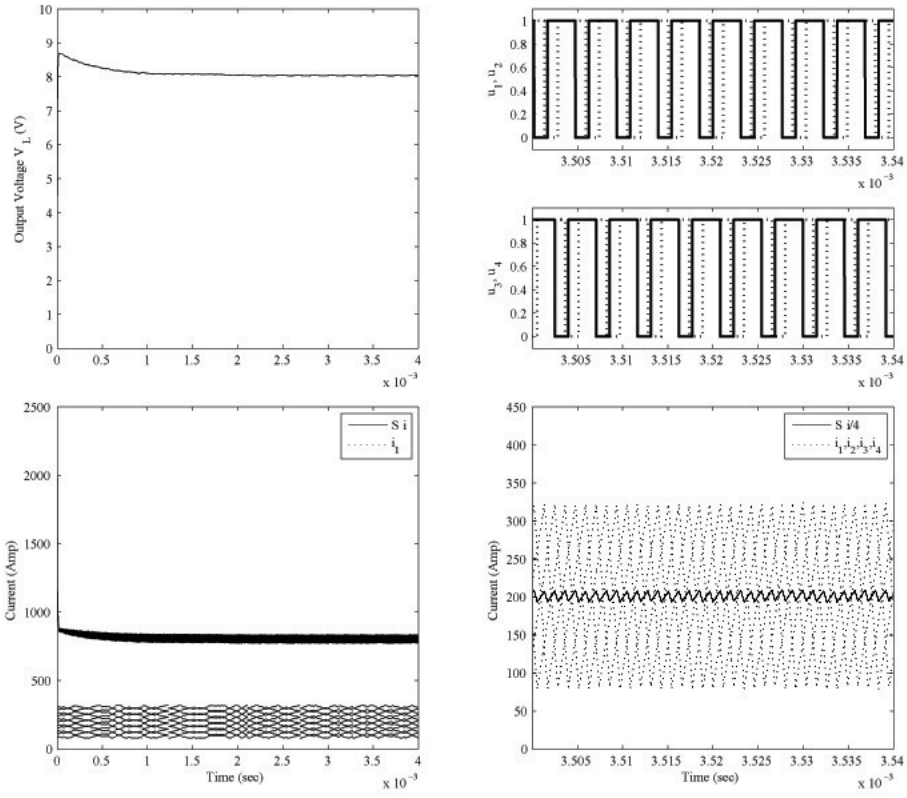
4.7 Chattering reduction under limitation of phase number

Let us assume that there are n phases available. As discussed in earlier section, it is obvious that the effect of chattering suppression in multiphase power converter system can be maximized if two conditions are satisfied:

- There are n phases having phase shift of T/n between two consecutive phases so all the phases are evenly distributed through the period of oscillation.

- Each phase has equal duty cycle $D_n = \frac{1}{n} \times 100\%$, which implies that the sum of duty cycles of individual channel is equal to 100%.

For system (4.33) with control (4.36) in master-slave mode, the conditions are fulfilled simultaneously by using the methodology proposed in previous sections only if

$$|a| = \left(1 - \frac{2}{n}\right) \ (n \geq 2) \tag{4.38}$$

where $a = \left(\frac{V_s}{2L} - \frac{I_{ref}R_a}{mL} - \frac{V_L}{L}\right)\left(\frac{2L}{V_s}\right)$.

Let us consider the case that there are two phases in master-slave mode and the duty cycle of each phase happens to be $D = 0.33\%$. In order to maximize chattering reduction, three phases are needed, but only two phases are available for a certain limitation. As mentioned in previous section, $a = 0$ is only admissible value for two phases to have the same period of oscillation. However, the system is out of the admissible range from (4.25) for the duty cycle; therefore, the gain K in (4.36) should be selected as

$$K = \frac{1 + |a|}{2} \tag{4.39}$$

according to (4.37) ($M = 1$). Then, switching commands for the two phases occur as can be seen in Figure (4.28). In this case, one can find that none of the two
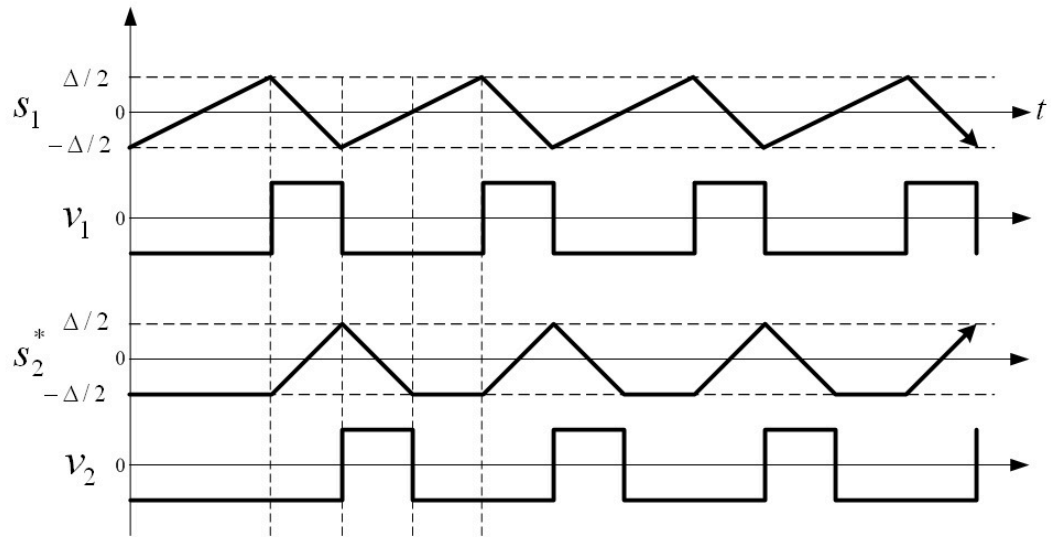
Figure 4.28: Switching commands v_1 and v_2 for two phases when duty cycle is $1/3$ $(K = \frac{1+|a|}{2})$.

conditions mentioned in the beginning of this section are satisfied; however, some level of chattering reduction is still expected since at least amplitude of $i_1 + i_2$ will not be greater than that of $2i_1$ or $2i_2$.

The magnitude of chattering is minimized by using 8-phase power converter as depicted in Figure (4.29) since the two conditions are fulfilled. But, if only four phases are available, level of ripple is comparably high even though the gain K is selected as (4.39) as can be observed in (4.30).

To improve chattering suppression in case that there are not enough phases available, the following method is proposed. Being different from (4.37) ($M = 1$), the gain K for master-slave mode implementation is selected as

$$K = \frac{n(1 - a^2)}{4} \tag{4.40}$$

even if $|a| > (1 - 2/n)$. Then the switching sequence shown in (4.10) is collapsed, and the period of switching command is changed from the second switching as can be seen in Figure (4.31). The main reason of this collapse is caused by the fact that the second switching is delayed due to speed ds_2^*/dt is not fast enough. This phenomenon may be fixed by increasing the speed of s_2^* or decreasing the width of hysteresis for s_2^* such that switchings occur consequently as originally designed. In master-slave mode for n number of phases, speed of slave channels can be adjusted as follows.

$$
\begin{aligned}
u_1 &= V_s \frac{1-sign(s_1)}{2}, \quad u_k = V_s \frac{1-sign(s_k^*)}{2}, \quad (k = 1, \cdots, n) \\
\dot{s}_1 &= -b_1 sign(s_1) - b_2 s_1 + a^* \\
\dot{s}_2^* &= K^* b_1 [sign(s_1) - sign(s_2^*)] \\
\dot{s}_k^* &= K^* b_1 [sign(s_{k-1}^*) - sign(s_k^*)]
\end{aligned}
\tag{4.41}
$$

Figure 4.29: Simulation results of 8-phase power converter. $V_s = 12V$, $V_{ref} = 1.5V$, $R_L = 1m\Omega$, and other parameters are specified in Set II of Table (4.1).
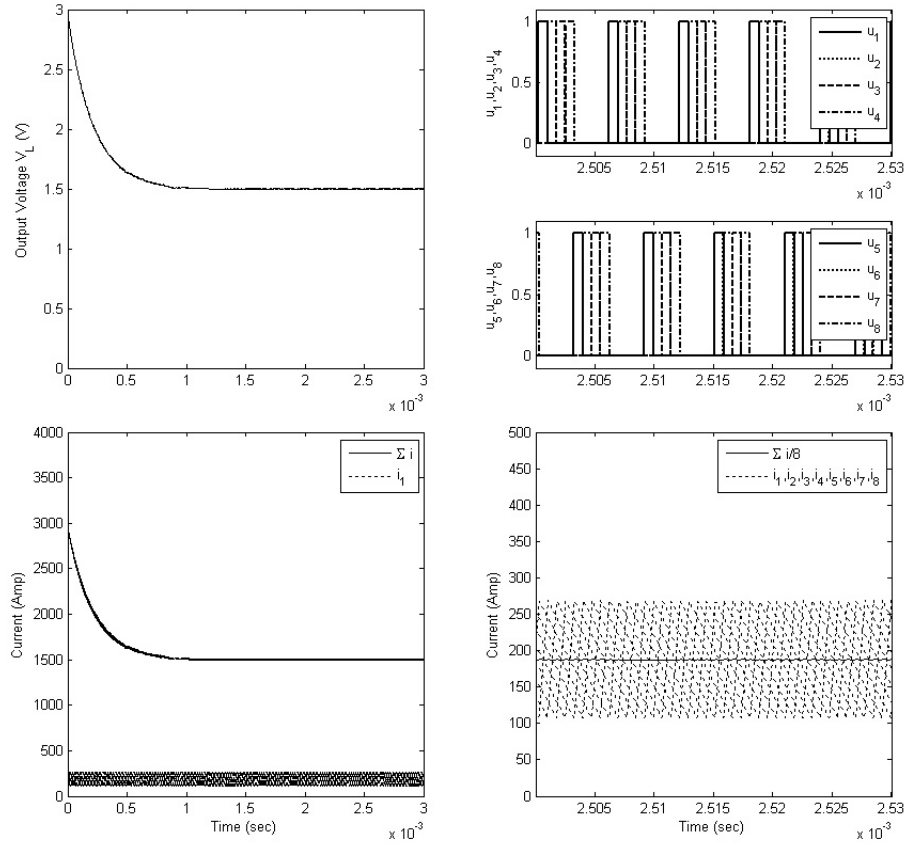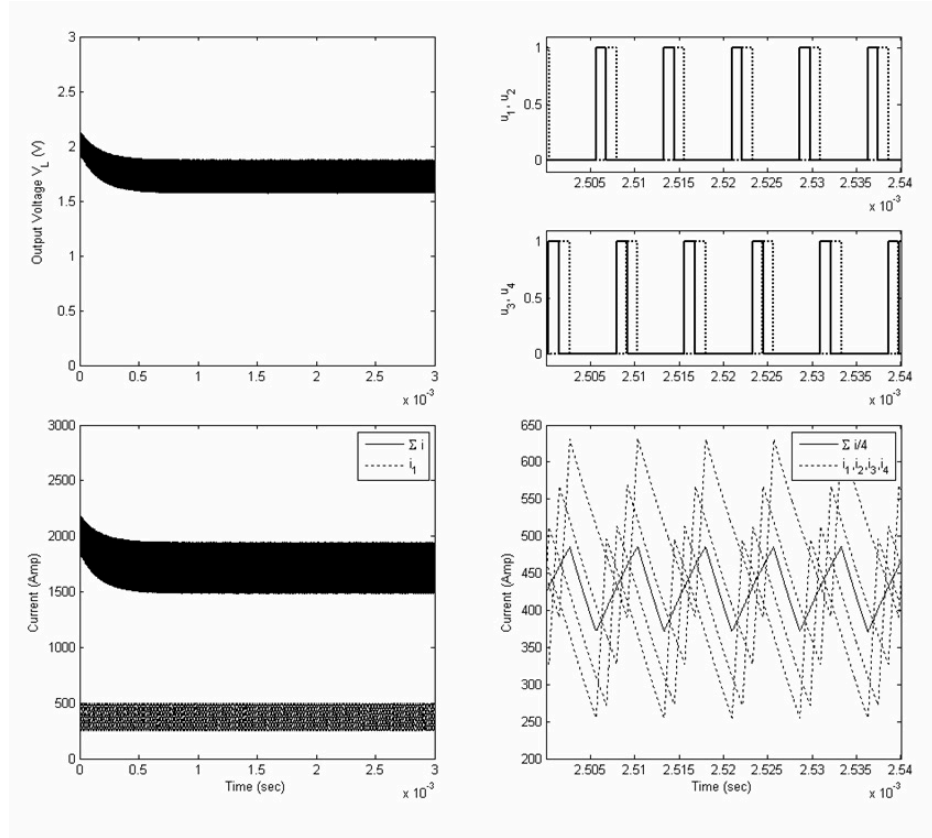
Figure 4.30: Simulation results of 4-phase power converter. $V_s = 12V$, $V_{ref} = 1.5V$, $R_L = 1m\Omega$, and other parameters are specified in Set II of Table (4.1).
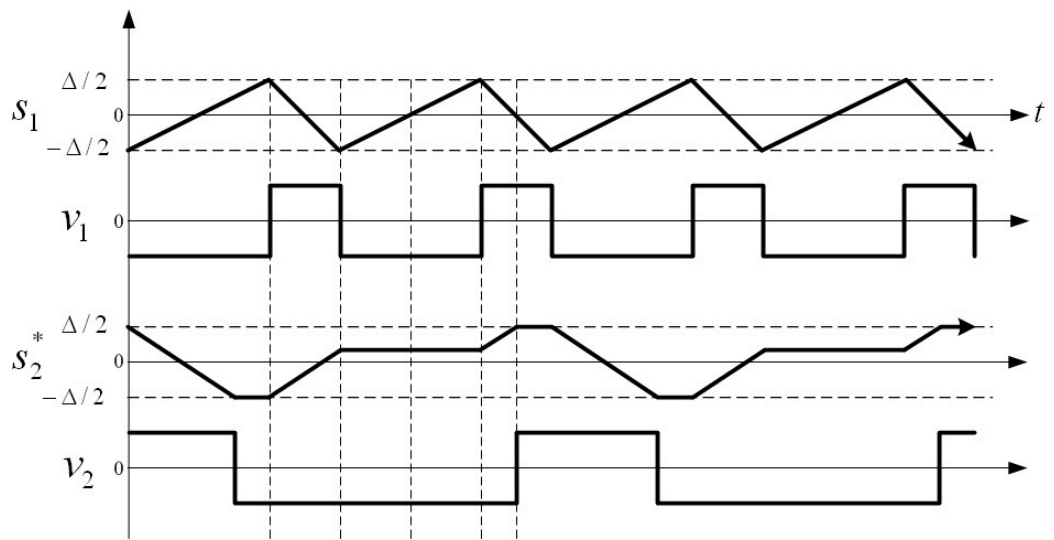
Figure 4.31: Switching commands v_1 and v_2 for two phases when duty cycle is $1/3$ $(K = \frac{n(1-a^2)}{4}, \ n = 2)$.

and $K^* = 3K$. Then period of oscillations in s_1 and s_2^* are the same as can be seen in Figure (4.32), and the phase difference between corresponding switchings v_1 and $v_{2,1}$ is found as

$$\phi = \frac{\Delta}{2K^*} = \frac{\Delta}{6K}. \tag{4.42}$$

From (4.40) and (4.15) for $M = 1$, the gain K becomes $K = \frac{n\Delta}{2T}$; therefore, (4.43) can be rewritten as

$$\phi = \frac{T}{3n} \tag{4.43}$$

which means that it is possible to have phase shift of T/n if two more subsystems are combined together as illustrated in Figure (4.32). As can be seen in Figure (4.33), the phase shift between two channels becomes T/n with the help of additional subsystems, and it is noted that the first condition mentioned in the beginning of this section is satisfied. A simulation is performed for a 4-phase power converter with the application of proposed methodology. Comparing to the results shown in Figure (4.30), it is observed that the effect of chattering reduction is improved by suggested method even though the ripple magnitude is higher than that of 8-phase converter model in Figure (4.29).

4.8 Chattering reduction for systems with dynamic loads

In previous sections of this chapter, it is shown that the level of chattering can be reduced by using multiple phases with phase shift method for power converter systems with resistance as loads. In this section, chattering suppression in similar systems with dynamic loads is discussed.

We may consider a DC motor operated by an external RLC circuit with on/off switching as illustrated in Figure (4.35). One can easily find that the structure of
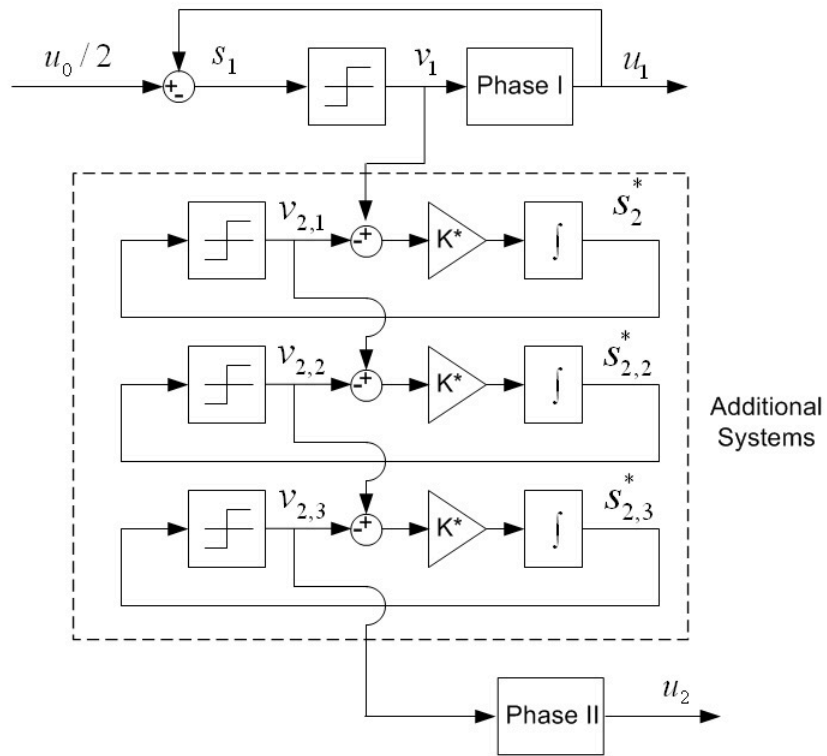
Figure 4.32: A modified master-slave mode schematic with two more additional systems. $v_{2,3}$ is switching command for the second channel.
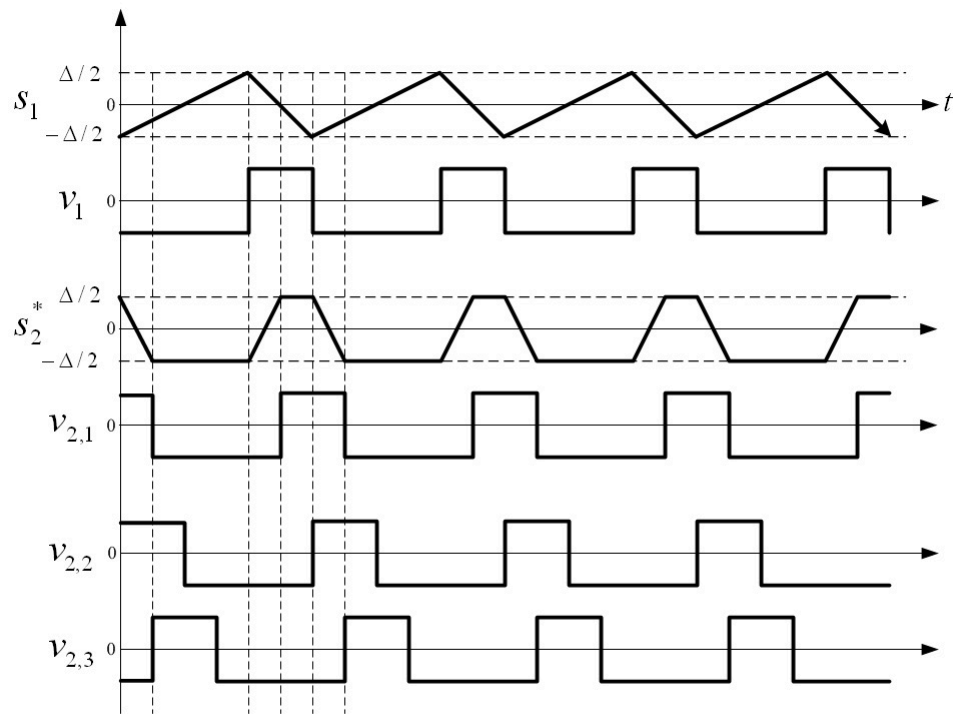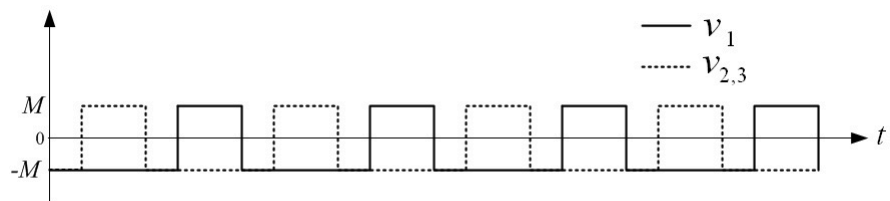
Figure 4.33: (a) Switching commands v_1, $v_{2,1}$, $v_{2,2}$, and $v_{2,3}$ for two phases when duty cycle is $1/3$ ($K^* = \frac{3n(1-a^2)}{4}$, $n = 2$). (b) With the help of two additional systems, $v_{2,3}$ is phase-shifted from v_1 by T/n.
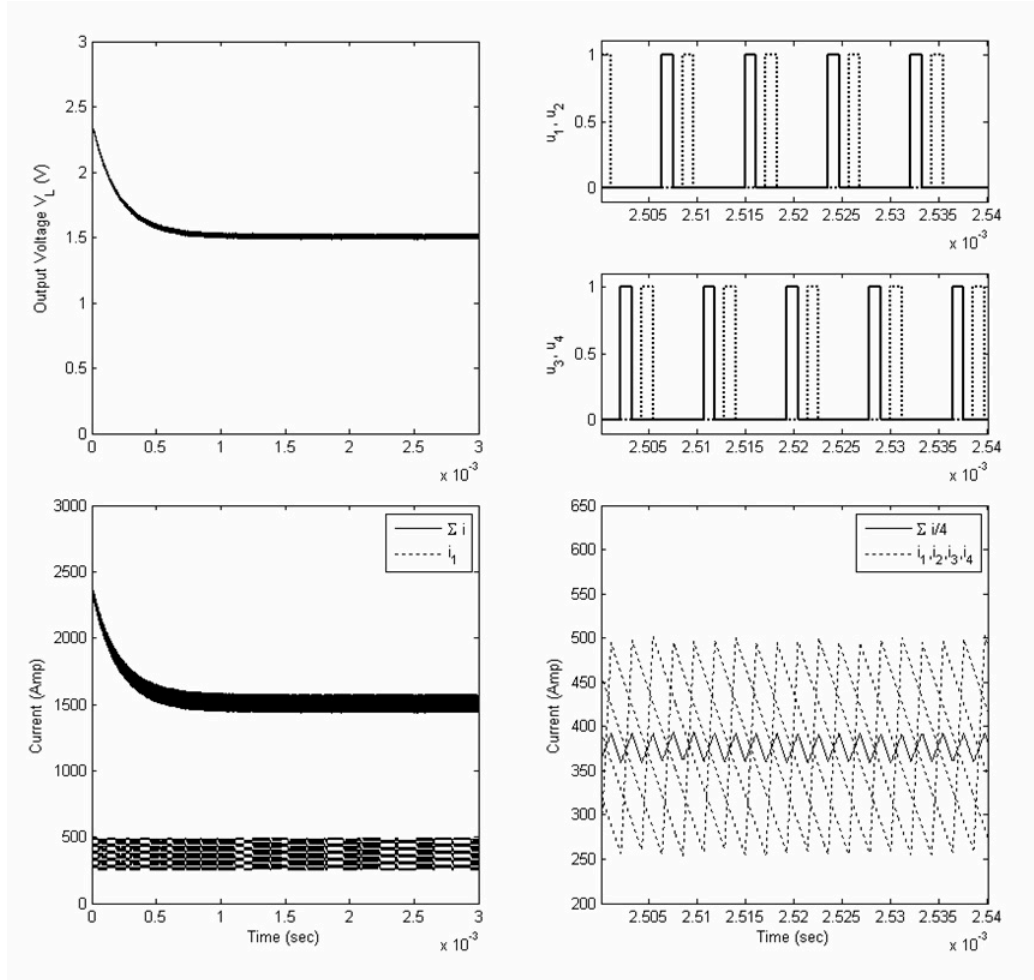
Figure 4.34: Simulation results of 4-phase power converter in modified structure as shown in Figure (4.32). $V_s = 12V$, $V_{ref} = 1.5V$, $R_L = 1m\Omega$, and other parameters are specified in Set II of Table (4.1).

Figure 4.35: A DC motor operated by an external circuit. (a) The external circuit has single module. (b) The external circuit consists of m modules.

external circuit is very similar to the one of DC-DC power converter depicted in Figure (1.3), and the only difference is that the load resistance is now replaced by DC motor system which is governed by following equations
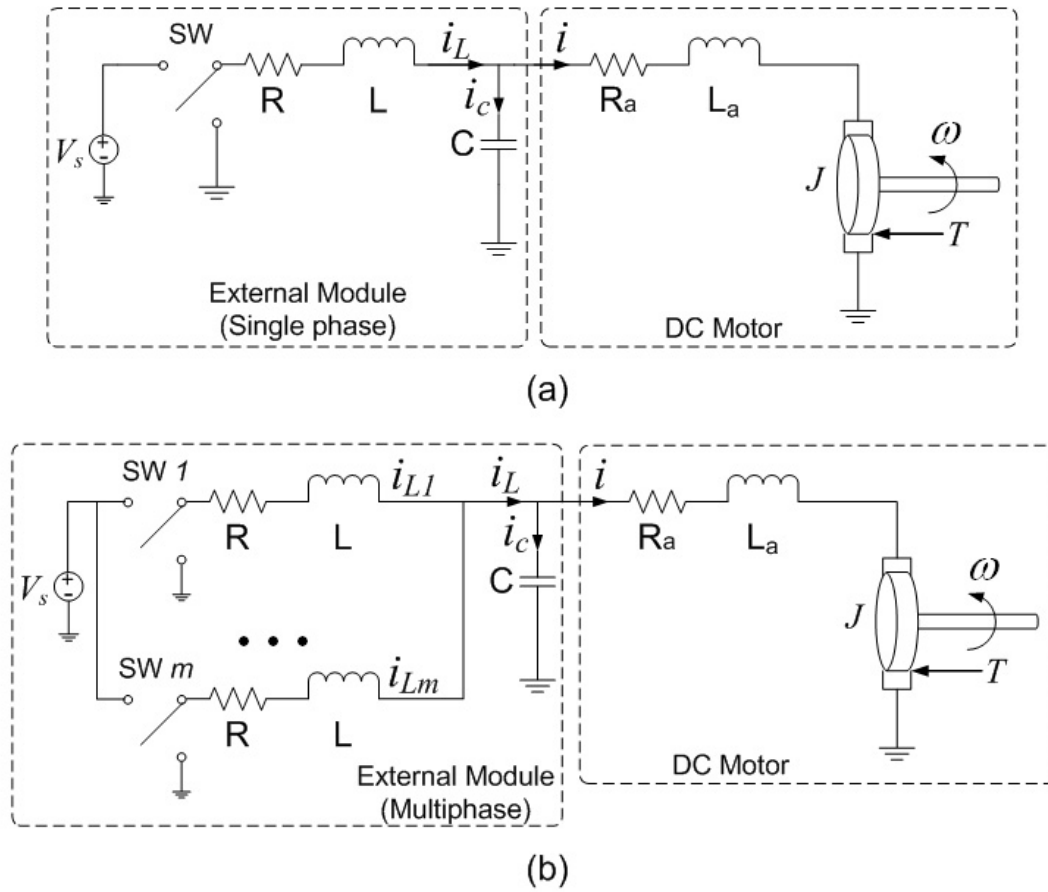
$$
\begin{aligned}
L_a \frac{di}{dt} &= -R_a i - K_e \omega \\
J \frac{d\omega}{dt} &= K_t i - B\omega
\end{aligned}
\tag{4.44}
$$

where

L_a = armature inductance

i = armature current

R_a = armature resistance

K_e = back EMF constant

J = total inertia

ω = shaft speed

K_t = torque constant

B = friction coefficient.

And the dynamics of external circuit module having m phases can be written as

$$
\begin{aligned}
L \frac{di_{Lj}}{dt} &= -R i_{Lj} - V_c + V_s u_j \quad (j = 1, \ldots, m) \\
C \frac{dV_c}{dt} &= i_L - i \quad \left(i_L = \sum_{j=1}^{m} i_{Lj}\right)
\end{aligned}
\tag{4.45}
$$

where

L = inductance in external circuit

R = resistance in external circuit

i_{Lj} = current through inductance in j-th phase

V_s = source voltage

u_j = switching command for j-th phase

V_c = voltage across capacitance.

To control DC motor speed ω, so-called the cascade control principle is used. The motor current is considered as and intermediate control and designed as a function of motor speed mismatch. Then, control is designed to reduce the difference between real and desired values of the current to zero in sliding mode. For the system of one phase with PI controller, a control law may be designed as

$$
\begin{aligned}
e &= \omega^* - \omega \\
f(e) &= c_1 e + c_2 \int e \, dt \\
s &= i_{L1} - \frac{f(e)}{m} \\
u_1 &= \frac{1 - sign(s)}{2}
\end{aligned}
\tag{4.46}
$$

where c_1 and c_2 are constant, and ω^* is desired motor shaft speed. Note that $i_L = i$ in steady state. The frequency of switching devices in the external circuit is limited, which leads to chattering in DC motor current i and external circuit current i_L. Other modules in external operation circuit are connected to the first module in parallel as shown in DC-DC power converter model provided earlier. Thus, assuming that all the switching elements have hysteresis loops with the same width, the switching command from u_2 to u_m may be obtained from u_1 in the manner of master-slave mode discussed in previous sections in this chapter as follows

$$
\begin{aligned}
s_1 &= s \\
\dot{s}_k &= K[sign(s_{k-1}) - sign(s_k)] \quad (k = 2, \ldots, m) \\
u_k &= \frac{1 - sign(s_k)}{2}
\end{aligned}
\tag{4.47}
$$

and a phase shift between two consecutive phases to bring the ripple cancellation is achieved by finding proper value of K.

A simulation is performed to verify the design principle, and the parameters used are $L_a = 0.1$ mH, $R_a = 1.6$ Ω, $K_e = 0.0353$ V·sec/rad, $J = 0.0241$ in·oz·sec^2, $K_t = 5$ in·oz/amp, $B = 0.0134$ in·oz·sec/rad, $L = 0.1$ μH, $R = 0.01$ Ω, and $V_s = 20$ V. As can be seen in Figure (4.36) (2 phases) and (4.37) (4 phases), amplitudes of chattering in motor current and external circuit current are nearly eliminated by applying proposed methodology with multiple phases.

The idea of chattering suppression for cascade control can be generalized easily for the system in the regular form [1]:

$$
\begin{aligned}
\dot{x}_1 &= f_1(x_1, x_2) \\
\dot{x}_2 &= f_2(x_1, x_2) + bu \quad (x_1 \in \Re^{n-1},\ x_2, u \in \Re).
\end{aligned}
\tag{4.48}
$$

The fictitious control $x_2 = v(x_1)$ is selected as a function of x_1, and the real control is designed to enforce sliding mode in the surface $s = x_2 - v(x_1) = 0$. Again, the control u can be implemented using m phases similarly to what was designed for DC motor.

4.9   The equivalent width of hysteresis method for systems with unmodeled dynamics

Let us assume that there exist unmodeled dynamics in power converter system (4.33) with control (4.36), and they are supposed to be dynamics of a sensor to measure current in the first phase I_1 disregarded in system model. Then, the switching command
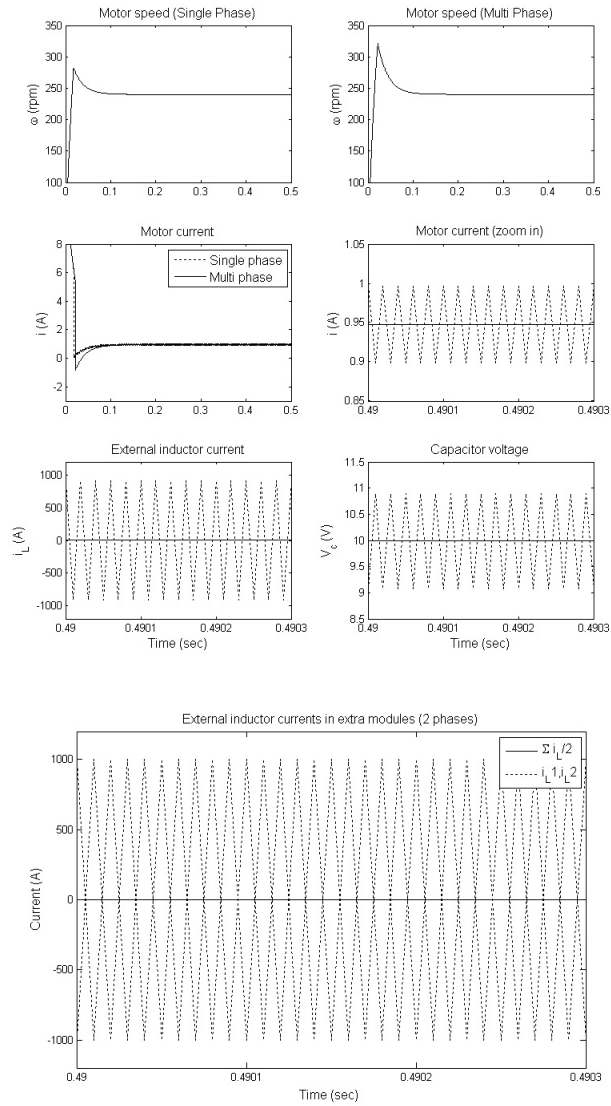
Figure 4.36: Simulation results for a DC motor operated by external modules ($m = 2$, $\omega^* = 240$ rpm).
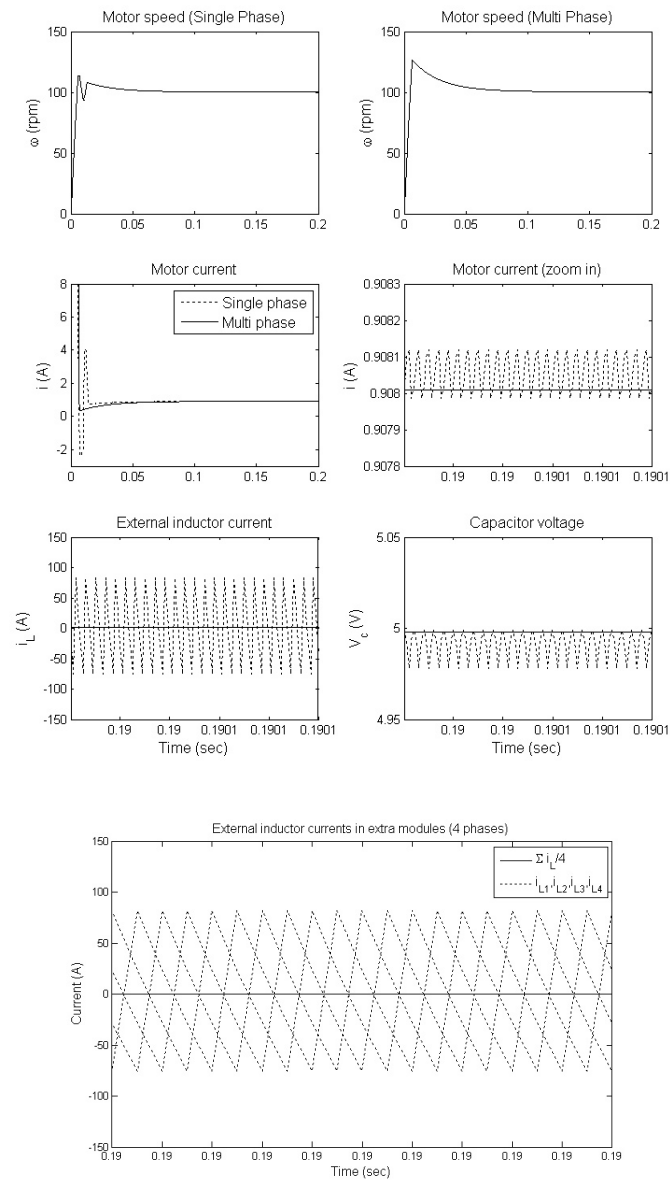
Figure 4.37: Simulation results for a DC motor operated by external modules ($m = 4$, $\omega^* = 100$ rpm).
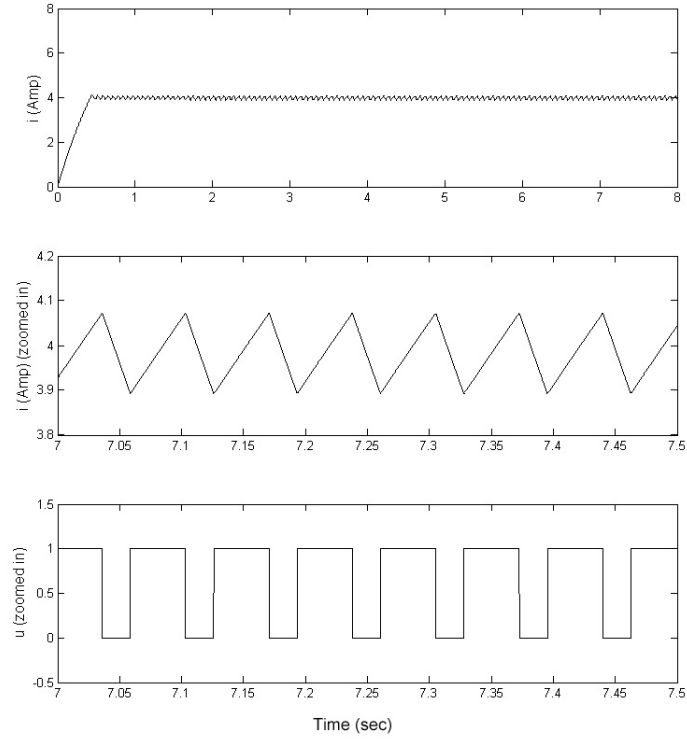
Figure 4.38: Chattering in load current due to unmodeled dynamics (single phase).

u_1 in (4.34) becomes

$$s_1 = \tilde{I}_1 - \frac{I_{ref}}{m}, \quad I_{ref} = \frac{V_{ref}}{R_L}$$
$$u_1 = V_s \frac{1 - sign(s_1)}{2} \tag{4.49}$$

where $\tilde{I}_1$ is a distorted measurement due to the unmodeled dynamics. The unmodeled dynamics discussed in this section are supposed to have the structure provided in (2.2). As analyzed in previous chapters, chattering occurs in load current as depicted in Figure (4.38), and the switching frequency of u_1 depends on the time constant value of the unmodeled dynamics. Note that there is no frequency control using hysteresis loop for the first phase. Assuming that the switching frequency can be

117

measured experimentally or estimated as in [69] or found analytically as proposed in chapter 2, a width of hysteresis in the second phase may be found such that the first and the second phase have the same switching frequency, and let us call the width of hysteresis in this case "the equivalent width of hysteresis". If there are m phases in the system, switching frequency of the first phase is determined by the parameter of unmodeled dynamics, and switchings in all the other phases from the second to the m-th will be in the same frequency if the equivalent width of hysteresis is applied to switching elements for the phases. Then, the desired phase shift between two consecutive phases is achieved by the methodology provided in the previous section. Figure (4.39) illustrates simulation results of two-phase converter, and it is observed that chattering in load current which is caused by unmodeled is nearly eliminated by using multiple number of phases with the equivalent width of hysteresis. When the duty cycle of switching command is different from 50%, number of phases needed to suppress chattering may be found by the method suggested in the section for selection of phase number.

Let us consider the DC motor system from the previous section. It is assumed that there exist unmodeled sensor dynamics in reading external inductance current as depicted in Figure (4.40) (c), then the sliding mode control in (4.46) becomes

$$
\begin{aligned}
s &= \tilde{i}_{L1} - \frac{f(e)}{m} \\
u_1 &= V_s sign(s)
\end{aligned}
\tag{4.50}
$$

where $\tilde{i}_{L1}$ is a distorted measurement due to the unmodeled dynamics, and chattering appears. Again, two phases are utilized to suppress chattering. The second phase has the equivalent width of hysteresis, and phase shift is obtained by using master-slave mode connection. As can be seen in Figure (4.41), chattering in motor shaft speed
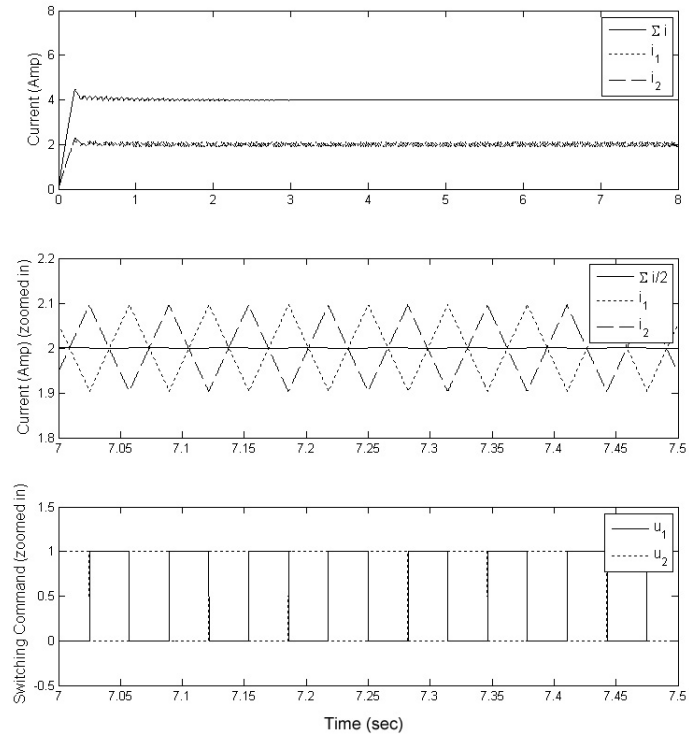
Figure 4.39: Chattering in load current due to unmodeled dynamics is suppressed by using two phases.
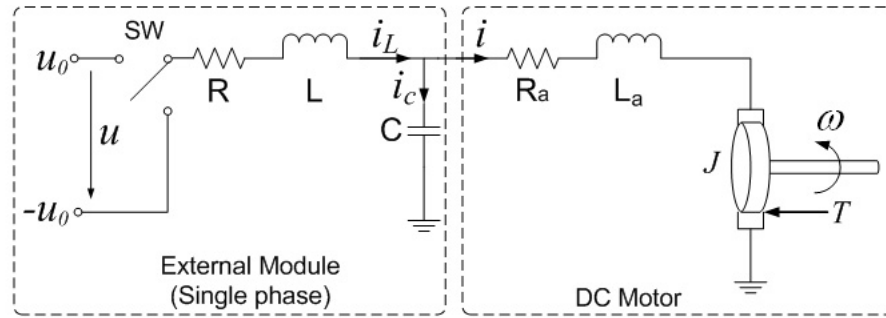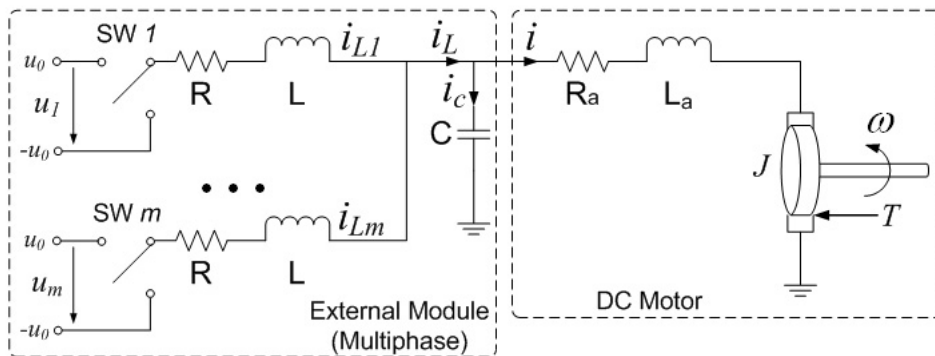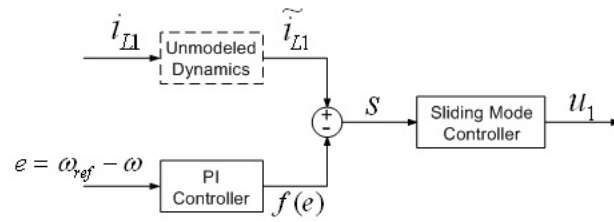
Figure 4.40: A DC motor operated by an external circuit. (a) The external circuit has single module. (b) The external circuit consists of m modules (c) Unmodeled dynamics in measurement of i_{L1}.
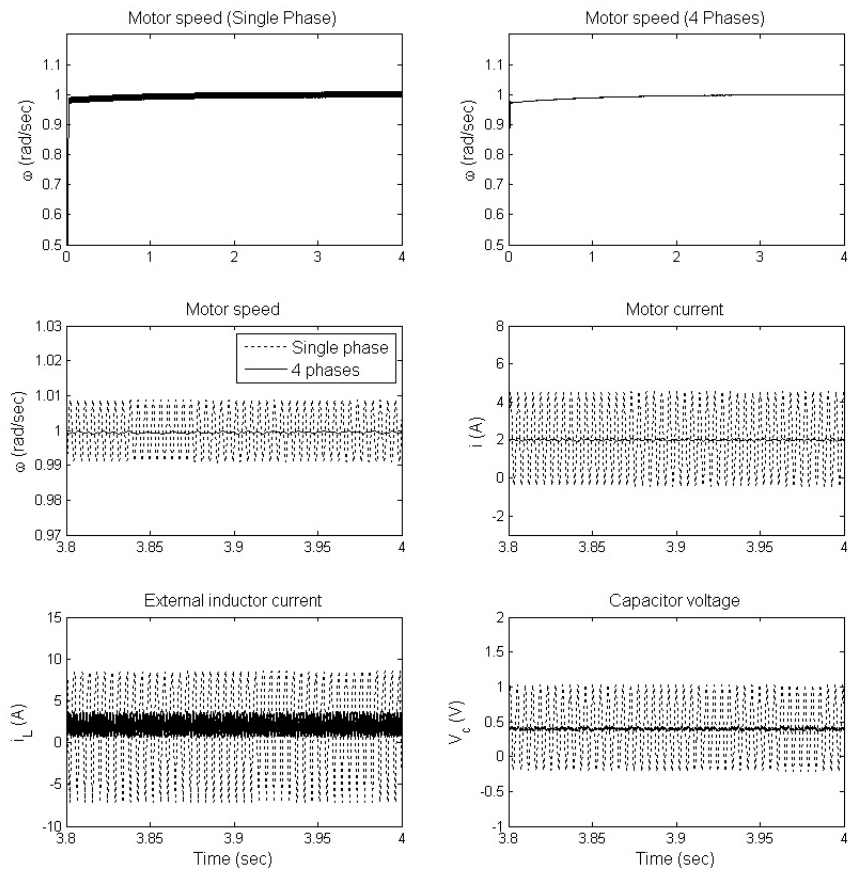
Figure 4.41: Simulation result of DC motor depicted in Figure (4.40).
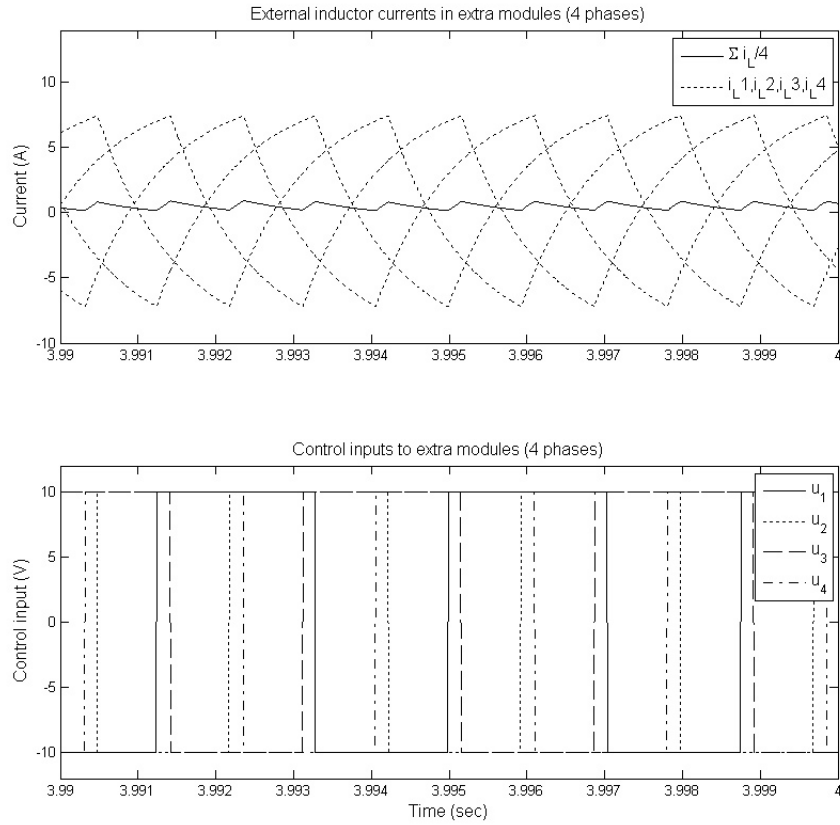
Figure 4.42: Simulation result shows ripple cancellation by 4 phases in DC motor system.

is nearly eliminated, and levels of current in motor and external circuit is greatly reduced by using the proposed methodology. The ripple cancellation effect with 4 phases can be observed in Figure (4.42).

Finally, one more example of the systme unmodeled dynamics:

$$
\begin{aligned}
\dot{x} &= a_1 x^2 \sin x + a_2 y \quad \text{(Block 1)} \\
\dot{y} &= b_1 y + b_2 x + u \quad \text{(Block 2)}.
\end{aligned}
\tag{4.51}
$$

The system state y in the first equation can be regarded as a fictitious control to obtain desired motion in x based on the cascade control principle. A sliding mode control for the system is designed as follows.

$$
\begin{aligned}
s &= y - y^* \\
u &= -M sign(s) \\
y^* &= -\frac{a_1}{a_2} x^2 \sin x - \frac{c}{a_2} x \quad (a_2 \neq 0)
\end{aligned}
\tag{4.52}
$$

where M and c are positive constant. By selecting proper value of M, sliding mode may be enforced to occur along the sliding surface $s = 0$, then y becomes y^*. Thus, the motion of equation becomes $\dot{x} = -cx$, and x is stabilized. Now it is assumed that there exist unmodeled sensor dynamics in measuring y, which implies that the sliding surface changes to $s = \tilde{y} - y^* = 0$ where $\tilde{y}$ is the output from the unmodeled dynamics as depicted in Figure (4.43) (a), and consequently chattering may appear in the system state x as can be seen in Figure (4.44). Now, it is assumed that additional subsystem modules may be attached to the original system to utilize multiple phases as illustrated in Figure (4.43) (b). One can find that the structure is not different from the master-slave mode connection in a power converter system. Then, with m
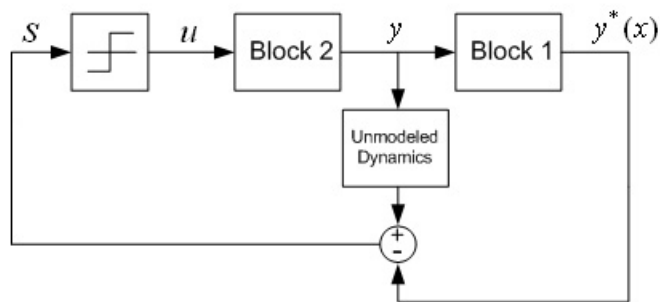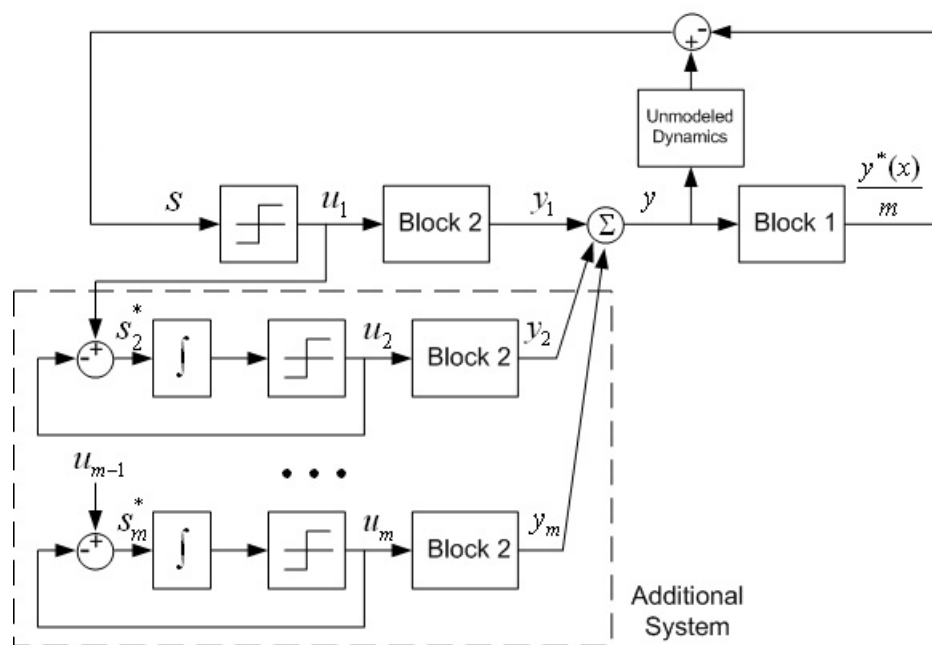
Figure 4.43: (a) Block diagrams of system (4.51). (b) The system has additional modules to suppress chattering. Note that the relay for u_1 does not have hysteresis while the others have hysteresis loops with the equivalent width.
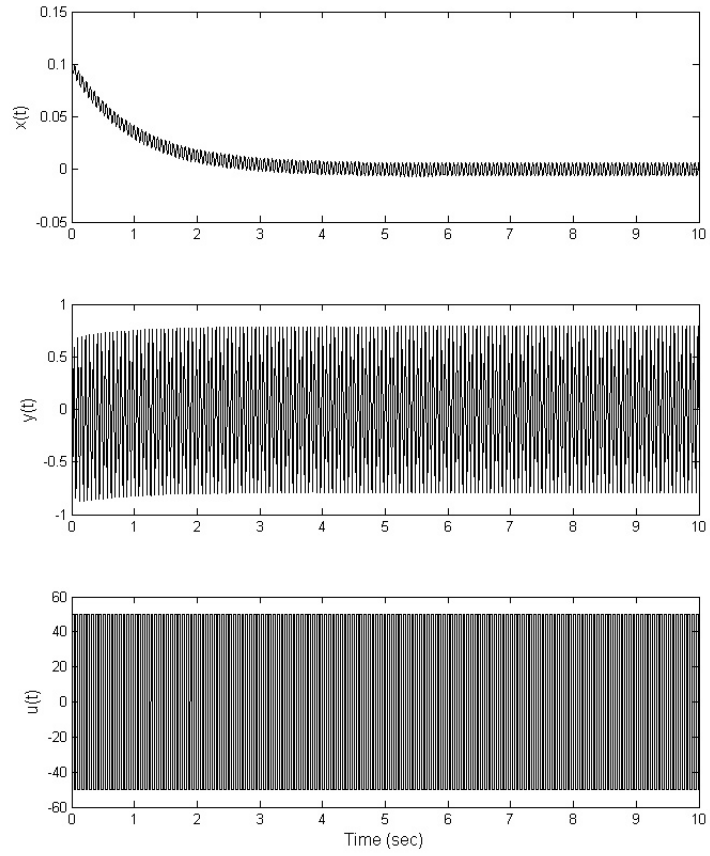
Figure 4.44: Simulation result of system (4.51) with control (4.52) in the presence of unmodeled dynamics.

modules for Block 2, the system equations (4.51) become

$$\dot{x} = a_1 x^2 \sin x + a_2 \sum_{j=1}^{m} y_j$$

$$\dot{y}_k = b_1 y_k + b_2 x + u_k \quad (k = 1, \ldots, m)$$

(4.53)

and controller is designed as

$$s_1 = y - \frac{y^*}{m}$$

$$y^* = -\frac{a_1}{a_2} x^2 \sin x - \frac{c}{a_2} x \quad (a_2 \neq 0)$$

$$\dot{s}_n = K\{sign(s_{n-1}) - sign(s_n)\} \quad (n = 2, \ldots, m)$$

$$u_n = -M sign(s_n)$$

(4.54)

and the gain K can be found to have desired phases shift. Figure (4.45) shows that chattering in system state x is almost eliminated by using 2 modules.

In this chapter, chattering reduction methods based on the idea of ripple cancellation is proposed, and simulation results for various systems confirm that the level of chattering may be decreased by multiple phases having proper phase shift with the help of adaptation in hysteresis loop. As it was discussed previously, the design methodology can be used for the systems of an arbitrary order in the regular form with scalar control. To apply the proposed methods to real systems, control can be implemented in low-power parts using amplifiers.
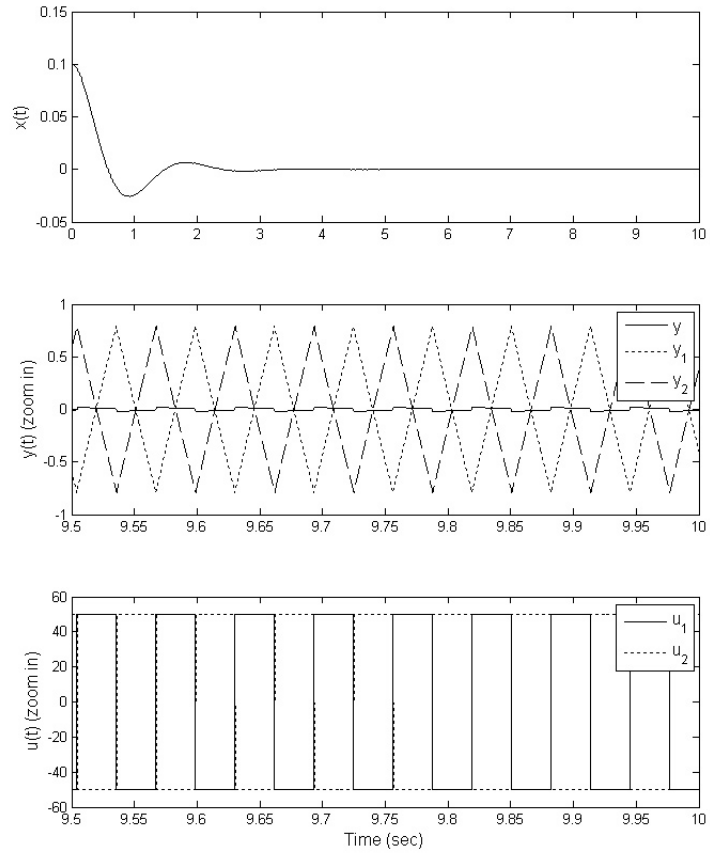
Figure 4.45: Simulation result of system (4.53) with control (4.54) in the presence of unmodeled dynamics when there are two phases.

CHAPTER 5

SUMMARY AND FUTURE WORK

The main obstacle in sliding mode implementation is chattering. One of the reasons that cause the chattering is certain dynamics disregarded in ideal model which may be excited by discontinuous control.

In this dissertation, the method based on the describing function approach was developed for chattering analysis of the system in the presence of unmodeled dynamics. Adopting the concept of the describing function method, it has been shown that the amplitude of chattering is proportional to relay gain in sliding mode control and also that the chattering frequency is inversely proportional to the time constant of unmodeled dynamics.

From the fact that smaller relay gain leads to lower level of chattering, chattering suppression methodology using adaptive relay gain was suggested. The idea is motivated from the original concept of the Variable Structure System. For the methodology, the switching gain of sliding mode control is designed such that it depends on the system state or the equivalent control that can be obtained by using a low-pass filter. The behavior of the system with the proposed controllers was analyzed, and simulation results were provided to show that chattering amplitudes were considerably reduced. Unlike the other known solutions for chattering suppression reviewed in the introduction of this dissertation, the method is strictly in the frame-

work of the principle concept of sliding mode and does not invite any complexity in controller design.

For systems controlled by on/off switching, chattering may exist if the switching frequency is restricted to be below a certain level. This situation is similar to so-called 'discretization chattering' problem that occurs due to finite sampling interval; however, the known solution to the problem, the equivalent control, cannot be applicable to the system with on/off switching. In power systems, which are generally operated by on/off switching, switching frequency is commonly limited to prevent power losses, and chattering or 'ripple' appears especially in system current. Common methods to decrease the ripple are based on 'harmonic cancellation' using multiple numbers of phase channels having desired phase shift that brings cancellation in the sum of outputs from individual channels. In this dissertation, a design principle of sliding mode control for power converters and similar systems was proposed. The methodology provided desired phase shifts between phases with the help of adaptive width of hysteresis loop in switching elements. The method is originated from the concept of multidimensional sliding mode and also based on the harmonic cancellation, which is a contrast to conventional control strategy that requires additional elements in the system to obtain phase shifts such as transformers or time delays. The chattering suppression effect is demonstrated by simulation for systems in various situations. For the system having unmodeled dynamics, it is also shown that the chattering may be reduced applying the same methodology of multiphase with the width of hysteresis that generates equivalent frequency of chattering in all phases.

In future work, a research is suggested to be performed to develop multidimensional sliding mode for chattering suppression in the system having two or more different types of unmodeled dynamics in control channels. For example, a system with two dimensional vector control may have two different types of unmodeled ac-

tuator dynamics. Then the chattering will be simultaneously affected by the two different dynamics. This problem needs a special method because chattering consists of periodic functions with different fundamental frequencies. The theory may be developed to be applied for dynamic systems with vector control such as induction motors, synchronous motors or generators.

BIBLIOGRAPHY

[1] V.I. Utkin, J. Guldner, J. Shi (1999) Sliding Mode Control in Electromechanical Systems, Taylor and Francis, London

[2] H. Lee and V.I. Utkin (2006) The Chattering Analysis, In: Edwards, Christopher; Fossas Colet, Enric; Fridman, Leonid (Eds.) Advances in Variable Structure and Sliding Mode Control, Lecture Notes in Control and Information Sciences, Vol. 334 , Springer, London

[3] V.I. Utkin and H. Lee (2006) The Chattering Analysis, Proc. 12th International Power Electronics and Motion Control Conference, EPE-PEMC 2006, Portoroz, Slovenia, pp. 2014-2019

[4] V.I. Utkin and H. Lee (2006) Chattering Problem in Sliding Mode Control Systems, Proc. 9th International Workshop on Variable Structure Systems, VSS 2006, Alghero, Sardinia, Italy, pp. 346-350

[5] V.I. Utkin (1993) Sliding mode control in discrete-time and difference systems, In: A. Zinober (Ed.) Variable Sturucture and Lyapunov Control, Springer-Verlag, London

[6] H. Lee (2002) Sliding mode control of read/write head positioning in hard disk drive, Master's thesis, The Ohio State University, Columbus

[7] V.I. Utkin (1978) Sliding modes and their application in variable structure systems, Mir Publishers, Moscow

[8] V.I. Utkin (1977) Variable structure systems with sliding modes, IEEE Transactions on Automatic Control, 22, pp. 212-222

[9] V.I. Utkin (1993) Application-oriented trends in sliding mode theory, Proceedings of the IEEE Industrial Electronics Conference, Maui HA, pp. 1937-42

[10] L. Fridman (2002) Singularly perturbed analysis of chattering in relay control systems, IEEE Transaction on Automatic Control, 47, 12, pp. 2079-2084

[11] L. Fridman (1999) The problem of chattering: an averaging approach. In: Young K.D. and Ozguner U. (eds.) Variable Structure, Sliding Mode and Nonlinear Control, Lecture Notes in Control and Information Science, no.247, Springer Verlag, London, pp. 363-386

[12] L. Fridman (2002) Sliding Mode Control for Systems with Fast Actuators: Singularly Perturbed Approach In Variable Structure Systems: Towards the 21st Century, X.Yu and J.-X.Xu Ed., Lecture Notes in Control and Information Science, v. 274,Springer Verlag, London, pp. 391-415

[13] L. Fridman (2003) Chattering analisys in sliding mode systems with inertial sensors, International Journal of Control, 76, no. 9/10, pp. 906-912

[14] L. Fridman (2001) An averaging approach to chattering, IEEE Transaction on Automatic Control, 46(8), pp. 1260-1265

[15] L.S. Goldfarb (1948) On the theory of vibrational regulators, Automation and Remote Control, Vol. IX, 6, 413-431

[16] K.K. Zhil'cov (1974) Approximate Methods of Variable Structure Systems Analysis, Mahsinostroeniye, Moscow (in Russian)

[17] Y.B. Shtessel and L. Young-Ju (1996) New approach to chattering analysis in systems with sliding modes, Decision and Control, Proceedings of the 35th IEEE Conference on, Volume: 4, pp. 4014-4019

[18] Y.Z. Tsypkin (1984) Relay Control Systems, Cambridge, England

[19] S.C. Chung and C.L. Lin (1999) A transformed Lure problem for sliding mode control and chattering reduction, IEEE Transaction on Automatic Control, 44, No. 3, pp. 563-568

[20] I. Boiko (2005) Analysis of sliding modes in the frequency domain, International J. Control, vol. 78, 10, pp. 969-981

[21] I. Boiko (2003) Frequency domain analysis of fast and slow motions in sliding modes, Asian Journal of Control, 5, No.4, pp. 445-453

[22] S.V. Emelyanov, S.K. Korovin (1981) Applying the principle of control by deviation to extend the set of possible feedback types, Soviet Physics, Doklady, 26 (6), pp. 562-564

[23] J.J. Slotine and W. Li (1991) Applied Nonlinear Control, Prentice-Hall

[24] J.J. Slotine and S.S. Sastry (1983) Tracking control of nonlinear systems using sliding surfaces, with application to robot manipulators, International Jounal of Control, 38, pp. 465-492

[25] J.J. Slotine (1984) Sliding controller design for nonlinear systems, International Jounal of Control, 40, pp. 421-434

[26] M. Chen, Y. Hwang, and M. Tomizuka (2002) A state-dependent boundary layer design for sliding mode control, IEEE Transactions on Automatic Control, 47, pp. 1677-81

[27] H. Lee, E. Kim, H.-J. Kang, and M. Park (2001) A new sliding-mode control with fuzzy boundary layer, Fuzzy Sets and Systems, Vol. 120, 147, pp. 135-143

[28] S. Huang and K. Chiou (2006) An Adaptive Neural Sliding Mode Controller for MIMO Systems, Journal of Intelligent and Robotic Systems, Vol. 46, 3, pp. 285-301

[29] A.G. Bondarev, S.A. Bondarev, N.E. Kostyleva, and V.I. Utkin (1985) Sliding modes in systems with asymptotic state observers, Automation and Remote Control, 46(6), pp. 49-64

[30] A. Kawamura, H. Itoh, and K. Sakamoto (1994) Chattering reduction of disturbance observer based sliding mode control, IEEE Transactions on industry applications, Vol. 30, 2, pp. 456-461

[31] S.V. Drakunov, D.B. Izosimov, A.G. Lukjanov, V.A. Utkin, and V.I. Utkin (1991) Block control principle, Automation and Remote Control, 51, Nb.6, pp. 601-8

[32] V.I. Utkin, S.V. Drakunov, D.B. Izosimov, A.G. Lukjanov, and V.A. Utkin (1984) A hierarchical principle of the control systems decomposition based on motion separation, Preprints of the 9th IFAC Congress, Budapest, Vol.V, pp. 134-39

[33] M. Krstic, I. Kanellakopoulos, and P. Kokotovic (1995) Nonlinear and Adaptive Control Design, J. Wiley, New York

[34] V.I. Utkin and J. Shi (1996) Integral sliding mode in systems operating under uncertainty conditions, Proceedings of the IEEE Conference on Decision and Control, Kobe, Japan, pp. 4591-4596

[35] R.A. DeCarlo, S.H. Zak, and G.P. Matthews (1988) Variable structure control of nonlinear multivariable systems: a tutorial, Proceedings of the IEEE, 76, pp. 212-232

[36] A. Levant (2003) Higher-order sliding modes, differentiation and ouptut feedback control, International Jounal of Control, 76, pp. 924-941

[37] L. Fridman and A. Levant (2002) Higher order sliding modes, In: W. Perruquetti, J. P. Barbot, eds. "Sliding Mode Control in Engineering", Marcel Dekker, Inc., 53-101

133

[38] L.V. Levantovsky (1985) Second order sliding algorithms. Their realization. In Dynamics of Heterogeneous Systems (Moscow: Institute for System Studies), pp. 32.43

[39] A. Levant (1993) Sliding order and sliding accuracy in sliding mode control. International Journal of Control, 58, pp. 1247-1263

[40] J.J Slotine and J.A. Coetsee (1986) Adaptive sliding controller synthesis for nonlinear systems, International Jounal of Control, 43, 6

[41] J.K. Hedrick and W.H. Yao (1993) Adaptive sliding control of a magnetic suspension system, in Variable Structure Control for Robotics and Aerospace Applications, Amsterdam, Netherlands

[42] L.C. Fu (1992) Robust adaptive decentralized control of robot manipulators, IEEE Transaction on Automatic Control, 37, 1, pp. 106-110

[43] C.Y. Su (1994) Adaptive sliding mode control of nonlinear robot system with time-varying parameters, Systems and Control Letters, 23, pp. 35-41

[44] K. Park and J. Lee (1996) Adaptive sliding mode controller with monotonically nonincreasing gain for nonlinear uncertain systems, Variable Structure Systems '96 Proceedings, 1996 IEEE International Workshop, pp. 139-142

[45] C.C. Kung and C.C. Liao (1994) Fuzzy-slding mode controller design for tracking control of non-linear system, Proceedings of the American Control Conference, Balimore, Maryland, pp. 180-184

[46] F.C. Sun, Z.Q. Sun, and G. Feng (1996) Design of adaptive fuzzy sliding mode controller for robot manipulators, Fuzzy systems, Proceedings of the 5th IEEE International Conference on, 1, pp. 62-67

[47] P. Kachroo and M. Tomizuka (1996) Chattering reduction and error convergence in the sliding-mode cotrol of a class of nonlinear systems, IEEE Transactions on Automatic Control, 41, 7, pp. 1063-1068

[48] R. Gessing (2000) Siding mode control with decreased chattering - model and simulations, Preceedings of the 2000 IEEE International Symposium on Computer-Aided Control System Design, Anchorage, Alaska, pp. 273-278

[49] C.L. Hwang (1996) Siding mode control using time-varying gain and boundary layer for electrohydraulic position and differential pressure control, IEE Proceedings Control Theory and Applications, 143, 4, pp. 325-332

[50] P.V. Kokotovic, R.B. O'Malley, and P. Sannuti (1976) Singular perturbations and order reduction in control theory, Automatica, 12, pp. 123-132

[51] P.V. Kokotovic (1984) Applications of singular perturbation techniques to control problems, SIAM Review, 26, pp. 501-550

[52] H.K. Khalil (1996) Nonlinear systems, 2nd Edition, Prentice-Hall, New Jersey

[53] A. Kawamura and R.G. Hoft (1983) Analysis of PWM Inverter with Instantaneous Feedback Control, IPEC-1983, Tokyo, pp. 1665-1675

[54] R. Venkataramanan, A. Sabanovic, and S. Cuk (1985) Sliding mode control of dc-to-dc converters, in Proc. IECON'85, pp. 251-258

[55] F. Bilalovic, O. Music, and A. Sabanovic (1983) Buck Converter Regulator Operating in Sliding Mode, Proceedings of 1983 PCI, pp. 331-340

[56] N. Sabanovic, T. Ninomiya, A. Sabanovic, and B. Perunicic (1995) Sliding Mode Approach to Control of Three-Phase Switching Converter, Elektrik Vol. 3, No.1, pp. 22-31

[57] A. Aroudi, B. Robert, and R. Leyva (2005) Sliding mode control of a high voltage DC-DC buck converter, Circuit Theory and Design, Proc. of the 2005 European Conference, Vol. 3, 28, pp. III/55-III/59

[58] V.M. Nguyen and C.Q. Lee (1996) "Indirect implementations of sliding-mode control law in buck-type converters," in Proc. IEEE Applied Power Electronics Conf. Expo. (APEC), Vol. 1, pp. 111-115

[59] A. Sabanovic (2003) Sliding modes in power electronics and motion control systems, International Journal of Control, The 29th Annual Conference of the IEEE, Vol. 1, 2-6, pp. 997-1002

[60] D. Cortes and J. Alvarez (2002) Robust sliding mode control for the boost converter, Power Electronics Congress, 2002. Technical Proceedings. CIEP 2002. VIII IEEE International, 20-24, pp. 208-212

[61] V.M. Nguyen and C.Q. Lee (1995) Tracking control of buck converter using sliding-mode with adaptive hysteresis, Power Electronics Specialists Conference, PESC '95 Record., 26th Annual IEEE, Vol. 2, 18-22, pp. 1086-1093

[62] M. Lopez, L. Garcia De Vicuna, M. Castilla, O. Lopez, J. Majo (1998) Interleaving of parallel DC-DC converters using sliding mode control, Industrial Electronics Society, Proceedings of the 24th Annual Conference of the IEEE Vol. 2, 31 pp. 1055 - 1059

[63] B. Miwa, D. Wen, and M. Schecht (1992) High Efficiency Power Factor Correction Using Interleaving Techniques, IEEE Applied Power Electronics Conference, Boston, pp. 557-568

[64] W. Woo, N.-C. Lee, and G. Schuellein (2006) Multi-phase buck converter design with two-phase coupled inductors , Applied Power Electronics Conference and Exposition, 2006. APEC '06. Twenty-First Annual IEEE, pp. 6

[65] R. Taylor and W. Liu (2007) Phase Shifting Optimizes Multistage Buck Converters, Power Electronics Technology, http://www.powerelectronics.com

[66] P, Xu, J. Wei, and F.C. Lee (2003) Multiphase Coupled-Buck Converter.A Novel High Efficient 12 V Voltage Regulator Module, Power Electronics, IEEE Transactions, Vol.18, 1, pp. 74-82

[67] P.-L. Wong, P. Xu, B. Yang, and F.C. Lee, (2001) Performance Improvements of Interleaving VRMs with Coupling Inductors, IEEE transactions on Power Electronics, VOL. 16, 4, pp. 499-507

[68] H. Lee and V.I. Utkin (2006) Sliding mode control of multiphase DC to DC converters, Technical report for research project with *IKOR*

[69] V. Utkin, D. Chen, S. Zarei, and J. Miller (2000) Real-time implementation of sliding mode observer for synchronous rectification of the automotive electric power supply systems, JSDMC Special Issue on Variable Structure Control, Vol. 122, Dec.,pp. 594-598